Rheology and dynamics of elastic waves in fluid-saturated porous media with gas bubbles

A Thesis submitted by

Adham Abdul Wahab Ali ALI

For the award of

Doctor of Philosophy

2019

Abstract

Elastic wave propagation in fluid-saturated porous media presents significant practical and theoretical interest for science and engineering. In such media at least two types of the waves can propagate: the Frenkel-Biot compressional waves of P1 and P2 type. Usually the waves are modelled by partial differential equations (PDEs) ranging from the classical wave equation to its nonlinear high-order extensions. A popular extension of this kind is the Nikolaevsky equation (1989). In this thesis we extend it further to included bubbles.

The thesis consists of seven chapters. Chapter 1 presents the literature review and motivation. Chapter 2 gives general concepts from dynamics. In Chapter 3 for the cases when there are no neutral modes, the wave decays exponentially quickly under the linear dispersion relation (which dynamically expresses dissipation). The wave dynamics depend on the grain rheology, which should take into account bubbles in the fluid-saturated pores. We consider the standard linear solid rheological model to include a special element representing a bubble. We derive the 2nd-order evolution PDEs for the P1-wave governing the velocity of the solid matrix in the moving reference frame. Then we derive the corresponding dispersion relation, and compare it to the case without the bubbles. We observe that the increase of the radius and number of the bubbles leads to the increase in the decay rate.

In Chapter 4 of the thesis we use the full rheological model, based on the model by Nikolaevsky. The full model consists of three segments representing the solid

continuum, fluid continuum and a bubble surrounded by the fluid. We derive the 4th-order PDE for the wave without the bubbles and 6th-order PDE for the wave with the bubbles, and obtain the corresponding dispersion relations. We discover that the increase of the radius of the bubbles leads to faster decay, while the increase of the number of the bubbles leads to slower decay of the wave. This latter result manifests the opposite trend to the one observed in the second part. We attribute this result to the more complete and, therefore, more realistic structure of the rheological model used.

In Chapter 5 of the thesis we evaluate the influence on the decay rate by the rheological parameters and other parameters of the medium such as pressure and porosity. Each of them has an appreciable effect on the decay rate, as detailed in the thesis. We discover that the model gives complex wave velocity and/or wave growth, which indicates limitations of the model applicability at extremely large amounts of bubbles. However, we calculate some of acceptable values of the parameters. They belong to finite-size cloud(s) of acceptable values in the multi-dimensional parametric space. Full study of this space is a possible direction of future research.

In Chapter 6 we use the centre manifold theory to describe the dynamics of the elastic wave for the special case when there is one neutral mode. After quickly falling onto the centre manifold, the system then exhibits slow algebraic decay or tends to a steady state depending on the initial conditions and the neutral wave number.

Finally, Chapter 7 gives the conclusions and suggestions for future work.

Certification of Thesis

This Thesis is entirely the work of **Adham Abdul Wahab Ali ALI** except where otherwise acknowledged. The work is original and has not previously been submitted for any other award, except where acknowledged.

Student and supervisors signatures of endorsement are held at the University.

Principal Supervisor: Assoc. Prof. Dmitry Strunin.....Date.....

Associate Supervisor: Prof. Nam Mai-Duy.....Date.....

Dedication

‘‘We all have dreams. But in order make dreams come into reality, it takes an awful lot of determination, dedication, self-discipline, and effort.’’ Jesse Owens

This thesis is
dedicated with love and
affection to the memory of my
father and to all my family, who inspire
me and make me so proud.
Always be the best
you can be.

Acknowledgments

Undertaking this Ph.D. has been a truly life-changing experience for me, both as a researcher and as a person and it would not have been possible to do without the support, motivation and guidance that I received from many people. I would like to take this opportunity to extend my sincere gratitude and appreciation to all those who made this Ph.D. thesis possible.

First and foremost, I praise God, the almighty for giving me this opportunity and capability to persevere my postgraduate research degree successfully. My special words of thanks should go to my academic Supervisor, Associate Professor Dmitry Strunin for the constant guidance, support, and encouragement he has provided to me during the entire period of my studies at the University of Southern Queensland. Dmitry Strunin provided me with every bit of guidance, assistance, enthusiasm, and immense knowledge that I needed during my first semester. He showed me different ways to approach a research problem and the need to be persistent to accomplish any goal. I wish to say you are a wonderful supervisor, professor and researcher. Additionally, I would like to express my special appreciation and thanks to my Associate Supervisor, Professor Nam Mai-Duy and previous Associate Supervisor Professor Thanh Tran-Cong for all their suggestions and comments.

I would like to extend my sincerest thanks and appreciation to my dear wife (Fatima) and my lovely children (Yousif, Zainab, and the little man Mustafa). Words can not express how grateful I am for all of the sacrifices that you all made and emotional

support that you provided during my journey. I also thank my family who encouraged me and prayed for me throughout the time of my research.

I greatly appreciate financial support from the University of Southern Queensland towards conference registrations and a journal fee. Further, I am extremely grateful to the Staff of the University of Southern Queensland, especially Mrs. Juanita Ryan, Mrs. Kathryn Schmacker and Mrs. Rebecca Darr who were always so helpful and provided me with their assistance throughout my study.

A special note of thanks should go to the Australian Commonwealth Government for the financial support through the Research Training Program (RTP) – fees offset scheme during my study.

Lastly, but most importantly, I am also truly grateful to my Iraqi Government represented by the Ministry of Higher Education and Scientific Research for offering the Ph.D. scholarship here at the University of Southern Queensland, Australia, without which this research would not have been possible.

Adham Abdul Wahab Ali ALI

University of Southern Queensland

September 2019

‘‘To move the world we must move ourselves.’’Socrates

Associated Publications

The following publications were produced during the period of candidature:

1. Strunin, D. V. and Ali, A. A. (2016), 'On nonlinear dynamics of neutral modes in elastic waves in granular media', *Journal of Coupled Systems and Multiscale Dynamics* [American Scientific Publishers] **4**(3), 163–169.

2. Ali, A. A. and Strunin, D. V. (2018), 'Nonlinear stability in seismic waves', *Australian and New Zealand Industrial and Applied Mathematics (ANZIAM) Journal* [Oxford University Press] **57**, 382–397.

3. Ali, A. A. and Strunin, D. V. (2018), 'The effect of rheology with gas bubbles on linear elastic waves in fluid-saturated granular media', *International Journal of Applied Mechanics and Engineering* [De Gruyter Poland] **23**(3), 575–594.

4. Strunin, D. V. and Ali, A. A. (2018), 'Rheology and decay rate for Frenkel-Biot P1 waves in porous media with gas bubbles', The 29th International Symposium on Transport Phenomena (30 Oct - 2 Nov, 2018, Honolulu, USA) [The Japan Society of Mechanical Engineers], paper ISTP29-057, presented, not published; submitted to the *International Journal of Mechanics* [North Atlantic University Union] in August 2019.

5. Ali, A. A. and Strunin, D. V. (2019), 'The role of rheology in modelling elastic waves with gas bubbles in granular fluid-saturated media', *Journal of Mechanics of Materials and Structures* [Mathematical Sciences Publishers] **14**(1), 1–24.

Contents

List of Figures

List of Tables

Keywords

Elastic Granular Media, Rheology, Bubbles, Nonlinear Waves, Frenkel-Biot's Waves, Porous Media, Fluid.

Acronyms & Abbreviations

PDEs	Partial Differential Equations
P-wave	Primary wave
S-wave	Shear wave
P1-wave	Fast primary wave
P2-wave	Slow primary wave
GSLS	Generalized Standard Linear Solid
BZ	Belousov-Zhabotinsky

Nomenclature

$\beta^{(s)}$	:	Compressibility of solid, Pa^{-1}
$\beta^{(L)}$	:	Compressibility of water and gas, Pa^{-1}
$\rho_0^{(s)}$	:	Density of solid, $\mathrm{kg/m}^3$
$\rho_0^{(L)}$	:	Density of water, $\mathrm{kg/m}^3$
$\rho_0^{(g)}$	:	Density of gas, $\mathrm{kg/m}^3$
R_0	:	Bubble radius, m
ε	:	Small parameter
n_0	:	Number of bubbles, $1/\mathrm{m}^3$
μ	:	Viscosity, Pa·s
ℓ	:	Permeability, m^2
E_i	:	Elastic moduli, Pa
M_i	:	Masses, kg/m
k_b	:	Bulk modulus, Pa
p	:	Pressure, Pa
$\sigma^{(ef)}$	:	Effective stress, Pa
ϕ	:	Volume gas content
m	:	Porosity
ζ	:	Adiabatic exponent
k	:	Wave number, 1/m
c	:	Wave velocity, m/s
v	:	Particle velocity, m/s
λ	:	Decay rate, 1/s

Chapter 1

Literature review and motivation

SUMMARY: This chapter gives a brief literature review of the wave propagation in porous media including Biot's theory and some related concepts. The rest of this chapter goes to presenting the motivation. Next, we explain the purpose of the study. Finally, the outline of this thesis is presented.

1.1 A review of wave propagation in porous media

The main purpose of this section is to give a brief review of propagation seismic wave in fluid saturated and partially saturated porous media. We also describe basics of stress-strain relations, in order to prepare the ground for deriving the constitutive equation for the new rheological model used in this thesis.

1.1.1 Stress-strain relations in viscoelastic models

The propagation of seismic waves in a porous elastic solid is intimately linked to two basic concepts: the stress and the strain (a measure of deformation per unit length). Therefore, these waves are also called stress waves. Stress is the force applied to the

elastic solid, and strain represents the resulting changes in shape and size. The unit of stress is force per unit area. For the material that is stretched, the strain has positive sign; for the material that is compressed, the strain has negative sign. Such strain is sometimes called a normal strain, however there is another type of strain which is called a shear strain and the corresponding stress is called a shear stress. By the Hooke's law the stress σ is related to the strain e by the linear relation

$$\sigma = Ee\,, \tag{1.1}$$

where E is the elastic modulus called the Young's modulus and has the same units as stress (Holmes, 2009). A similar relation can be written for the shear strain and stress

$$\tau = G\gamma\,, \tag{1.2}$$

where G is the shear modulus. The stress-strain relations of a linear elastic material can be identified by two constants, the Young's modulus E and the Poisson's ratio υ which are connected by the following expressions (Vyalov, 2013),

$$E = \frac{3KG}{K+G}, \qquad \upsilon = \frac{K-2G}{2(K+G)}\,, \tag{1.3}$$

where K is bulk modulus of elasticity.

The relation between stress and strain can be very complicated, therefore many simplified models are introduced in rheology (Novotny, 1999). In general, materials can be classified as elastic solids and viscous liquids (Ferry, 1980). A material that exhibits both viscous and elastic characteristics is often called a viscoelastic material. Rheological models, also called viscoelastic models or mechanical models are usually used to illustrate the viscoelastic behavior and physical properties of the materials. Viscoelastic models are very useful in many disciplines of science especially in biomechanics, for example, most of biological tissues have viscoelastic features (Fung, 2013; Özkaya et al., 2017). We can build up the linear viscoelastic model by using different combinations of elements of the linear elastic springs and the linear viscous dashpots

that relate to stress-strain relations. The linear elastic and viscous deformation can be represented (modelled) by the spring and dashpot elements, respectively, as illustrated in Figure 1.1. A purely linear elastic spring follows Hooke's law (similar to the linear relation between the stress and strain (1.1)). For the case of purely linear viscous material, the stress-strain relation (the constitutive law) in the dashpot element follows the formula

$$\sigma = \mu \frac{de}{dt}\,, \tag{1.4}$$

where μ is the viscosity constant specified to the dashpot and has the unit $\mathrm{N/m^2}$, or Pascal·Second=Pa·s. This means that the shear stress is proportional to the change of the strain rate. At this point the main difference between elastic and viscoelastic materials is that the constitutive equation of the viscoelastic material involves time derivative(s) whereas for the elastic material it does not. For elastic materials, the size and shape of the material can return to its original when the applied force is removed and this is because the energy provided to deform the material is stored elastically in the material (Özkaya et al., 2017). This shows that there is no energy loss during the loading cycle. Therefore, the loading and unloading cycle for an elastic material coincide as shown in Figure 1.2. For viscoelastic materials, some of the energy is stored in the material and some of it is damped (dissipated) thermally. Consequently, there is loss of energy during the loading and unloading cycle because the Newton's dashpot generates the resistance to activate the deformation (Kim, 2008). The area enclosed by the loading and unloading paths represents the energy dissipated thermally and is known as the hysteresis, see Figure 1.3.

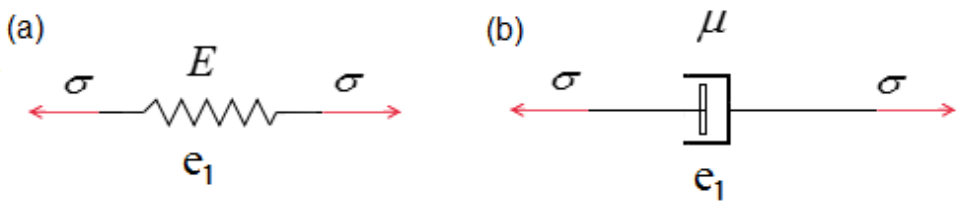

Figure 1.1: Rheological scheme for the linear: (a) elastic spring, (b) viscous dashpot .

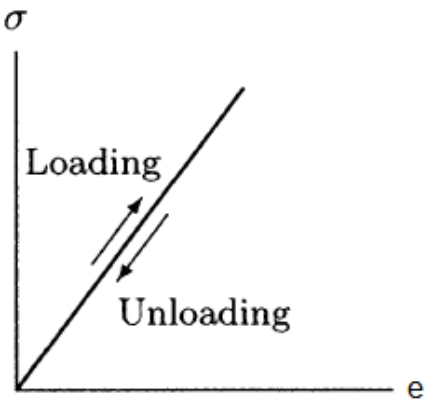

Figure 1.2: For an elastic material, loading and unloading paths coincide (Özkaya et al., 2017) .

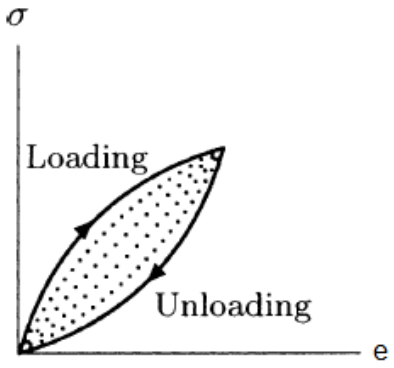

Figure 1.3: Hysteresis loop (Özkaya et al., 2017) .

The constitutive equation for a linear viscoelasticity can be presented either by a differential equation or an integral equation. There are several models that are used to describe the viscoelasticity of the materials. To make this review more concrete we give some basic examples to express the linear viscoelastic materials providing the details of the approach that we will use to obtain the governing equations for more complex viscoelastic models (Lemaitre, 2001; Banks et al., 2011; Fung, 2013; Findley and Davis, 2013; Zhi-jun et al., 2014; Skrzypek and Ganczarski, 2015).

- Maxwell model

  The Maxwell model is the simplest model for a viscoelastic material that connects a purely viscous dashpot with a purely elastic spring as shown in Figure 1.4. In the Maxwell model, the stress goes down exponentially with time. The equations of the model are

$$\begin{aligned} e &= e_1 + e_2\,, \quad \sigma = \sigma_1 = \sigma_2\,, \\ \sigma_1 &= Ee_1\,, \quad \sigma_2 = \mu\frac{de_2}{dt}\,. \end{aligned} \tag{1.5}$$

  The system (1.5) gives the constitutive equation for the model

$$\sigma + \frac{\mu}{E}\frac{d\sigma}{dt} = \mu\frac{de}{dt}\,. \tag{1.6}$$

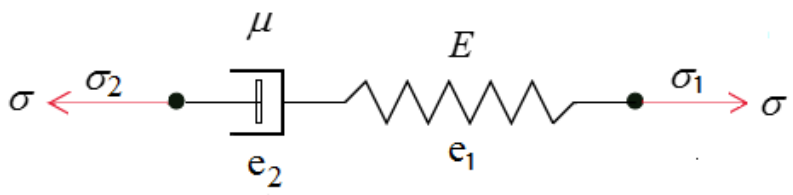

Figure 1.4: Rheological scheme for Maxwell model.

- Voigt-Kelvin model

  The Kelvin-Voigt model is another simple model which consists of a single elastic spring and a single viscous dashpot but in this case the two elements are connected in parallel as shown in Figure 1.5. The model generates the following equations

$$\begin{aligned} e &= e_1 = e_2\,, \quad \sigma = \sigma_1 + \sigma_2\,, \\ \sigma_1 &= \mu\frac{de_1}{dt}\,, \quad \sigma_2 = Ee_2\,. \end{aligned} \tag{1.7}$$

  Therefore, the stress-strain equation of the model is

$$\sigma = Ee + \mu\frac{de}{dt}\,. \tag{1.8}$$

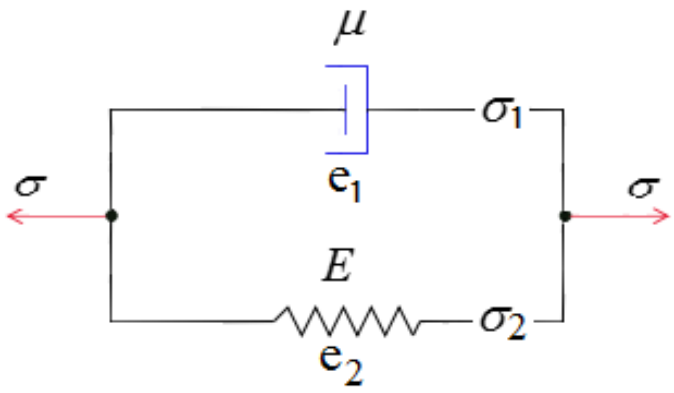

Figure 1.5: Rheological scheme for Voigt-Kelvin model .

- Standard linear solid model

  Standard linear solid model is the combination of a Maxwell model in parallel with an elastic spring element. This model is also called a Kelvin model. An illustration is given in Figure 1.6. The governing equations of the model are

$$\begin{aligned} e &= e_2 = e_1 + e_3\,, \\ \sigma &= E_1 e_1 + E_2 e_2\,, \\ E_1 e_1 &- \mu \frac{de_3}{dt} = 0\,. \end{aligned} \tag{1.9}$$

  This is a more complex model and below we show the derivation in detail. Differentiating the first and second equations of the system (1.9), we obtain the following equations in matrix form,

$$\begin{bmatrix} E_2 & E_1 & 0 & 0 & 0 \\ 0 & 0 & 0 & E_1 & 0 \\ 0 & E_1 & 0 & 0 & -\mu \\ -1 & 1 & 1 & 0 & 0 \\ 0 & 0 & 0 & 1 & 1 \end{bmatrix} \begin{bmatrix} e \\ e_1 \\ e_3 \\ \frac{de_1}{dt} \\ \frac{de_3}{dt} \end{bmatrix} = \begin{bmatrix} \sigma \\ \frac{d\sigma}{dt} - E_2 \frac{de}{dt} \\ 0 \\ 0 \\ \frac{de}{dt} \end{bmatrix}. \tag{1.10}$$

  Then solving system (1.10) for e yields

$$e = \frac{-E_1^2 \mu \frac{de}{dt} - E_1 E_2 \mu \frac{de}{dt} + E_1^2 \sigma + E_1 \mu \frac{d\sigma}{dt}}{E_1^2 E_2}\,. \tag{1.11}$$

Equation (1.11) leads to the constitutive law

$$\sigma + \theta \frac{d\sigma}{dt} = E_2 e + \theta(E_1 + E_2)\frac{de}{dt}\,, \tag{1.12}$$

where $\theta = \mu/E_1$.

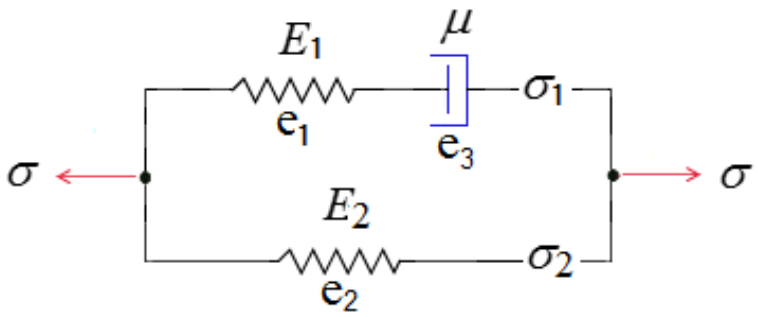

Figure 1.6: Rheological scheme for standard linear solid model.

- Burgers model

  This model is even more complicated than the former three models. The Burgers model is composed of the Maxwell model and the Kelvin-Voigt arranged in a series as shown in Figure 1.7. Now we write the equations for its elements,

$$\begin{aligned} e &= e_1 + e_2 + e_3\,, \\ \sigma &= E_1 e_1\,, \\ \sigma &= \mu_1 \frac{de_2}{dt}\,, \\ \sigma &= E_2 e_3 + \mu_2 \frac{de_3}{dt}\,. \end{aligned} \tag{1.13}$$

  Differentiating system (1.13) up to the second order, gives the following equations in matrix form,

$$\begin{bmatrix} 0 & 1 & 1 & 1 & 0 & 0 & 0 & 0 & 0 & 0 \\ -1 & 0 & 0 & 0 & 1 & 1 & 1 & 0 & 0 & 0 \\ 0 & 0 & 0 & 0 & 0 & 0 & 0 & 1 & 1 & 1 \\ 0 & E_1 & 0 & 0 & 0 & 0 & 0 & 0 & 0 & 0 \\ 0 & 0 & 0 & 0 & E_1 & 0 & 0 & 0 & 0 & 0 \\ 0 & 0 & 0 & 0 & 0 & 0 & 0 & E_1 & 0 & 0 \\ 0 & 0 & 0 & 0 & 0 & \mu_1 & 0 & 0 & 0 & 0 \\ 0 & 0 & 0 & 0 & 0 & 0 & 0 & 0 & \mu_1 & 0 \\ 0 & 0 & 0 & E_2 & 0 & 0 & \mu_2 & 0 & 0 & 0 \\ 0 & 0 & 0 & 0 & 0 & 0 & E_2 & 0 & 0 & \mu_2 \end{bmatrix} \begin{bmatrix} \frac{de}{dt} \\ e_1 \\ e_2 \\ e_3 \\ \frac{de_1}{dt} \\ \frac{de_2}{dt} \\ \frac{de_3}{dt} \\ \frac{d^2e_1}{dt^2} \\ \frac{d^2e_2}{dt^2} \\ \frac{d^2e_1}{dt^2} \end{bmatrix} = \begin{bmatrix} e \\ 0 \\ \frac{d^2e}{dt^2} \\ \sigma \\ \frac{d\sigma}{dt} \\ \frac{d^2\sigma}{dt^2} \\ \sigma \\ \frac{d\sigma}{dt} \\ \sigma \\ \frac{d\sigma}{dt} \end{bmatrix}. \tag{1.14}$$

Solving system (1.14) for $\frac{de}{dt}$ results in

$$\frac{de}{dt} = -\left[\frac{E_1^3 E_2 \mu_1^2 \mu_2 \frac{d^2e}{dt^2} - E_1^2 E_2 \mu_1 \left(((E_1+E_2)\mu_1 + E_1\mu_2)\frac{d\sigma}{dt} + \mu_1\mu_2 \frac{d^2\sigma}{dt^2}\right)}{E_1^3 E_2^2 \mu_1^2}\right]. \tag{1.15}$$

Then the stress-strain equation of the Burgers model takes the form

$$\sigma + \left(\frac{\mu_1}{E_1} + \frac{\mu_1}{E_2} + \frac{\mu_2}{E_2}\right)\frac{d\sigma}{dt} + \frac{\mu_1\mu_2}{E_1E_2}\frac{d^2\sigma}{dt^2} = \mu_1\frac{de}{dt} + \frac{\mu_1\mu_2}{E_2}\frac{d^2e}{dt^2}. \tag{1.16}$$

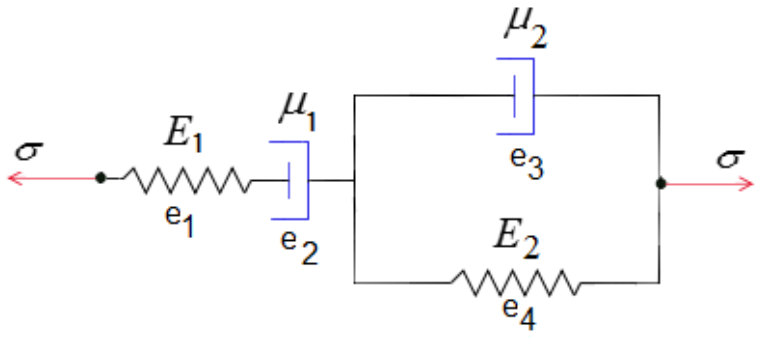

Figure 1.7: Rheological scheme for Burgers model.

1.1.2 Model of rheology with internal oscillators

This section gives a short introduction to the one-dimensional viscoelastic model with internal oscillators. Typically, the rheological models combine an elastic spring with a viscous dashpot. However, Nikolaevskiy (1985) in his analysis of seismic waves considered the standard mechanical model with an internal oscillator. The structure of the model is similar to the standard linear solid model but it also contains two oscillating masses M_1 and M_2 attached to the elastic springs, see Figure 1.8. The governing equations are

$$\begin{aligned} & e = e_2 = e_1 + e_3 \,, \\ & E_1 e_1 = \mu \frac{de_3}{dt} \,, \\ & M_1 \frac{\partial^2 e_1}{\partial t^2} + M_2 \frac{\partial^2 e_2}{\partial t^2} = \sigma - E_1 e_1 - E_2 e_2 \,. \end{aligned} \tag{1.17}$$

Now we differentiate system (1.17) up to the third order and get the following equations in matrix form,

$$\begin{bmatrix} E_2 & E_1 & 0 & 0 & 0 & M_1 & 0 & 0 & 0 \\ 0 & 0 & 0 & E_1 & 0 & 0 & 0 & M_1 & 0 \\ 0 & E_1 & 0 & 0 & -\mu & 0 & 0 & 0 & 0 \\ 0 & 0 & 0 & E_1 & 0 & 0 & -\mu & 0 & 0 \\ 0 & 0 & 0 & 0 & 0 & E_1 & 0 & 0 & -\mu \\ -1 & 1 & 1 & 0 & 0 & 0 & 0 & 0 & 0 \\ 0 & 0 & 0 & 1 & 1 & 0 & 0 & 0 & 0 \\ 0 & 0 & 0 & 0 & 0 & 1 & 1 & 0 & 0 \\ 0 & 0 & 0 & 0 & 0 & 0 & 0 & 1 & 1 \end{bmatrix} \begin{bmatrix} e \\ e_1 \\ e_3 \\ \frac{de_1}{dt} \\ \frac{de_3}{dt} \\ \frac{d^2e_1}{dt^2} \\ \frac{d^2e_3}{dt^2} \\ \frac{d^3e_1}{dt^3} \\ \frac{d^3e_3}{dt^3} \end{bmatrix} = \begin{bmatrix} \sigma - M_2 \frac{d^2e}{dt^2} \\ \frac{d\sigma}{dt} - E_2 \frac{de}{dt} - M_2 \frac{d^3e}{dt^3} \\ 0 \\ 0 \\ 0 \\ 0 \\ \frac{de}{dt} \\ \frac{d^2e}{dt^2} \\ \frac{d^3e}{dt^3} \end{bmatrix} . \tag{1.18}$$

Solving system (1.18) for e yields,

$$e = - \left[\frac{E_1 \big(M_2 \frac{d^2e}{dt^2} + \mu \frac{de}{dt} - \sigma \big) + \mu \big(E_2 \frac{de}{dt} + (M_1 + M_2) \frac{d^3e}{dt^3} - \frac{d\sigma}{dt} \big)}{E_1 E_2} \right] . \tag{1.19}$$

Equation (1.19) leads to the constitutive law presented in (Nikolaevskiy, 1985),

$$\sigma + \theta\frac{d\sigma}{dt} = E_2 e + (E_1 + E_2)\theta\frac{de}{dt} + M_2\frac{d^2e}{dt^2} + (M_1 + M_2)\theta\frac{d^3e}{dt^3}\,, \tag{1.20}$$

where $\theta = \mu_1/E_1$.

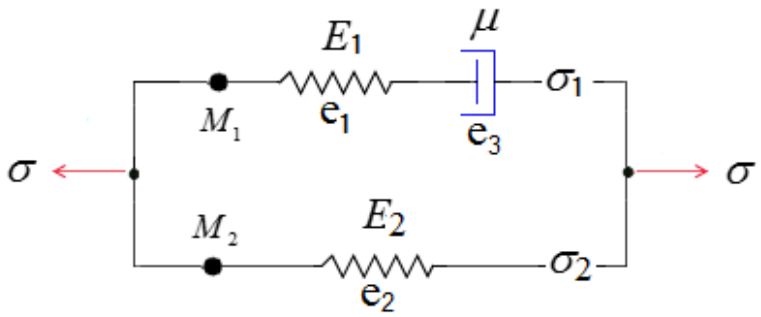

Figure 1.8: Rheological scheme with internal oscillators (Nikolaevskiy, 1985) .

In 1989, Nikolaevskiy extended his model by connecting the rheological model presented in Figure 1.8 and the Maxwell model in parallel (Nikolaevskiy, 1989), see Figure 1.9. The resulting constitutive equation has the form

$$\left(a_0 + \sum_{p=1}^{5} a_p\frac{D^p}{Dt^p}\right) e = \left(b_0 + \sum_{p=1}^{3} b_p\frac{D^p}{Dt^p}\right)\sigma\,, \tag{1.21}$$

where the mechanical parameters a_i and b_i are expressed as

$$a_0 = E_2, \quad a_1 = (E_1 + E_2)\theta_1 + (E_2 + E_3)\theta_2, \quad a_2 = E_2\Big(\frac{M_1}{E_1} + \frac{M_2}{E_2} + \theta_1\theta_2\Big)\,,$$

$$\begin{gathered} a_3 = (M_1 + M_2)\theta_1 + \big(M_1 + M_2\frac{E_2 + E_3}{E_1}\big)\theta_2\,, \\ a_4 = \frac{M_1 + M_2}{E_1} + \theta_1\theta_2 E_1, \quad a_5 = \frac{M_1 + M_2}{E_1}\theta_2\,, \\ b_0 = 0, \quad b_1 = \theta_1\theta_2 + \frac{M_1}{E_1}, \quad b_3 = \frac{M_1}{E_1}\theta_1, \quad \theta_1 = \frac{\mu_1}{E_1}, \quad \theta_2 = \frac{\mu_2}{E_3}\,. \end{gathered} \tag{1.22}$$

In this study, we will use an extended viscoelastic model relative to the model of Nikolaevskiy (1985, 1989) to take into account bubbles. In the new model, we will add

one more mass attached to an elastic spring and a viscous dashpot in the fluid branch in Figure 1.8. The new extended model will be discussed in more detail in Chapter 4.

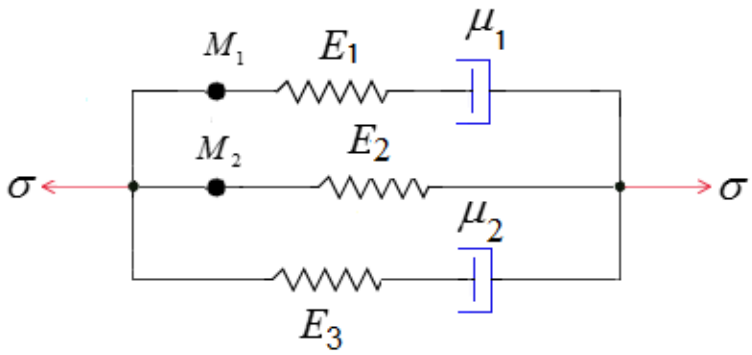

Figure 1.9: Rheological scheme with internal oscillators (Nikolaevskiy, 1989) .

1.1.3 Biot's theory for porous elastic solids

The problem of the wave propagation in porous media is important in various fields of science and engineering. Over the recent years, researchers studied diverse phenomena of this type in large-scale earthquakes, soil mechanics, acoustics, earthquake engineering, and many other areas. In 1956, Biot (1956*a*,*b*) presented his important work of wave propagation in a saturated porous medium for both low and higher frequencies. Today, most studies in acoustics, geophysical and geological mechanics rely on his theory. Biot identified the presence of three different wave types in fluid-saturated porous media, namely two types of compressional waves, also called longitudinal, dilatational, irrotational or primary waves (P-waves) with different speeds and one type of rotational, shear wave or secondary wave (S-wave). Note that the P- and S-waves are well known waves in seismology. The two compressional waves are a fast compressional wave called P1-wave and a slow compressional wave called P2-wave. Both compressional and shear elastic waves can move and propagate in solid rocks. However, only compressional waves can propagate in fluids and gases.

Figure 1.10 shows the particle motion for both P-wave and S-wave.

Biot (1962*b*,*a*) also derived the dynamical equations for the wave propagation in poroelastic media fully saturated with a single-phase fluid using Lagrange's equations. Many researchers re-derived the Biot's equations using different mathematical approaches, for example, homogenization for periodic structures (Lévy, 1979; Auriault, 1980; Burridge and Keller, 1981) and volume averaging processes (Pride et al., 1992). The Biot's equations involve four basic assumptions (Müller et al., 2010): first, the porous rock is isotropic and homogeneous; second, the porous rock is fully saturated with only one fluid; third, the motion between the solid and fluid is governed by the Darcy's law and fourth, the wavelength of the wave is larger than the size of the biggest grains or pores. A seismic wave is an elastic wave; and the elastic wave equation has been widely used to describe the wave propagation in a porous media, such as earth rocks and human body (ultrasonic waves). The standard form of the seismic wave equation in a homogeneous and isotropic medium can be expressed in vector notation as

$$\rho_0 \frac{\partial^2 \boldsymbol{u}}{\partial t^2} = (\lambda + 2\mu)\nabla(\nabla \cdot \boldsymbol{u}) - \mu \nabla \times (\nabla \times \boldsymbol{u}) \,, \tag{1.23}$$

here ∇ is the gradient operator, ρ is the density, λ and μ are the Lame parameters related to the Young's modulus, and $\boldsymbol{u}$ is the displacement. Because the equation is expressed in terms of the displacement of the material, it is also called the displacement equation of motion (Bedford and Drumheller, 1994). Additionally, we can write the P-wave equation as

$$\nabla^2(\nabla \cdot \boldsymbol{u}) - \frac{1}{\alpha^2} \frac{\partial^2 (\nabla \cdot \boldsymbol{u})}{\partial t^2} = 0 \,, \tag{1.24}$$

where α is the P-wave velocity,

$$\alpha = \sqrt{\frac{\lambda + 2\mu}{\rho}} \,. \tag{1.25}$$

Similarly, we can write the S-wave equation as

$$\nabla^2(\nabla \times \boldsymbol{u}) - \frac{1}{\beta^2} \frac{\partial^2 (\nabla \times \boldsymbol{u})}{\partial t^2} = 0 \,, \tag{1.26}$$

where β is the velocity of the S-wave,

$$\beta = \sqrt{\frac{\mu}{\rho}}\,. \tag{1.27}$$

(Müller et al., 2007; Shearer, 2010).

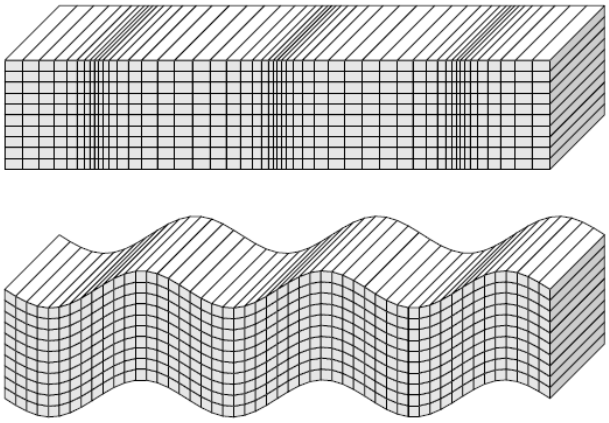

Figure 1.10: Displacements occurring from a harmonic plane P-wave (top) and S-wave (bottom) traveling horizontally across the page. S-wave propagation is pure shear with no volume change, whereas P-waves involve both a volume change and shearing (change in shape) in the material. Strains are highly exaggerated compared to actual seismic strains in the Earth (Shearer, 2010) .

Wave propagation in porous media and related Biot theory of deformation are extensively discussed in a number of papers and books (for example, Berryman, 1981; Nikolaevskiy, 1990; Tuncay and Corapcioglu, 1996; Wei and Muraleetharan, 2002; Lo et al., 2005; Nikolaevskiy, 2005; Kurzeja and Steeb, 2012; Beresnev, 2013; Cheng, 2014; Beresnev, 2016; Merxhani, 2016; Wang, 2017; Ciarletta et al., 2018; Agreste et al., 2019; Ali and Strunin, 2019). The propagating P2-wave in a fluid saturated porous medium has caught many scientists' interest since it was predicted by Biot (1956*a*,*b*). The P2-wave has first been observed experimentally in a laboratory by Plona (1980). This type of wave has a strongly dissipative behaviour (energy losses), and therefore is difficult to observe (Tuncay and Corapcioglu, 1996). Tun-

cay and Corapcioglu (1996), Wei and Muraleetharan (2002) and Lo et al. (2005) determined the minimum velocity of the P2-wave at fully saturated media. The former three studies documented that the wave velocity is gently declining from low to high wetting saturation until it reaches the minimum. However, Santos et al. (1990) and Lu et al. (2007) reported the opposite behavior, therefore further research is necessary to get a clear answer in this regard.

Yang et al. (2014) showed that the dispersion of velocity and attenuation of the fast (P1) wave are both affected by the viscoelasticity of the medium, but has almost no effect on the slow (P2) wave. In addition, they proved that the dominant frequency of the P1-wave shifts linearly toward lower frequencies due to the conditions of low permeability and low porosity; this plays a significant role in exploration for gas and oil. Lo et al. (2005) stated that the speed of the P1-wave in the oil-water saturated medium is higher than the air-water saturated medium and increases with the increasing of the water saturation. Moreover, they illustrated that the P1-wave is significantly affected by the saturating continuum, which can be oil or air, see Figures 1.11 and 1.12. The results of some experiments (Gardner, 2000) showed that the P2-wave velocity of the seismic waves for gassy soil which propagated at frequencies below resonance is ($\sim 200\,\mathrm{m/s}$), while, at higher frequencies, they propagated at the P1-wave velocity ($\sim 1500\,\mathrm{m/s}$). According to Toksöz et al. (1976) the velocity of the P-wave is higher when the rock is saturated with water than when it is dry or saturated with gas. Sharma and Saini (2012) considered the waves propagation in porous solid containing two viscous fluids with the existence of bound liquid film. The solution of the mathematical model for the propagation of harmonic waves provided the velocities of four attenuated waves in the medium. One of these waves is S-wave and the others are P-waves.

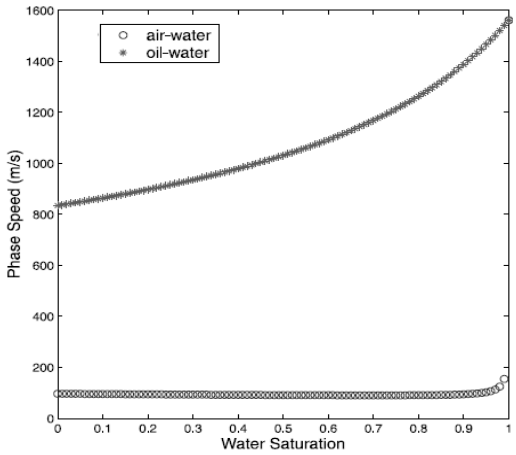

Figure 1.11: Effect of water saturation on the phase speed of the P1 wave at four excitation frequencies: the air-water and oil-water systems (Lo et al., 2005) .

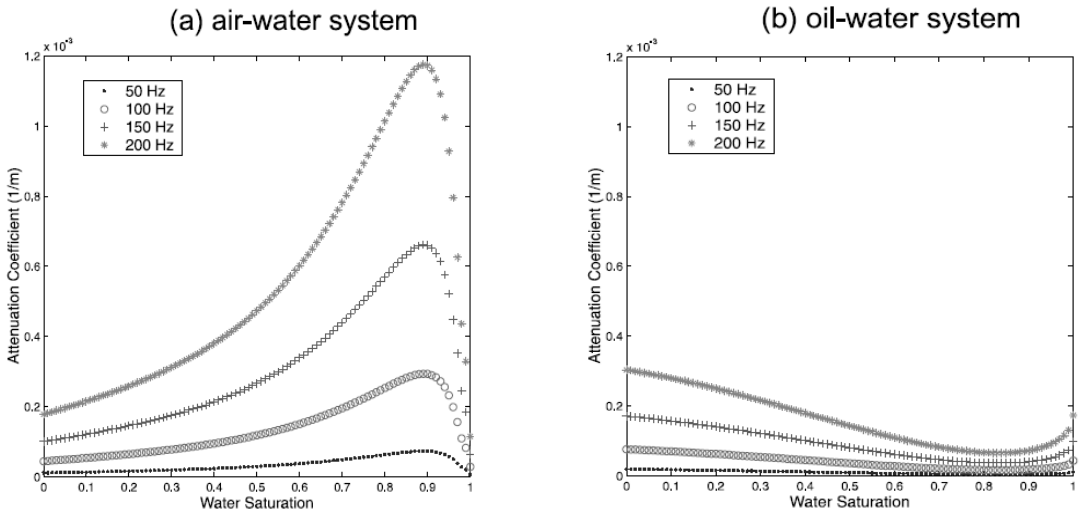

Figure 1.12: Effect of water saturation on the attenuation coefficient of the P1 wave at four excitation frequencies: (a) air-water system, (b) oil-water system (Lo et al., 2005) .

Still further, Tuncay and Corapcioglu (1996), Buckingham (1999), and Wei and Muraleetharan (2002) compared the phase velocities of the P- and S-waves, as a function of saturation. They showed that an increase in the degree of saturation leads

to decrease in the velocity of P1- and S-waves. A similar behavior is observed for the P2-wave, however, the velocity of P1- and P2-waves start to rapidly increase when the degree of saturation reaches 100% for the P1-wave and 85% for the P2-wave until the medium becomes fully saturated, see Figures 1.13 and 1.14. In contrast, Lu et al. (2007) presented quite different results for the P1- and the P2-waves. For P1-wave they demonstrated that the velocity decreases with increase in saturation at first, but when the saturation approaches 40%, it increases with increase in saturation. For P2-wave the velocity increases with increase in saturation, see Figure 1.15.

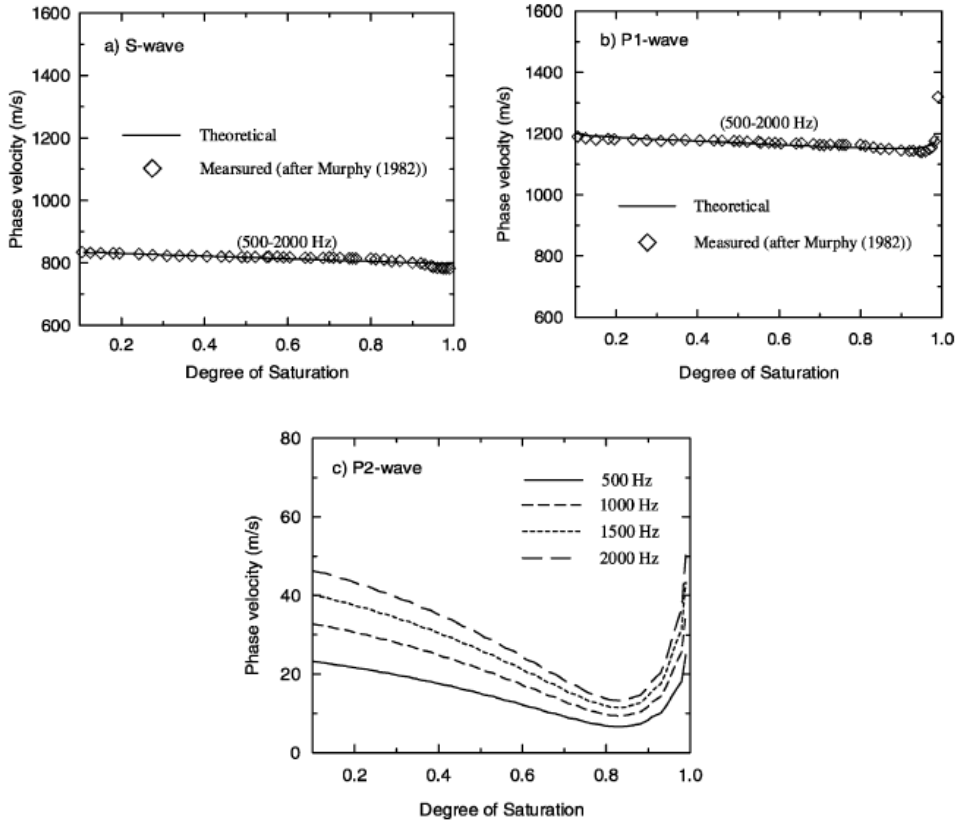

Figure 1.13: Variations of phase velocities with varying degree of saturation for the Massilon sandstone (Wei and Muraleetharan, 2002) .

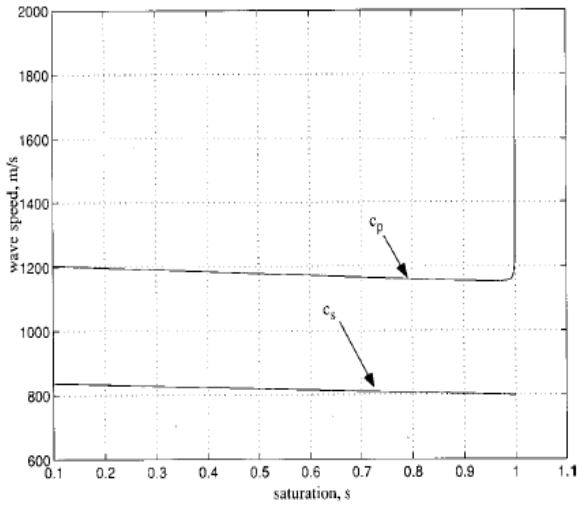

Figure 1.14: Compressional and shear wave speeds (Buckingham, 1999) .

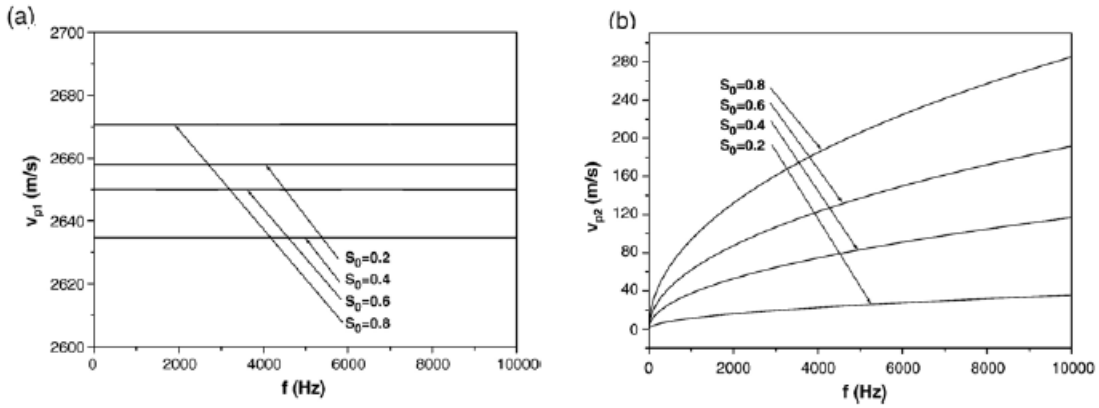

Figure 1.15: Velocities of P1- and P2-waves in porous medium with varying saturation of the wetting phase $S_0 = 0.2, 0.4, 0.6, 0.8$: (a) velocity for the P1-wave (v_{p1}); (b) velocity for the P2-wave (v_{p2}) (Lu et al., 2007) .

Beresnev (2013) compared the phase velocity of P1- and P2-waves as a function of porosity. Figure 1.16 illustrates the influence of porosity on the phase velocity of P-wave.

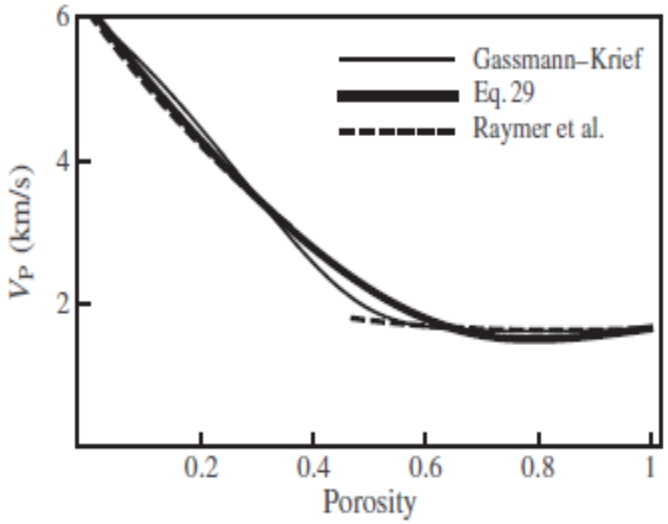

Figure 1.16: Compressional-wave velocity in the porous material, saturated with one fluid, as a function of porosity (Beresnev, 2013) .

1.2 Motivation

This section discusses the factors that motivate this research and the main objectives of the study.

1.2.1 Nikolaevskiy equation

In recent years, the theory of wave propagation in fluid saturated porous media developed very rapidly thanks to the efforts of both theorists and applied modellers. An important equation for such waves, which generated a widespread interest to redistribution of energy over the wave spectrum, is the Nikolaevskiy equation (1989). Based on the rheological model represented in Figure 1.9, Nikolaevskiy (1989) derived the following one-dimensional partial differential equation for the nonlinear longitudinal

seismic waves,

$$\frac{\partial v}{\partial t} + v\frac{\partial v}{\partial x} = \sum_{p=1}^{5} A_{p+1}\frac{\partial^{p+1} v}{\partial x^{p+1}}\,, \tag{1.28}$$

where v is the velocity of the solid matrix and the coefficients A_{p+1} are constants linked to mechanical parameters of the system. The terms in Eq.(1.28) account for the effects of nonlinearity, dissipation and dispersion. By interpretation of Nikolaevskiy (1989), the linear part of Eq. (1.28) describes the dominant frequency in the bounded interval of the oscillation spectrum. Later on, Nikolaevskiy (2008) investigated the effect of global dissipation of the wave described by the damped version of Eq. (1.28),

$$\frac{\partial v}{\partial t} + v\frac{\partial v}{\partial x} + \varsigma v = \sum_{p=1}^{5} A_{p+1}\frac{\partial^{p+1} v}{\partial x^{p+1}}\,. \tag{1.29}$$

In addition to the elastic/seismic systems, the Nikolaevskiy equation was also linked to Rayleigh-Benard convection (Bernoff, 1994), reaction-diffusion systems (Tanaka, 2004; Strunin, 2009; Strunin and Mohammed, 2015). The initial focus within the equation continuing up to the present time, was on the formation and stability of patterns such as stationary rolls, which emerge as a result of linear instability of a spatially uniform state (Beresnev and Nikolaevskiy, 1993; Tribelsky and Velarde, 1996; Matthews and Cox, 2000; Cox and Matthews, 2007; Tribelsky, 2008; Simbawa et al., 2010). Further attention was given to more complex dynamics, especially chaos (Tribelsky and Tsuboi, 1996; Tanaka, 2004; Poon, 2009; Tanaka and Okamura, 2010). In a broader context of earth sciences (Regenauer Lieb et al., 2013), the equation presents an interesting case of multiscale mode coupling. Strunin (2014) suggested an interpretation of dominant frequency, based on the $\lambda(k)$-curve lying entirely below zero but having a local maximum. He argued that any positive section of the $\lambda(k)$-curve would imply self-excitation of motion of the medium, which is impossible because of the absence of internal energy source. He pointed out that a local maximum below the zero level would allow slower decay of certain frequency and this frequency dominates over other frequencies. So far, interest to the equation

was largely due to its capacity to generate self-excited structures, for example rolls. However, solid matrices formed by rocks is an essentially passive system due to the absence of energy supply from inside the system. In other words, rocks cannot self-start moving from the rest, therefore only decaying dynamics have physical sense. For more details, see (Strunin, 2014). The absence of internal sources of energy in the rheological model is obvious from Figures 1.8 and 1.9. As we see from these figures there is no internal energy source in the models. Conversely, there is dissipation generated by the friction pistons. In this study, our main goal is to derive Nikolaevskiy type equations describing the propagation of elastic waves in fluid-saturated porous media including gas bubbles.

1.2.2 Aim and scope of the thesis

In this study our main goal is to explore the dynamics of the seismic waves in the granular medium with gas bubbles. We will explore two different rheological models: the first model is based on the standard linear solid model; the second model is based on the model from (Nikolaevskiy, 1985, 1989). We will derive the 2nd-, 4th- and 6th-order partial differential equations (PDEs) describing the velocity of the solid matrix in the moving reference frame. The equations are linearized to yield the decay rate λ of the wave as a function of the wave number k. Then we will compare the decay rate for the cases with and without the bubbles. Also, we will study the influence of the bubble-related physical parameters, including radius and density, on the decay rate. Lastly, for the special case when there is one neutral mode, we will use the centre manifold theory to describe the dynamics.

1.2.3 Outline of the thesis

This thesis is composed of seven chapters as follows:

Chapter 1: This chapter gives the literature review of elastic waves and motivation. Also, we outline the aims of the current study.

Chapter 2: As a background, we present some basic concepts from dynamics used in the current study.

Chapter 3: We use an extended rheological model relative to the standard linear solid model to derive the 2nd-order PDEs to describe the P-waves with and without bubbles.

Chapter 4: We use an extended rheological model relative to the model of Nikolaevskiy to derive the 4th- and 6th-order PDEs for the waves with and without bubbles.

Chapter 5: This chapter evaluates the decay rates of the wave with the bubbles, based on the literature values of the physical and mechanical parameters of the medium.

Chapter 6: We describe the dynamics of the wave with one neutral mode using the centre manifold theory. We conduct direct computations of the dynamical system for the modes to confirm the results.

Chapter 7: We conclude the thesis by the summery of the main results and present an outlook for future work.

1.3 Concluding remarks

This chapter gave a brief literature review on the wave propagation in porous media and the Biot's theory. The chapter then discussed the motivation for this study including the objectives and specific tasks. Finally, we presented the outline of this thesis.

Chapter 2

General concepts from dynamics

SUMMARY: In this chapter, we describe some basic concepts from dynamics that are used in this thesis.

2.1 Dissipative and conservative systems

Dissipative and conservative dynamical systems are relevant to many interesting and important phenomena in physics, chemistry, and biology. In a dissipative system the energy or phase volume is not preserved but continually decrease (Mukherjee and Poria, 2012; Cimellaro and Marasco, 2018). In contrast, in a conservative system or Hamiltonian system the total energy is preserved (constant) along the trajectories. Generally, a system is called conservative if the divergence of its vector field is zero while, it is dissipative if its vector field has negative divergence (Mukherjee and Poria, 2012; Layek, 2015). The study of dissipative systems is motivated by the fact that many important dynamical and physical systems often depend on input-output properties related to the dissipation and transport of energy. Many important phenomena in physical systems are naturally dissipative. It is dissipative system that is considered in our dissertation. Further classification of dynamical

systems is connected to linearity and nonlinearity. The linear systems whose stored energy remains unchanged or decreases are called Positive Real systems while for the nonlinear systems we usually use the term dissipative in general (Lozano et al., 2013). The dissipative systems exchange energy with its surroundings by the balance between the energy income and outcome (Johnson et al., 2016). The notion of dissipativity arises in physical contexts associated with friction, viscosity, or other forms of dissipation of energy (Wayne, 2012; Strogatz, 2018). All characteristics of open systems that are relevant to analysis and synthesis are based on dissipative systems. Some examples of dissipative dynamical systems are thermodynamic systems, the Belousov-Zhabotinsky (BZ) reaction (polymer systems), mechanical systems with friction, electrical circuits, etc. (Willems, 2007; Socolar, 2007; Hara, 2014). From preceding discussion we recall that the dissipative systems are characterized by the presence of attractors and repellers in the phase space as opposed to conservative systems which do not have attractors (Hadjidemetriou and Voyatzis, 2011).

2.2 Active and passive systems and oscillations

Dissipative systems can be classified into two types: passive and active systems. A system is said to be passive if it does not have any energy sources (Landa, 2013). However, a system is called active if it contains a constant or varying energy source. From the definition above, we can see that the active systems are able to present oscillatory dynamics in the form of self-excited oscillations. Therefore, in active systems self-oscillations are expressed as limit cycles in the phase space. Notably, limit cycle oscillations play a significant role in natural science especially in biology. Nowadays, many biological rhythms can be described by a limit cycle such as circadian rhythms, Calcium oscillations, cell cycle, etc. (Gonze and Kaufman, 2015). The concept of self-oscillations was first introduced by Andronov et al. (2013, first edition 1937). In an autonomous system, he defined self-oscillations as the oscillations satisfying the

following conditions:

1. The amplitude of the oscillations is determined by the properties of the system and not by the initial conditions.

2. The inner forces of the system excite and maintain these oscillations.

In this case the system is called self-oscillating system. For more details on the concept and history of self-oscillations, see (Pechenkin, 2002; Ginoux, 2015; Ginoux and Poincaré, 2017).

The system that does not depend on an initial impulse is called a soft-excitation system, on the other hand, the system is called a hard-excitation system when the self-oscillation arises spontaneously only from an initial impulse of certain amplitude (Rabinovich and Trubetskov, 2012; Borisov and Zverev, 2016).

Of course, the oscillatory dynamic is not the only possible outcome of nonlinear differential equations. The nonlinear dynamical systems can be subdivided into three groups: bistable, excitable, and oscillatory (Mikhailov, 2012; Mikhailov and Loskutov, 2013). The main feature of a bistable system is the existence of two different stable equilibrium states. Excitability is a well known phenomenon and it has applications in various fields. An excitable system has a unique stable attractor or fixed point, but it has two ways of returning to the steady state–monotonic and non-monotonic. For small perturbations away from the equilibrium, the return is monotonic. However, for perturbations beyond a certain threshold amplitude, the return is non-monotonic, and many undergo a large excursion before returning to rest. For the current study, we aim at analyzing the passive system featuring the propagating linear elastic waves in fluid-saturated granular media based on different viscoelastic models.

2.3 Centre manifold theory

This section elaborates the concept of centre manifold and the associated theory following Roberts (1989) and the book of Carr (2012). In the current study it will be used to investigate the dynamics of the neutral mode of seismic wave described by the Nikolaevskiy equation.

2.3.1 Preliminaries

Consider the system

$$\begin{aligned} \frac{dx}{dt} &= Ax + f(x, y)\,, \\ \frac{dy}{dt} &= By + g(x, y)\,, \end{aligned} \tag{2.1}$$

where $x \in R^n$, $y \in R^m$ and A and B are constant matrices such that all the eigenvalues of A are pure imaginary, while all the eigenvalues of B are negative real part.

Definition 1: A curve, $y = h(x)$ defined for $|x|$ small, is called an invariant manifold for the system (2.1), if the solution $(x(t), y(t))$ of (2.1) evaluated at $(x_0, h(x_0))$ lies on the curve $y = h(x)$, that is, $y(t) = h(x(t))$.

Definition 2: Let $y = h(x)$ be a smooth invariant manifold of the system (2.1). Then $h(x)$ is called a centre manifold of the origin if $h(0) = 0$, $h'(0) = 0$. Here, h' is the Jacobian matrix of h.

If f and g are both zero, then

- The system (2.1) has two invariant manifolds, $x = 0$ and $y = 0$. The invariant manifold $x = 0$ is stable manifold, while the invariant manifold $y = 0$ is centre manifold.

- The solutions of the system (2.1) tend exponentially fast, as $t \to \infty$, to solutions of

$$\frac{dx}{dt} = Ax\,.$$

In the centre manifold theory the modes are exponentially quickly attracted to the surface (manifold) and then they evolve slowly. This explains how the center manifold may reduce the dimensionality of the dynamical systems. Now we present the analogue of some results of the centre manifold theory when f and g are non-zero (Watt and Roberts, 1995; Carr, 2012). These results enable us to solve the centre manifold of the system.

Theorem 1: Let $y = h(x)$ is a centre manifold for the system (2.1) such that $|x|$ is small and h is C^2. The evolution on the centre manifold is governed by the n-dimensional system

$$\frac{dy}{dt} = Au + f(u, h(u))\,, \tag{2.2}$$

where u is a new variable to determine the location of the system on the centre manifold. The following theorem contains the information needed to determine the asymptotic behaviour of small solutions of the system (2.1).

Theorem 2:

1. If the zero solution of the system (2.2) is stable, asymptotically stable, or unstable, then the zero solution of the system (2.1) is stable, asymptotically stable, or unstable.

2. If the zero solution of the system (2.2) is stable. Let $(x(t), y(t))$ be a solution of the system (2.1) with small $(x(0), y(0))$. Then there exists a solution $u(t)$ of (2.2), as $t \to \infty$, such that

$$\begin{aligned} x(t) &= u(t) + o(e^{-\gamma t})\,, \\ y(t) &= h(u(t)) + o(e^{-\gamma t})\,, \end{aligned} \tag{2.3}$$

where $\gamma > 0$ is a constant. Let we substitute $y(t) = h(x(t))$ into the second equation in system (2.1), to obtain

$$h'(x)[Ax + f(x, h(x))] = Bh(x) + g(x, h(x)) . \tag{2.4}$$

The equation (2.4) together with the conditions $h(0) = 0$, $h'(0) = 0$ is the system to be solved for the centre manifold. In the next theorem we show that the centre manifold can be approximated to any degree of accuracy. Let function $\phi : R^n \longrightarrow R^m$ which are C^1 in a neighborhood of the origin define

$$M(\phi(x)) = \phi'(x)[Ax + f(x, \phi(x))] - B\phi(x) - g(x, \phi(x)) .$$

Theorem 3: Let $\phi : R^n \longrightarrow R^m$ be a C^1 function of a neighborhood of the origin such that $\phi(0) = 0$ and $\phi'(0) = 0$. If $M(\phi(x)) = o(|x|^q)$, as $x \to 0$ where $q > 0$, then $|h(x) - \phi(x)| = o(|x|^q)$, as $x \to 0$.

2.3.2 Examples

To illustrate the use of the above theorems we give the following examples.

Example 1: Consider the system (Carr, 2012)

$$\begin{aligned} \frac{dx}{dt} &= xy + ax^3 + by^2x , \\ \frac{dy}{dt} &= -y + cx^2 + dx^2y . \end{aligned} \tag{2.5}$$

By theorem 1, the centre manifold of the system (2.5) is $y = h(x)$. To approximate h using the second equation of the system we get

$$M(\phi(x)) = \phi'(x)[x\phi(x) + ax^3 + bx\phi^2(x)] + \phi(x) - cx^2 - dx^2\phi(x) .$$

If $\phi(x) = cx^2$, $M(\phi(x)) = o(x^4)$ then by theorem 3, $h(x) = cx^2 + o(x^4)$. Hence, by theorem 2 the equation which governs the flux is

$$\frac{du}{dt} = uh(u) + au^3 + buh^2(u) = (a + c)u^3 + o(u^5) .$$

Then the zero solution of system (2.5) is asymptotically stable if $a + c < 0$ and unstable if $a + c > 0$. If $a + c = 0$, then we have to get a better approximation to h. Suppose a+c = 0. Let $\phi(x) = cx^2 + \psi(x)$, where $\psi(x) = o(x^4)$. Thus, $M(\phi(x)) = \psi(x) - cdx^4 + o(x^6)$. Therefore, if $\phi(x) = cx^2 + cdx^4$ then $M(\phi(x)) = o(x^6)$ so that by theorem 3, $h(x) = cx^2 + cdx^4 + o(x^6)$. The equation that governs the solution is

$$\frac{du}{dt} = uh(u) + au^3 + buh^2(u) = (cd + bc^2)u^5 + o(u^7)\,.$$

The zero solution of system (2.5) is asymptotically stable if $cd + bc^2 < 0$, and unstable if $cd + bc^2 > 0$. If $cd + bc^2 = 0$, then we have to obtain a better approximation to h.

Example 2: Consider the system (Roberts, 1989)

$$\begin{aligned} \frac{dx}{dt} &= -xy\,, \\ \frac{dy}{dt} &= -y + x^2 - 2y^2\,. \end{aligned} \tag{2.6}$$

The linearized state of the system (2.6), $dx/dt = 0$, $dy/dt = -y$, is characterised by the zero eigenvalue for the slow variable x and the negative eigenvalue, -1, for the fast variable y. According to Roberts (1989) it can be shown that all trajectories of system (2.6) are attracted to the parabola

$$y = x^2 \tag{2.7}$$

called the centre manifold, Figure 2.1. If it was not for the nonlinear perturbative terms $x^2 - 2y^2$, the variable y would quickly fall onto the equilibrium state $y = 0$ (the analogue to quickly decaying vertical non-uniformities under diffusion) while x would stay in the neutral state $x = const$ (analogue of the neutral state of constant concentration). For the full system (2.6) the trajectories drop onto the manifold or attractor, Eq. (2.7), on which the perturbation, $x^2 - 2y^2$ is comparable to the linear term,$-y$. On the manifold the motion is slow and described by $dx/dt = -xy$, where $y = x^2$ so that

$$\frac{dx}{dt} = x^3 \tag{2.8}$$

On the manifold the variable y depends on t via x to which it is connected by Eq. (2.7).

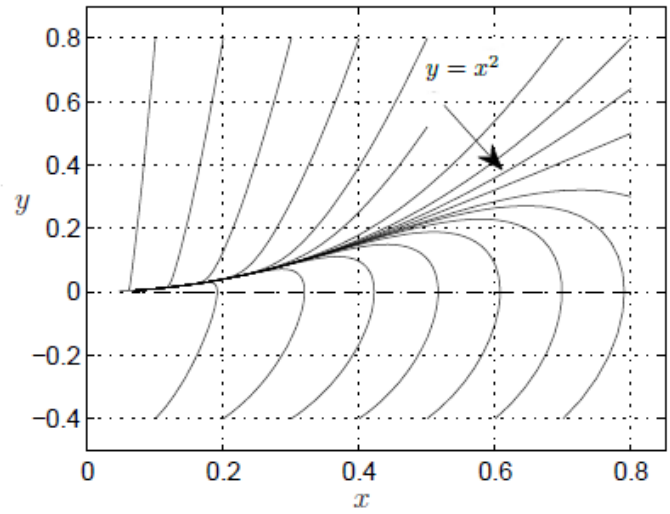

Figure 2.1: Attraction of the trajectories to parabola $y = x^2$ is system (2.6) (Roberts, 1989) .

2.4 Concluding remarks

This chapter discussed essential concepts of the current work. These include dissipative and conservative systems, active and passive systems and oscillations, and then centre manifold theory.

Chapter 3

Simple rheology and decay rate for P1 waves in porous granular media with gas bubbles

SUMMARY: In this chapter we study the effect of using different rheological models when describing Frenkel-Biot elastic waves of P1-type in porous media. Two rheological models are considered – one with the bubbles and the other without. The bubble-including model consists of segments representing the solid continuum and bubbles inside the fluid, while the bubble-free model is represented by the standard solid-fluid rheological model. We derive the dispersion relations for the wave equations in their linear forms and analyzed the decay rate, λ, versus the wave number, k. We compare the $\lambda(k)$-dependence for the two rheologies under consideration using typical values of the mechanical parameters of the model. We observe, in particular, that an increase of the radius and the number of the bubbles leads to an increase in the decay rate.

3.1 Introduction

The problem of elastic wave propagation through the liquid-saturated granular medium containing gas bubbles was studied in many theoretical works started by (Silberman, 1957; Wijngaarden, 1968, 1972; Nakoryakov et al., 1972). The gas bubbles represent one of the key physical factors in liquid-saturated porous systems, and naturally attract significant attention from the researchers in mechanics and physics. Of particular interest, due to their geophysical and industrial applications and because of theoretical importance, are the wave phenomena in such media and the influence on the wave characteristics by the interaction between the bubbles, fluid and solid (Anderson and Hampton, 1980; Commander and Prosperetti, 1989; Watanabe and Prosperetti, 1994; Matsumoto and Kameda, 1996; Dunin and Nikolaevskiy, 2005; Kudryashov and Sinelshchikov, 2014; Ali and Strunin, 2019; Thiessen and Cheviakov, 2019). These studies showed that the presence of the bubbles substantially affects the properties of the waves such as the velocity and attenuation.

This chapter studies the influence of different rheologies including the bubbles on the wave attenuation in the liquid-saturated porous media. We will use an extended stress-strain relation relative to the standard linear solid model to take into account the bubbles in modelling the P-type waves. Dunin et al. (2006) used the simple stress-strain relation, $\sigma = Ee$, in such modelling, while Nikolaevskiy (1989, 2008) used a considerably complicated stress-strain relation that involves higher-order time derivatives of the stress σ and strain e. This relation is the result of the rheological model shown in Figure 3.1. Eventually it leads to a higher-order partial differential equation with respect to the velocity of the solid matrix. However, the original rheological model (Nikolaevskiy, 1989) does not include gas bubbles. Nikolaevskiy and Strunin (2012) pointed out the place in this model that the bubbles should take, see Figure 3.2.

In the present work we aim to include the bubble into the rheological model and de-

rive the P-wave equations, where the coefficients will depend on the bubble-related parameters. We will investigate the influence of the bubble-related parameters, including their radius and concentration, on the decay rate.

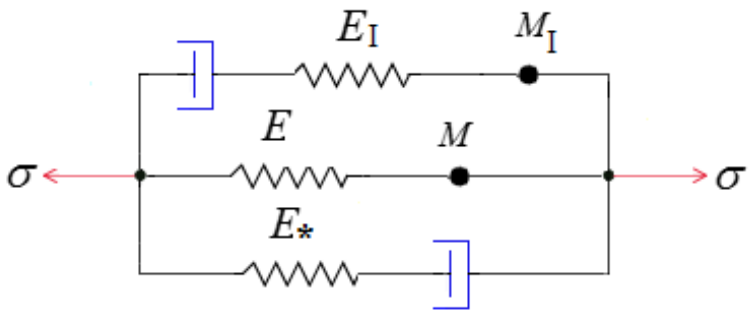

Figure 3.1: Three–branch rheological scheme from (Nikolaevskiy, 1989) .

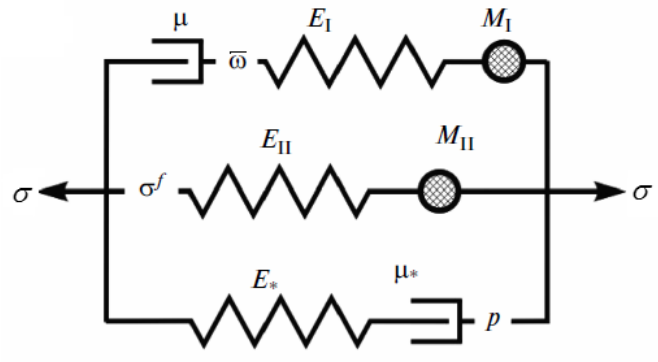

Figure 3.2: The modified rheological scheme relative to Figure 3.1. It shows the position of the bubble-representing element ϖ, which may generally include spring, mass and friction piston (Nikolaevskiy and Strunin, 2012) .

3.2 Basic equations of motion

3.2.1 Conservation of mass and momentum

For a one-dimensional case the momentum and mass balance equations (Nikolaevskiy, 1990) are

$$\begin{aligned}
\frac{\partial}{\partial t}(1-m)\rho^{(s)}v + \frac{\partial}{\partial x}(1-m)\rho^{(s)}vv &= \frac{\partial}{\partial x}\sigma - (1-m)\frac{\partial p}{\partial x} - I\,, \\
\frac{\partial}{\partial t}m\rho^{(f)}u + \frac{\partial}{\partial x}m\rho^{(f)}uu &= -m\frac{\partial p}{\partial x} + I\,, \\
\frac{\partial}{\partial t}(1-m)\rho^{(s)} + \frac{\partial}{\partial x}(1-m)\rho^{(s)}v &= 0\,, \\
\frac{\partial}{\partial t}m\rho^{(f)} + \frac{\partial}{\partial x}m\rho^{(f)}u &= 0\,,
\end{aligned} \tag{3.1}$$

where, the subscripts s and f label the solid and gas-liquid mixture respectively, ρ, v, and u are the corresponding densities and mass velocities, m is the porosity, σ is the true stress, p is the pore pressure, and I is the interfacial viscous force approximated by

$$I = \delta m(v-u), \quad \delta = \frac{\mu^{(f)}m}{\ell}\,,$$

where $\mu^{(f)}$ is the gas-liquid mixture viscosity and ℓ is the intrinsic permeability.

Now we add to the system (3.1) the equation of the dynamics of a bubble (Dontsov et al., 1987)

$$R\frac{\partial^2}{\partial t^2}R + \frac{3}{2}\left(\frac{\partial}{\partial t}R\right)^2 + \frac{4\mu}{\rho^{(L)}}\left(\frac{1}{R} + \frac{m}{4\ell}R\right)\frac{\partial}{\partial t}R = (p_g - p)/\rho^{(L)}\,, \tag{3.2}$$

where R is the bubble radius, p is the pressure in the liquid, $p_g = p_0(R_0/R)^\chi$ is the gas pressure inside the bubble (here $\chi = 3\varsigma$, ς is the adiabatic exponent), $\rho^{(L)}$ is the density of the liquid without the bubbles, and μ is the viscosity of the liquid without the bubbles. The density equations for the solid and liquid without gas are

$$\rho^{(s)} \;=\; \rho_0^{(s)}(1 - \beta^{(s)}\sigma)\,, \tag{3.3}$$

$$\rho^{(L)} = \rho_0^{(L)}(1 + \beta^{(L)}p)\,. \tag{3.4}$$

The mean density of the gas-liquid mixture is

$$\rho^{(f)} = (1 - \phi)\rho^{(L)} + \phi\rho^{(g)}, \tag{3.5}$$

where

$$\phi = (4\pi/3)R^3 n_0\,.$$

Here σ is the stress, ϕ is the volume gas content and n_0 is the number density of the bubbles per unit volume. In Eq. (3.5) we can neglect the density of the gas $\rho^{(g)}$ due to the low gas content. The change in ϕ is due to the change in the bubble radius R. Then Eq. (3.5) becomes

$$\rho^{(f)} = \rho_0^{(L)}(1 + \beta^{(L)}p)\Big(1 - \frac{4\pi}{3}R_0^3 n_0\Big)\,. \tag{3.6}$$

Similarly to Dunin et al. (2006) we also assume that the pore pressure p is equal to the pressure in the liquid far from the bubble.

3.2.2 Rheological model

In this section we consider a simplified rheological model compared to Figure 3.1 and Figure 3.2. It includes three elastic springs with the elastic moduli E_1, E_2, and E_3, and one dashpot with viscosity μ as shown in Figure 3.3. Applying the Newton's law, this model generates the following equations

$$\begin{aligned} &e = e_2 = e_1 + e_3 + e_4\,,\\ &E_3 e_3 - \mu\frac{de_4}{dt} = 0\,,\\ &E_1 e_1 - E_3 e_3 = 0\,,\\ &E_1 e_1 + E_2 e_2 = \sigma\,. \end{aligned} \tag{3.7}$$

Using system (3.7) we arrive at the following matrix system

$$\begin{bmatrix} E_2 & E_1 & 0 & 0 & 0 & 0 & 0 \\ 0 & 0 & 0 & 0 & E_1 & 0 & 0 \\ 0 & 0 & E_3 & 0 & 0 & 0 & -\mu \\ -1 & 1 & 1 & 1 & 0 & 0 & 0 \\ 0 & 0 & 0 & 0 & 1 & 1 & 1 \\ 0 & E_1 & -E_3 & 0 & 0 & 0 & 0 \\ 0 & 0 & 0 & 0 & E_1 & -E_3 & 0 \end{bmatrix} \begin{bmatrix} e \\ e_1 \\ e_3 \\ e_4 \\ \frac{de_1}{dt} \\ \frac{de_3}{dt} \\ \frac{de_4}{dt} \end{bmatrix} = \begin{bmatrix} \sigma \\ \frac{d\sigma}{dt} - E_2 \frac{de}{dt} \\ 0 \\ 0 \\ \frac{de}{dt} \\ 0 \\ 0 \end{bmatrix} . \tag{3.8}$$

Solving system (3.8) for e we get

$$e = \frac{-((E_1 + E_3)E_2 + E_1E_3)\mu\frac{de}{dt} + E_1E_3\sigma + (E_1 + E_3)\mu\frac{d\sigma}{dt}}{E_1E_2E_3} . \tag{3.9}$$

Equation (3.9) leads to the following stress-strain relation

$$\sigma + b_1\frac{d\sigma}{dt} = E_2e + a_1\frac{de}{dt} , \tag{3.10}$$

where $a_1 = ((E_1 + E_3)E_2 + E_1E_3)\theta$, $b_1 = (E_1 + E_3)\theta$, and $\theta = \mu/E_1E_3$.

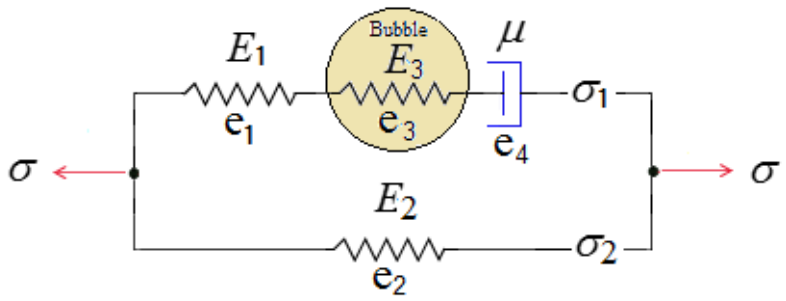

Figure 3.3: A simplified rheological scheme including the bubble .

The system of equations (3.1)- (3.10) is closed by the relation between the deformation e and the velocity of the solid v,

$$\frac{De}{Dt} \equiv \frac{\partial e}{\partial t} + v\frac{\partial e}{\partial x} = \frac{\partial v}{\partial x} . \tag{3.11}$$

3.3 Propagation of P1-waves including gas bubbles

We consider the slowly varying wave in space and time. Accordingly we use the running coordinate system with simultaneous scale change,

$$\begin{aligned} &\xi = \varepsilon(x - ct)\,, \qquad \tau = \frac{1}{2}\varepsilon^2\, t\,, \\ &\frac{\partial}{\partial x} = \varepsilon\frac{\partial}{\partial \xi}\,, \qquad \frac{\partial}{\partial t} = \varepsilon\left(\frac{1}{2}\varepsilon\frac{\partial}{\partial \tau} - c\frac{\partial}{\partial \xi}\right)\,, \end{aligned} \tag{3.12}$$

where ε is the small parameter. Thus, the constitutive law (3.10) transforms into the following form

$$\sigma + b_1\,\varepsilon\left(\frac{1}{2}\varepsilon\frac{\partial}{\partial \tau} + (v-c)\frac{\partial}{\partial \xi}\right)\sigma = E_2 e + a_1\,\varepsilon\left(\frac{1}{2}\varepsilon\frac{\partial}{\partial \tau} + (v-c)\frac{\partial}{\partial \xi}\right) e\,. \tag{3.13}$$

Now, we seek the unknown functions as power series

$$\begin{aligned} &v = \varepsilon v_1 + \varepsilon^2 v_2 + \dots\,, && u = \varepsilon u_1 + \varepsilon^2 u_2 + \dots\,, \\ &\sigma = \sigma_0 + \varepsilon\sigma_1 + \varepsilon^2\sigma_2 \dots\,, && p = p_0 + \varepsilon p_1 + \varepsilon^2 p_2 \dots\,, \\ &m = m_0 + \varepsilon m_1 + \varepsilon^2 m_2 \dots\,, && e = e_0 + \varepsilon e_1 + \varepsilon^2 e_2 \dots\,, \\ &\phi = \phi_0 + \varepsilon\phi_1 + \varepsilon^2\phi_2 \dots\,, && R = R_0(1 + \varepsilon R_1 + \varepsilon^2 R_2 \dots)\,. \end{aligned} \tag{3.14}$$

3.3.1 First approximation

Using Eqs. (3.14), we collect the linear terms $\sim \varepsilon$ in Eqs. (3.1), (3.2), (3.11) and (3.13) to get

$$\begin{gathered}
\rho_0^{(s)} c\frac{\partial m_1}{\partial \xi} - (1-m_0)c\frac{\partial \rho_1^{(s)}}{\partial \xi} + (1-m_0)\rho_0^{(s)}\frac{\partial v_1}{\partial \xi} = -\frac{1}{2}(1-m_0)\frac{\partial \rho_0^{(s)}}{\partial \tau}\,, \\
-m_0 c\frac{\partial \rho_1^{(f)}}{\partial \xi} - \rho_0^{(f)} c\frac{\partial m_1}{\partial \xi} + m_0\rho_0^{(f)}\frac{\partial u_1}{\partial \xi} = -\frac{1}{2}m_0\frac{\partial \rho_0^{(f)}}{\partial \tau}\,, \\
-(1-m_0)\rho_0^{(s)} c\frac{\partial v_1}{\partial \xi} = \frac{\partial \sigma_1}{\partial \xi} - (1-m_0)\frac{\partial p_1}{\partial \xi}\,, \\
-m_0\rho_0^{(f)} c\frac{\partial u_1}{\partial \xi} = -m_0\frac{\partial p_1}{\partial \xi},\ \ \mu c\left[\frac{4}{R_0} + \frac{m_0 R_0}{\ell}\right]\frac{\partial R_0}{\partial \xi} = (p_0\,\chi\,R_1 + p_1)\,, \\
\frac{1}{2}\frac{\partial e_0}{\partial \tau} - c\frac{\partial e_1}{\partial \xi} + v_1\frac{\partial e_0}{\partial \xi} = \frac{\partial v_1}{\partial \xi}\,,\ \ \sigma_1 - E_2\,e_1 = -a_1 c\frac{\partial e_0}{\partial \xi} + b_1 c\frac{\partial \sigma_0}{\partial \xi}\,.
\end{gathered} \tag{3.15}$$

Further,

$$\begin{gathered}
\rho_1^{(s)} = -\rho_0^{(s)}\beta^{(s)}\sigma_1\,, \\
\rho_1^{(f)} = \rho_0^{(L)}\left(\beta^{(L)}\kappa_1 p_1 - 4\pi n_0\kappa_2 R_0^3 R_1\right)\,, \\
\rho_0^{(f)} = \kappa_1\kappa_2\rho_0^{(L)}\,,
\end{gathered} \tag{3.16}$$

where

$$\kappa_1 = 1 - \frac{4\pi}{3}R_0^3\,n_0\,,\ \kappa_2 = 1 + \beta^{(L)}p\,.$$

Inserting Eqs. (3.16) into the system (3.15) gives the following integrals,

$$\begin{gathered}
(1-m_0)\rho_0^{(s)}v_1 + c(1-m_0)\rho_0^{(s)}\beta^{(s)}\sigma_1 + c\rho_0^{(s)}m_1 = 0\,, \\
m_0\rho_0^{(L)}\kappa_1\kappa_2 u_1 - c\rho_0^{(L)}\kappa_1\kappa_2 m_1 - cm_0\kappa_1\rho_0^{(L)}\beta^{(L)}p_1 + 4c\kappa_2\rho_0^{(L)}\pi\,n_0 m_0 R_0^3\,R_1 = 0\,, \\
c(1-m_0)\rho_0^{(s)}v_1 + \sigma_1 - (1-m_0)p_1 = 0\,,\quad c\kappa_1\kappa_2 m_0\rho_0^{(L)}u_1 - m_0 p_1 = 0\,, \\
ce_1 + v_1 = 0,\quad \sigma_1 - E_2\,e_1 = 0,\quad p_1 + p_0\,\chi\,R_1 = 0\,.
\end{gathered} \tag{3.17}$$

Now we have seven equations with seven unknowns: v_1, u_1, p_1, σ_1, m_1, R_1, and e_1. In order to find the velocity of the wave from the system (3.17) we require that

$$\det(a_{nm}) = 0\,, \tag{3.18}$$

where

$$a_{11} = c(1-m_0)\rho_o^{(s)}\,,\ a_{12} = 0\,,\ a_{13} = (1-m_0)\,,\ a_{14} = 1\,,\ a_{15} = 0\,,\ a_{16} = 0\,,\ a_{17} = 0\,,$$

$$a_{21} = 0\,,\ a_{22} = c\kappa_1\kappa_2 m_0\rho_0^{(L)}\,,\ a_{23} = -m_0\,,\ a_{24} = 0\,,\ a_{25} = 0\,, a_{26} = 0\,,\ a_{27} = 0\,,$$

$$a_{31} = (1-m_0)\,,\ a_{32} = 0\,,\ a_{33} = 0\,,\ a_{34} = c\beta^s(1-m_0)\,,\ a_{35} = c\,,\ a_{36} = 0\,,\ a_{37} = 0\,,$$

$$a_{41} = 0\,,\ a_{42} = \kappa_1\kappa_2 m_0\,,\ a_{43} = -c\kappa_1\beta^{(L)}m_0\,,\ a_{44} = 0\,,\ a_{45} = -c\kappa_1\kappa_2\,, m_0 n_o R_0\,,$$

$$a_{46} = 4c\kappa_2\pi\,,\ a_{47} = 0\,,\ a_{51} = 1\,,\ a_{52} = 0\,,\ a_{53} = 0\,,\ a_{54} = 0\,,\ a_{55} = 0\,,\ a_{56} = 0\,,\ a_{57} = c\,,$$

$$a_{61} = 0\,,\ a_{62} = 0\,,\ a_{63} = 0\,, a_{64} = 1\,,\ a_{65} = 0\,,\ a_{66} = 0\,,\ a_{67} = -E_2\,,$$

$$a_{71} = 0\,,\ a_{72} = 0\,,\ a_{73} = 1\,,\ a_{74} = 0\,,\ a_{75} = 0\,,\ a_{76} = \chi p_0\,,\ a_{77} = 0\,.$$

This gives

$$\begin{aligned} &c^4\left[m_0(1-m_0)\rho_0^{(s)}\rho_0^{(L)}\left(\kappa_1\chi\beta^{(L)}p_0 + 4\kappa_2\pi n_0 R_0^3\right)\right] \\ -c^2&\left[\rho_0^{(L)}\Big(\kappa_1\chi p_0(\kappa_2(1-E_2\beta^{(s)})(-1+m_0)^2 + E_2\beta^{(L)}m_0) + 4E_2\kappa_2\pi m_0 n_0 R_0^3\Big)\right. \\ &\left.+\chi(1-m_0)m_0 p_0\rho_0^{(s)}\right] + E_2\chi m_0 p_0 = 0\,. \end{aligned} \tag{3.19}$$

From equation (3.19) we find the velocity of the wave with the bubbles,

$$c^2 = \frac{-\beta_1 \pm \sqrt{\beta_1^2 - 4\alpha_1\gamma_1}}{2\alpha_1}\,, \tag{3.20}$$

where

$$\begin{aligned} \alpha_1 &= m_0(1-m_0)\rho_0^{(s)}\rho_0^{(L)}\left(\kappa_1\chi\beta^{(L)}p_0 + 4\kappa_2\pi n_0 R_0^3\right)\,, \\ \beta_1 &= -\left[\rho_0^{(L)}\Big(\kappa_1\chi p_0(\kappa_2(1-E_2\beta^{(s)})(-1+m_0)^2 + E_2\beta^{(L)}m_0)\right. \\ &\left.+4E_2\kappa_2\pi m_0 n_0 R_0^3\Big) + \chi(1-m_0)m_0 p_0\rho_0^{(s)})\right]\,, \\ \gamma_1 &= E_2 m_0\chi p_0\,. \end{aligned}$$

Thus, all the variables are expressed through any one selected variable, for example, the velocity v_1. From the last three equations of system (3.17), we have

$$e_1 = -\frac{v_1}{c}, \quad \sigma_1 = -E_2\,\frac{v_1}{c}, \quad p_1 = -p_0\,\chi\,R_1\,. \tag{3.21}$$

Substituting of σ_1, and p_1 into the remaining equations of the system (3.17), we obtain

$$(1-m_0)\rho_0^{(s)}v_1 - E_2(1-m_0)\rho_0^{(s)}\beta^{(s)}v_1 + c\rho_0^{(s)}m_1 = 0\,. \tag{3.22}$$

$$m_0u_1 - cm_1 + \left(\frac{p_0\,\chi\beta^{(L)}}{\kappa_2} + \frac{4\pi\,n_0R_0^3}{\kappa_1}\right)cm_0\,R_1 = 0\,. \tag{3.23}$$

$$c(1-m_0)\rho_0^{(s)}v_1 - \frac{E_2}{c}v_1 + (1-m_0)p_0\,\chi\,R_1 = 0\,. \tag{3.24}$$

$$c\kappa_1\kappa_2m_0\rho_0^{(L)}u_1 + m_0p_0\,\chi\,R_1 = 0\,. \tag{3.25}$$

Equation (3.22) gives

$$m_1 = -(1-m_0)(1-E_2\beta^{(s)})\frac{v_1}{c}\,. \tag{3.26}$$

Then from Eq. (3.24) we get

$$R_1 = -\left(\frac{c^2(1-m_0)\rho_0^{(s)} - E_2}{(1-m_0)p_0\,\chi}\right)\frac{v_1}{c}\,. \tag{3.27}$$

Substituting Eq. (3.27) into the value of p_1 from Eq. (3.21), leads to

$$p_1 = \left(\frac{c^2(1-m_0)\rho_0^{(s)} - E_2}{(1-m_0)}\right)\frac{v_1}{c}\,. \tag{3.28}$$

Moreover, we derive the proportionality between v_1 and u_1 as

$$u_1 = \left(\frac{c(1-m_0)\rho_0^{(s)} - \frac{E_2}{c}}{\kappa_1\kappa_2\rho_0^{(L)}(1-m_0)}\right)\frac{v_1}{c}\,. \tag{3.29}$$

3.3.2 Second approximation

In the second approximation for the full system we have

$$
\begin{gathered}
\frac{\partial}{\partial\xi}\left((1-m_0)v_2+c(1-m_0)\beta^{(s)}\sigma_2+cm_2\right)=\Lambda^{(s)}\,,\\
\frac{\partial}{\partial\xi}\left(m_0u_2-\left[m_2+\frac{m_0\beta^{(L)}p_2}{\kappa_2}-\frac{4\pi\,m_0\,n_0R_0^3(R_2+R_1^2)}{\kappa_1}\right.\right.\\
\left.\left.+\frac{4\pi\,m_0\,n_0R_0^3\,p_0\,\chi\,\beta^{(L)}R_1^2}{\kappa_1\kappa_2}\right]c\right)=\Lambda^{(L)}\,,\\
\frac{\partial}{\partial\xi}\left(c(1-m_0)\rho_0^{(s)}v_2+\sigma_2-(1-m_0)p_2\right)=\Sigma_1\,,\\
\frac{\partial}{\partial\xi}\left(c\kappa_1\kappa_2m_0\rho_0^{(L)}u_2-m_0p_2\right)=\Sigma_2\,,\\
\frac{\partial}{\partial\xi}\left(p_1+p_0\,\chi\,R_1\right)=\frac{\partial\Gamma}{\partial\xi},\quad\frac{\partial}{\partial\xi}\left(ce_2+v_2\right)=F\,,\\
\frac{\partial}{\partial\xi}\left(\sigma_2-E_2\,e_2\right)=\frac{\partial T}{\partial\xi}\,,
\end{gathered}
\tag{3.30}
$$

where

$$
\begin{gathered}
\Lambda^{(s)}=\frac{1}{2}\frac{\partial}{\partial\tau}\left[(m_1+\,(1-m_0)\beta^{(s)}\sigma_1)\right]\,,\\
\Lambda^{(L)}=-\frac{1}{2}\frac{\partial}{\partial\tau}\left[\kappa_1\left(m_1\kappa_2+m_0\beta^{(L)}p_1\right)-4\pi n_0\kappa_2R_0^3R_1\right],\\
\Sigma_1=(1-m_0)\rho_0^{(s)}\frac{1}{2}\frac{\partial v_1}{\partial\tau}\,,\ \Sigma_2=m_0\rho_0^{(f)}\frac{1}{2}\frac{\partial u_1}{\partial\tau}\,,\\
\Gamma=\mu c\left(4+\frac{m_0R_0^2}{\ell}\right)\frac{\partial R_1}{\partial\xi}\,,\ F=-\frac{1}{2c}\frac{\partial v_1}{\partial\tau}\,,\\
T=-a_1c\frac{\partial e_1}{\partial\xi}+b_1c\frac{\partial\sigma_1}{\partial\xi}\,.
\end{gathered}
$$

The determinant of the left-hand side of the system (3.30) coincides with the determinant of (3.18), which equals zero. Therefore, a non-zero solution for v_2 exists only if the following compatibility condition takes place,

$$
\det(b_{nm})=0\,,
\tag{3.31}
$$

where

$$
b_{11}=\frac{\partial T}{\partial\xi}\,,\ b_{12}=0\,,\ a_{13}=0\,,\ b_{14}=1\,,\ b_{15}=0\,,\ b_{16}=0\,,\ b_{17}=-E_2\,,
$$

$$b_{21} = \Sigma_1\,,\; b_{22} = 0\,,\; b_{23} = (1-m_0)\,,\; b_{24} = 1\,,\; b_{25} = 0\,,\; b_{26} = 0\,,\; b_{27} = 0\,,$$

$$b_{31} = \Sigma_2\,,\; b_{32} = c\kappa_1\kappa_2 m_0 \rho_0^{(L)}\,,\; a_{33} = -m_o\,,\; b_{34} = 0\,,\; b_{35} = 0\,,\; b_{36} = 0\,,\; b_{37} = 0\,,$$

$$b_{41} = \frac{\partial \Gamma}{\partial \xi}\,,\; b_{42} = 0\,,\; b_{43} = 1\,,\; b_{44} = 0\,,\; b_{45} = 0\,,\; b_{46} = \chi p_0\,,\; b_{47} = 0\,,$$

$$b_{51} = F\,, b_{52} = 0\,,\; b_{53} = 0\,,\; b_{54} = 0\,,\; b_{55} = 0\,,\; b_{56} = 0\,,\; b_{57} = c\,,$$

$$b_{61} = \Lambda^{(s)}\,,\; b_{62} = 0\,,\; b_{63} = 0\,,\; b_{64} = c(1-m_0)\beta^{(s)}\,,\; b_{65} = c\,,\; b_{66} = 0\,,\; b_{67} = 0\,,$$

$$b_{71} = \Lambda^{(L)}\,,\; b_{72} = m_0\,,\; b_{73} = -\frac{c\beta^{(L)} m_0}{\kappa_2}\,,\; b_{74} = 0\,,$$

$$b_{75} = -c\,,\; b_{76} = \frac{4c\pi m_0 n_0 R_0^3}{\kappa_1}\,,\; b_{77} = 0\,.$$

This gives the evolution equation for $v \cong v_1$

$$\begin{aligned}
&\chi\Big(c\Sigma_2 + \Big(E_2F - c\Big(\Sigma_1 + \Sigma_2 - \frac{\partial T}{\partial \xi}\Big)\Big)m_0\Big)p_0 + c^2\Big[- 4\kappa_2\pi m_0\Big(E_2F - c\Big(\Sigma_1 \\
&- \frac{\partial T}{\partial \xi} + \frac{\partial \Gamma}{\partial \xi}\Big) + c\frac{\partial \Gamma}{\partial \xi}m_0\Big)n_o R_0^3 + \kappa_1\chi p_0\Big(\Big(- E_2F - c\Big(\frac{\partial T}{\partial \xi} - \Sigma_1\Big)\Big)\beta^{(L)}m_0 \\
&- \kappa_2(1-m_0)\Big(\Big(E_2F + c\frac{\partial T}{\partial \xi}\Big)\beta^{(s)}(-1+m_0) + \Lambda^{(L)} + \Lambda^{(s)}\Big)\Big)\Big]\rho_0^{(L)} = 0\,.
\end{aligned} \tag{3.32}$$

We re-write equation (3.32) in terms of v and re-arrange with the help of Mathematica software,

$$\begin{aligned}
&\frac{1}{2}\Big[c(1-m_0)\rho_0^{(s)}\,\Upsilon_1 + c\,\Upsilon_2 + c^2\kappa_1\kappa_2\chi p_0\rho_0^{(L)}((1-m_0)^2 - \Upsilon_3) - E_2\Upsilon_4\Big]\frac{\partial v}{\partial \tau} \\
&\qquad + c^2\left[\Upsilon_4(a_1 - b_1E_2) - 4\Upsilon_5\right]\frac{\partial^2 v}{\partial \xi^2} + c\,\Upsilon_6\,\frac{\partial v v}{\partial \xi} = 0\,,
\end{aligned} \tag{3.33}$$

where

$$\Upsilon_1 = cm_0\big(- \chi p_0 + c^2\rho_0^{(L)}(\kappa_1\chi p_0\beta^{(L)} + 4\kappa_2\pi n_0 R_0^3)\big)\,,$$

$$\Upsilon_2 = \chi p_0 m_0\Big(c(1-m_0)\rho_0^{(s)} - \frac{E_2}{c}\Big)\,,$$

$$\Upsilon_3 = \kappa_1\kappa_2(1-m_0)^2(1-E_2\beta^{(s)}) - (c^2(1-m_0)\rho_0^{(s)} - E_2)(\kappa_1 m_0\rho_0^{(L)} + 4\kappa_2\pi n_0 R_0^3)\,,$$

$$\Upsilon_4 = p_0\,\chi m_0 + c^2\rho_0^{(L)}\Big(\kappa_1 p_0\,\chi\big(\kappa_2\beta^{(s)}(-1+m_0)^2 - \beta^{(L)}m_0\big) - 4\pi n_0 m_0\kappa_2 R_0^3\Big)\,,$$

$$\Upsilon_5 = c^2\pi n_0 m_0\kappa_2 R_0^3\rho_0^{(L)}\mu\big(4 + \frac{m_0R_0^2}{\ell}\big)\Big(\frac{c^2(1-m_0)\rho_0^{(s)} - E_2}{p_0\,\chi}\Big)$$

and Υ_6 is the nonlinearity coefficient, which we do not present here because our further analysis focuses on the linear part of equation (3.33).

Finally, we re-write the wave equation (3.33) as

$$A_1\frac{\partial v}{\partial \tau} + A_2\frac{\partial^2 v}{\partial \xi^2} + A_N\frac{\partial vv}{\partial \xi} = 0\,, \tag{3.34}$$

where

$$A_1 = \frac{1}{2}\left[c(1-m_0)\rho_0^{(s)}\,\Upsilon_1 + c\,\Upsilon_2 + c^2\kappa_1\kappa_2\chi p_0\rho_0^{(L)}((1-m_0)^2 - \Upsilon_3) - E_2\Upsilon_4\right]\,,$$

$$A_2 = c^2\left[\Upsilon_4(a_1 - b_1E_2) - 4\Upsilon_5\right],\; A_N = c\,\Upsilon_6\;.$$

3.4 P1-waves without gas bubbles

3.4.1 Rheological model

By removing one elastic spring segment, which represents the gas bubble, from the rheological model in Figure 3.3 we get Figure 3.4, for which we derive the following constitutive law (Findley and Davis, 2013),

$$\sigma + b_1\frac{d\sigma}{dt} = E_2 e + a_1\frac{de}{dt}\,, \tag{3.35}$$

where $a_1 = (E_1 + E_2)\theta,\; b_1 = \theta,\;\; \theta = \mu/E_1$. This equation was discussed in detail in Chapter 1.

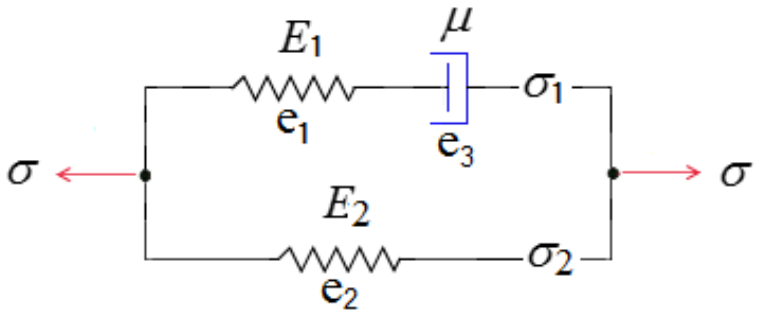

Figure 3.4: Rheological scheme without gas bubble.

3.4.2 The equations of dynamics

In the case without the bubbles, the equations of motion reduce to the six equations

$$\begin{gathered}
\frac{\partial}{\partial t}(1-m)\rho^{(s)} + \frac{\partial}{\partial x}(1-m)\rho^{(s)}v = 0\,, \\
\frac{\partial}{\partial t}m\rho^{(L)} + \frac{\partial}{\partial x}m\rho^{(L)}u = 0\,, \\
\frac{\partial}{\partial t}(1-m)\rho^{(s)}v + \frac{\partial}{\partial x}(1-m)\rho^{(s)}vv = \frac{\partial \sigma}{\partial x} - (1-m)\frac{\partial p}{\partial x} - I\,, \\
\frac{\partial}{\partial t}m\rho^{(L)}u + \frac{\partial}{\partial x}m\rho^{(L)}uu = -m\frac{\partial p}{\partial x} + I\,, \\
\sigma + b_1\frac{d\sigma}{dt} = E_2 e + a_1\frac{de}{dt}\,, \\
\frac{De}{Dt} \equiv \frac{\partial e}{\partial t} + v\frac{\partial e}{\partial x} = \frac{\partial v}{\partial x}\,.
\end{gathered} \tag{3.36}$$

The density equation (3.3) for the solid remains unchanged, but for the gas-liquid mixture we neglect the volume gas content ϕ in equation (3.5),

$$\rho^{(f)} = \rho^{(L)} = \rho_0^{(L)}(1+\beta^{(L)}p)\,. \tag{3.37}$$

3.4.3 First approximation

The linear terms in the order $\sim \varepsilon$ in system (3.36)

$$\begin{gathered}
c(1-m_0)\rho_0^{(s)}v_1 + \sigma_1 - (1-m_0)p_1 = 0\,, \\
m_0u_1 - cm_1 - cm_0\beta^{(L)}p_1 = 0\,, \\
(1-m_0)v_1 + c(1-m_0)\beta^{(s)}\sigma_1 + cm_1 = 0\,,\ cm_0\rho_0^{(L)}u_1 - m_0p_1 = 0\,, \\
\sigma_1 - E_2\,e_1 = 0\,, \quad ce_1 + v_1 = 0\,.
\end{gathered} \tag{3.38}$$

In system (3.38), to find the velocity c we require

$$\det(a_{nm}) = 0\,, \tag{3.39}$$

where

$$a_{11} = c(1-m_0)\rho_0^{(s)}\,,\ a_{12} = 0\,,\ a_{13} = (1-m_0)\,,\ a_{14} = 1\,,\ a_{15} = 0\,,\ a_{16} = 0\,,$$

$$a_{21} = 0\,,\ a_{22} = m_0\,,\ a_{23} = -c\beta^{(L)}m_0\,,\ a_{24} = 0\,,\ a_{25} = -c\,,\ a_{26} = 0\,,$$

$$a_{31} = (1-m_0)\,,\ a_{32} = 0\,,\ a_{33} = 0\,,\ a_{34} = c\beta^{(s)}(1-m_0)\,,\ a_{35} = c\,,\ a_{36} = 0\,,$$

$$a_{41} = 0\,,\ a_{42} = cm_o\rho_0^{(L)}\,,\ a_{43} = -m_0\,,\ a_{44} = 0\,,\ a_{45} = 0\,,\ a_{46} = 0\,,$$

$$a_{51} = 0\,,\ a_{52} = 0\,,\ a_{53} = 0\,,\ a_{54} = 1\,,\ a_{55} = 0\,,\ a_{56} = -E_2\,,$$

$$a_{61} = 1\,,\ a_{62} = 0\,,\ a_{63} = 0\,,\ a_{64} = 0\,,\ a_{65} = 0\,,\ a_{66} = c\,.$$

This gives

$$\begin{aligned} c^4\rho_0^{(s)}\rho_0^{(L)}\beta^{(s)}(1-m_0)m_0 - c^2\Big(\rho_0^{(L)}\big((1-E_2\beta^{(s)})(-1+m_0)^2 + E_2\beta^{(L)}m_0\big) \\ + \rho_0^{(s)}m_0(1-m_0)\Big) + E_2m_0 = 0\,. \end{aligned} \tag{3.40}$$

Equation (3.40) gives the velocity of the wave without the bubbles,

$$c^2 = \frac{-\beta_2 \pm \sqrt{\beta_2^2 - 4\alpha_2\gamma_2}}{2\alpha_2}\,, \tag{3.41}$$

where

$$\begin{aligned} \alpha_2 &= \rho_0^{(s)}\rho_0^{(L)}\beta^{(s)}(1-m_0)m_0\,, \\ \beta_2 &= -\Big(\rho_0^{(L)}\big((1-E_2\beta^{(s)})(-1+m_0)^2 + E_2\beta^{(L)}m_0\big) + \rho_0^{(s)}m_0(1-m_0)\Big)\,, \\ \gamma_2 &= E_2m_0\,. \end{aligned}$$

The terms for e_1, σ_1, p_1, and m_1 remain the same, while the proportionality between v_1 and u_1 becomes

$$u_1 = \left(\frac{c(1-m_0)\rho_0^{(s)} - \frac{E_2}{c}}{\rho_0^{(L)}(1-m_0)}\right)\frac{v_1}{c}\,. \tag{3.42}$$

3.4.4 Second approximation

Collecting the quadratic terms$\sim \varepsilon^2$ in system (3.36) gives

$$\begin{gathered}
\frac{\partial}{\partial\xi}(\sigma_2 - E_2\, e_2) = \frac{\partial T}{\partial\xi}\,, \quad \frac{\partial}{\partial\xi}(ce_2 + v_2) = F\,. \\
c(1-m_0)\rho_0^{(s)}\frac{\partial v_2}{\partial\xi} + \frac{\partial\sigma_2}{\partial\xi} - (1-m_0)\frac{\partial p_2}{\partial\xi} = \Sigma_1\,, \\
(cm_0\rho_0^{(L)}\frac{\partial u_2}{\partial\xi} - m_0\frac{\partial p_2}{\partial\xi}) = \Sigma_2\,,\ (1-m_0)\frac{\partial v_2}{\partial\xi} + c(1-m_0)\beta^{(s)}\frac{\partial\sigma_2}{\partial\xi} + c\frac{\partial m_2}{\partial\xi} = \Lambda^{(s)}\,, \\
m_0\frac{\partial u_2}{\partial\xi} - c\frac{\partial m_2}{\partial\xi} - cm_0\beta^{(L)}\frac{\partial p_2}{\partial\xi} = \Lambda^{(L)}\,,
\end{gathered} \tag{3.43}$$

where the formulas of F, Σ_1, and $\Lambda^{(s)}$ are the same, while the formulas for Σ_2, $\Lambda^{(L)}$, and T are changed to

$$\begin{gathered}
\Sigma_2 = m_0\rho_0^{(L)}\frac{1}{2}\frac{\partial u_1}{\partial\tau}\,, \\
\Lambda^{(L)} = -\frac{1}{2}\frac{\partial}{\partial\tau}\left(m_1 + m_0\beta^{(L)}p_1\right)\,, \\
T = -a_1 c\frac{\partial e_1}{\partial\xi} + b_1 c\frac{\partial\sigma_1}{\partial\xi}\,.
\end{gathered}$$

In analogy to Eq. (3.31), the compatibility condition for the system (3.43) has the form

$$\det(b_{nm}) = 0\,, \tag{3.44}$$

where

$$\begin{gathered}
b_{11} = \frac{\partial T}{\partial\xi}\,,\ b_{12} = 0\,,\ b_{13} = 0\,,\ b_{14} = 1\,,\ b_{15} = 0\,,\ b_{16} = -E_2\,, \\
b_{21} = F\,,\ b_{22} = 0\,,\ b_{23} = 0\,,\ b_{24} = 0\,,\ b_{25} = 0\,,\ b_{26} = c\,, \\
b_{31} = \Sigma_1\,,\ b_{32} = 0\,,\ b_{33} = (1-m_0)\,,\ b_{34} = 1\,,\ b_{35} = 0\,,\ b_{36} = 0\,, \\
b_{41} = \Sigma_2\,,\ b_{42} = cm_o\rho_0^{(L)}\,,\ b_{43} = -m_0\,,\ b_{44} = 0\,,\ b_{45} = 0\,,\ b_{46} = 0\,, \\
b_{51} = \Lambda^{(s)}\,,\ b_{52} = 0\,,\ b_{53} = 0\,,\ b_{54} = c\beta^{(s)}(1-m_0)\,,\ b_{55} = c\,,\ b_{56} = 0\,, \\
b_{61} = \Lambda^{(L)}\,,\ b_{62} = m_0\,,\ b_{63} = -c\beta^{(L)}m_0\,,\ b_{64} = 0\,,\ b_{65} = -c\,,\ b_{66} = 0\,.
\end{gathered}$$

Then the evolution equation for $v \cong v_1$ is

$$\begin{aligned} & c\Sigma_2 + \left(E_2 F - c\left(\Sigma_1 + \Sigma_2 - \frac{\partial T}{\partial \xi} \right) \right) m_0 \\ & +c^2 \left(\left(-E_2 F - c\left(\frac{\partial T}{\partial \xi} - \Sigma_1 \right) \right) \beta^{(L)} m_0 \right. \\ & \left. -(1-m_0) \left(\left(E_2 F + c\frac{\partial T}{\partial \xi} \right) \beta^s (-1+m_0) + \Lambda^{(L)} + \Lambda^{(s)} \right) \right) \rho_0^{(L)} = 0 \,. \end{aligned} \tag{3.45}$$

Now, we re-write equation (3.45) in terms of v and re-arrange,

$$\frac{1}{2}\big(\lambda_1 + \lambda_2 - (\lambda_3 + \lambda_4 + E_2 \lambda_5) \big) \frac{\partial v}{\partial \tau} + c^2 \, \lambda_5 \, (a_1 - b_1 E_2) \frac{\partial^2 v}{\partial \xi^2} + c \, \lambda_6 \, \frac{\partial v v}{\partial \xi} = 0 \,, \tag{3.46}$$

where

$$\lambda_1 = c m_0^2 \Big(c(1-m_0)\rho_0^{(s)} - \frac{E_2}{c} \Big) \,,$$

$$\lambda_2 = c^2 m_0 (1-m_0)^2 \rho_0^{(L)} \,,$$

$$\lambda_3 = c^2 m_0 \rho_0^{(L)} \Big((1-m_0)^2 (1 - E_2 \beta^{(s)}) - m_0 \beta^{(L)} (c^2 (1-m_0)\rho_0^{(s)} - E_2) \Big) \,,$$

$$\lambda_4 = c^2 m_0^2 \rho_0^{(s)} (1-m_0)(1 - c^2 \rho_0^{(L)} \beta^{(L)}) \,,$$

$$\lambda_5 = m_0 \Big(m_0 + c^2 \rho_0^{(L)} (\beta^{(s)} (-1+m_0)^2 - m_0 \beta^{(L)}) \Big) \,,$$

and λ_6 is the nonlinearity coefficient. The above equation then becomes

$$B_1 \frac{\partial v}{\partial \tau} + B_2 \frac{\partial^2 v}{\partial \xi^2} + B_N \frac{\partial v v}{\partial \xi} = 0 \,, \tag{3.47}$$

where

$$B_1 = \frac{1}{2}\big(\lambda_1 + \lambda_2 - (\lambda_3 + \lambda_4 + E_2 \lambda_5) \big) \,,$$

$$B_2 = c^2 \, \lambda_5 \, (a_1 - b_1 E_2) \,, \; B_N = c \, \lambda_6 \, .$$

3.5 Linearized model

In this section we consider the linearized version of the models (3.34) and (3.47). Our main interest is its dissipative part responsible for decay (attenuation) of the wave.

3.5.1 Evaluation of the parameters and the wave velocity

From (Dunin and Nikolaevskiy, 2005; Dunin et al., 2006; Mikhailov, 2010), the values of the parameters are: densities, $\rho_0^{(L)} = 1000\,\mathrm{kg/m^3}$ for water, $\rho^{(g)} = 2\,\mathrm{kg/m^3}$ for gas, $\rho_0^{(s)} = 2500\,\mathrm{kg/m^3}$ for solid; porosity $m_0 = 0.25$; compressibility $\beta^{(L)} = 2\times10^{-9}\,\mathrm{Pa^{-1}}$ for water, $\beta^{(L)} = 2.4\times10^{-6}\,\mathrm{Pa^{-1}}$ for gas, $\beta^{(s)} = 2\times10^{-10}\,\mathrm{Pa^{-1}}$ for solid; steady pressure $p_0 = 10^3\,\mathrm{Pa}$; bubble radius $R_0 = 10^{-4}\,\mathrm{m}$; volume gas content $\phi_0 = 10^{-3}$; viscosity $\mu = 10^{-3}\,\mathrm{Pa{\cdot}s}$; adiabatic exponent $\zeta = 1.4$, and permeability $\ell = 1.8\times10^{-11}\,\mathrm{m^2}$. Using the data from (Nikolaevskiy, 1985; Nikolaevskiy and Stepanova, 2005; Nikolaevskiy and Strunin, 2012; Nikolaevskiy, 2016), the values of the parameters of the rheological model in Figure 3.3 are

$$(a)\quad E_1 = 1/\beta^{(L)} = 4\times10^5\,\mathrm{Pa}\,,\quad E_2 = c^2\rho_0 = 2\times10^7\,\mathrm{Pa}\,,$$

$$E_3 = 3\chi\,p_0 = 4\times10^7\,\mathrm{Pa}\,,$$

where we used, just for the purpose of evaluating of E_i and M_i, the typical velocity $c \sim 100\,\mathrm{m/s}$ and the linear size of the oscillator $L_s = 0.3\,\mathrm{cm}$ from (Nikolaevskiy, 1985; Vilchinska et al., 1985).

We will also explore the values of E_i obtained by a different method, namely by using the formula $c^2\rho$ for all three phases, with ρ being the density of the liquid, solid and gas, respectively,

$$(b)\quad E_1 = c^2\rho^{(L)} = 1000\times10^4\,\mathrm{Pa}\,,\quad E_2 = c^2\rho^{(s)} = 2500\times10^4\,\mathrm{Pa}\,,$$

$$E_3 = c^2\rho^{(g)} = 2\times10^4\,\mathrm{Pa}\,.$$

According to Biot (1956*a*,*b*), the equation (3.20) gives the velocity of P-waves with the bubbles: for the P1-wave $c \approx 103\,\mathrm{m/s}$ and $c \approx 116\,\mathrm{m/s}$ for the both variants (a) and (b) respectively; for the P2-wave $c \approx 3\,\mathrm{m/s}$ for the both variants (a) and (b). We see that the velocity of P2-wave is indeed smaller than the velocity of P1-wave.

The results of equation (3.41) gives the velocity of P-waves without the bubbles. For the P1-wave using the variants (a) and (b) gives $c \approx 1050\,\mathrm{m/s}$, while for the P2-wave

$c \approx 70\,\mathrm{m/s}$ and $c \approx 78\,\mathrm{m/s}$ for the both variants (a) and (b) respectively. These results confirm that the presence of gas bubbles significantly decreases the P-waves velocities (Gubaidullin et al., 2017; Ali and Strunin, 2019).

Furthermore, we observed that the velocity (3.41) of the P-waves without the bubbles is almost the same as the velocity of P-waves with the bubbles (3.20) when we set ($n_0 = 0$ and $R_0 = 0$) for the both variants (a) and (b).

3.5.2 Dispersion (dissipation) relation

In this section we are again interested in the effect of the bubbles on the wave dissipation. Therefore, we consider the linearized wave equations (3.34) and (3.47). The linearized form of Eq. (3.34) can be written as

$$\frac{\partial v}{\partial \tau} = -\frac{A_2}{A_1}\frac{\partial^2 v}{\partial \xi^2}\,. \tag{3.48}$$

Now using the Fourier modes $v \sim \exp(\lambda t + ikx)$, we get the dissipation relation

$$\lambda(k) = \frac{A_2}{A_1}k^2\,, \tag{3.49}$$

where λ is the decay rate and k is the wave number. For the case without the bubbles the linearized form of equation (3.47) is

$$\frac{\partial v}{\partial \tau} = -\frac{B_2}{B_1}\frac{\partial^2 v}{\partial \xi^2}\,. \tag{3.50}$$

Then the dissipation relation is

$$\lambda(k) = \frac{B_2}{B_1}k^2\,. \tag{3.51}$$

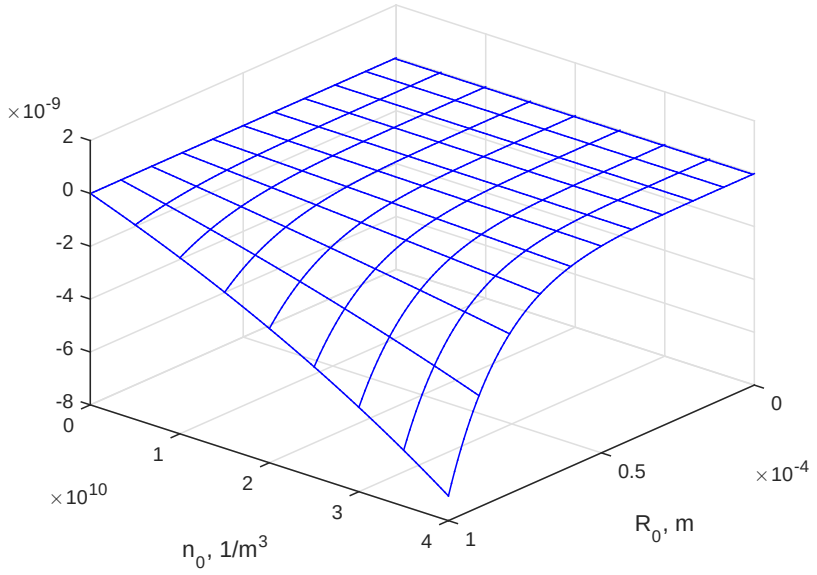

Figure 3.5: The decay rate by formula (3.49) for variant (a), $k_* = 0.25\ 1/\mathrm{m}$.

The plot in Figure 3.5 shows the decay rate at fixed $k_* = 0.25$ 1/m Nikolaevskiy (1989) against R_0 and n_0. As mentioned earlier, the decay rate is significantly affected by the increase in R_0 and becomes large in absolute value; this is because the bubbles affect the system through the pressure $p_1 = -p_0\,\chi\,R_1$. As for n_0, one should disregard the region of small n_0 in Figure 3.5 where the equations of continuum mechanics cease to be valid. This is because the used assumption that each bubble is embedded in its own fluid particle (see Eq. (3.2)) is no longer inapplicable due to the large size of the particle.

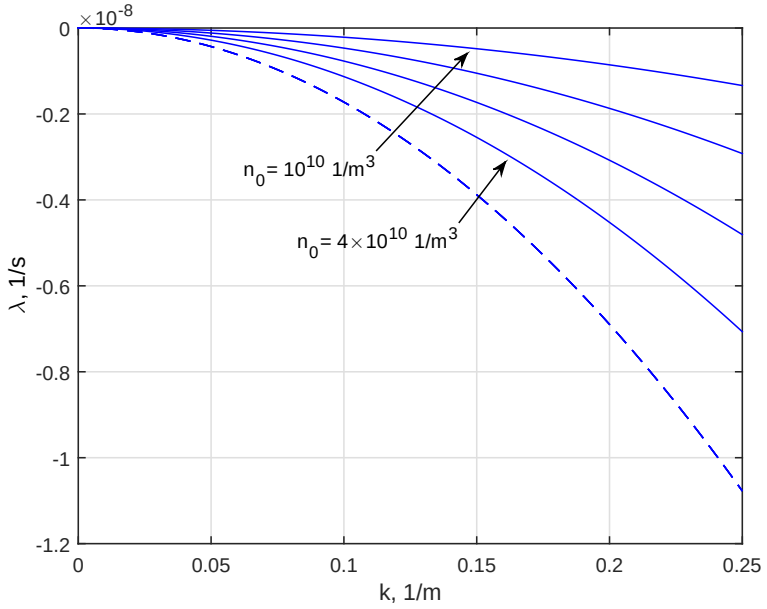

Figure 3.6: The decay rate by formulas (3.49) and (3.51) for variant (a): n_0 varies, $R_0 = 10^{-4}$.

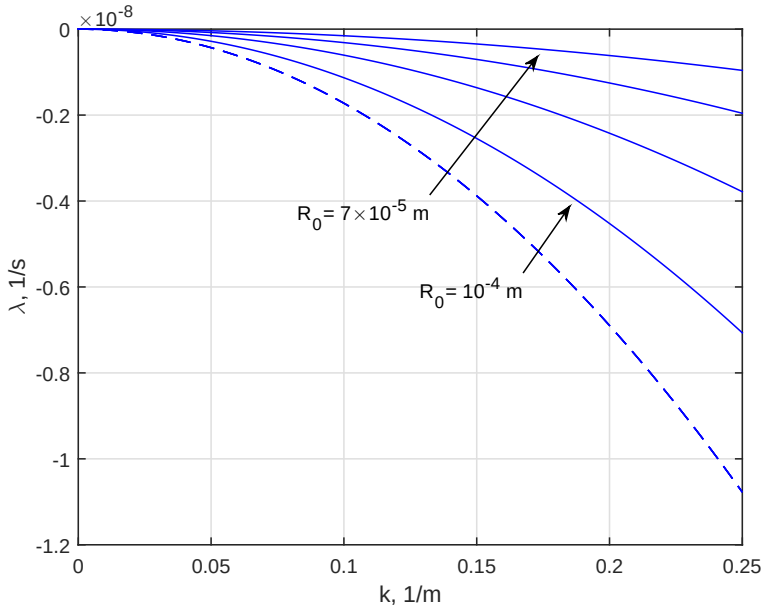

Figure 3.7: The decay rate by formulas (3.49) and (3.51) for variant (a): R_0 varies, $n_0 = 4 \times 10^{10}$.

Figures 3.6 and 3.7 compare the decay curves of the wave with the bubbles and the wave without the bubbles. The dashed line describes the case without the bubbles and the solid lines correspond to the wave with the bubbles. Figure 3.6 is for varying n_0 and fixed R_0. Figure 3.7 is for varying R_0 and fixed n_0. We clearly see that the curves lie entirely below zero, which means that the wave decays and the decay rate depends on the number and radius of the bubbles. This result agrees with the conception emphasized in Strunin (2014); Strunin and Ali (2016) about the essentially dissipative nature of the freely propagating elastic wave. Similar results are obtained for variants (b) as shown in Figures 3.8–3.10.

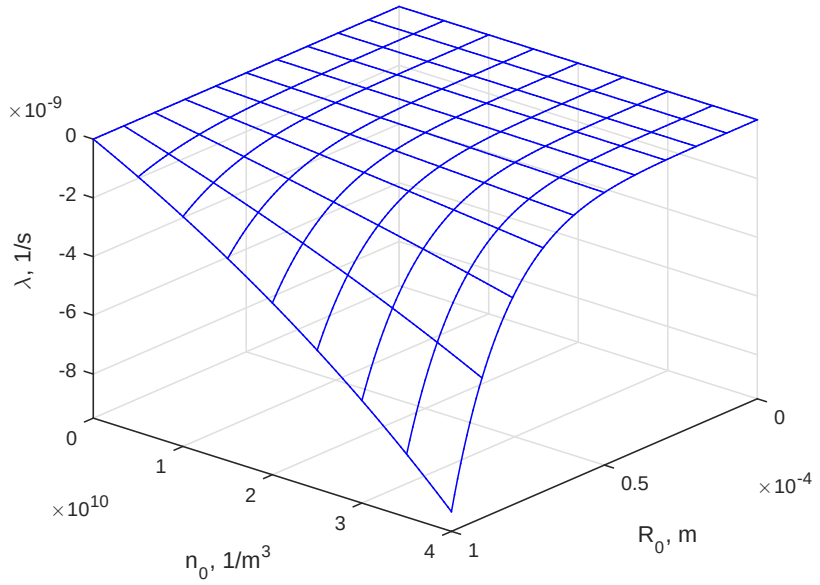

Figure 3.8: The decay rate by formula (3.49) for variant (b), $k_* = 0.25\ 1/\mathrm{m}$.

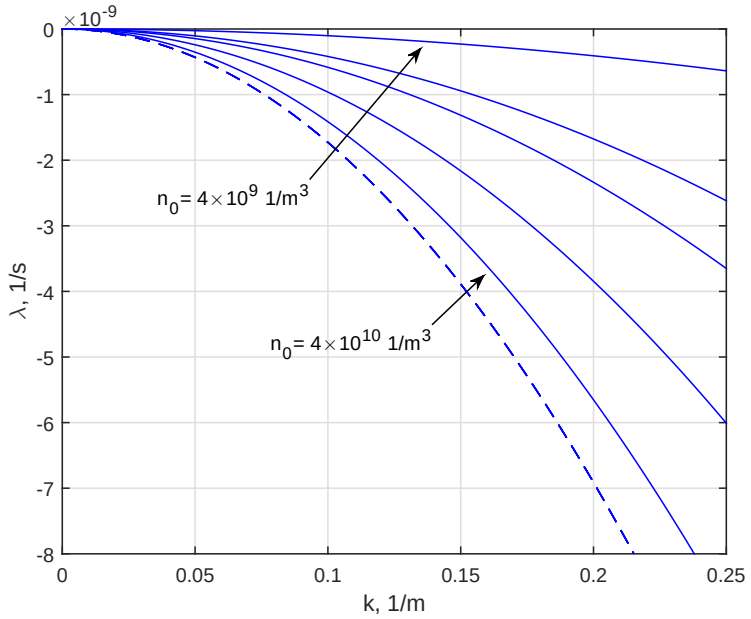

Figure 3.9: The decay rate by formulas (3.49) and (3.51) for variant (b): n_0 varies, $R_0 = 10^{-4}$.

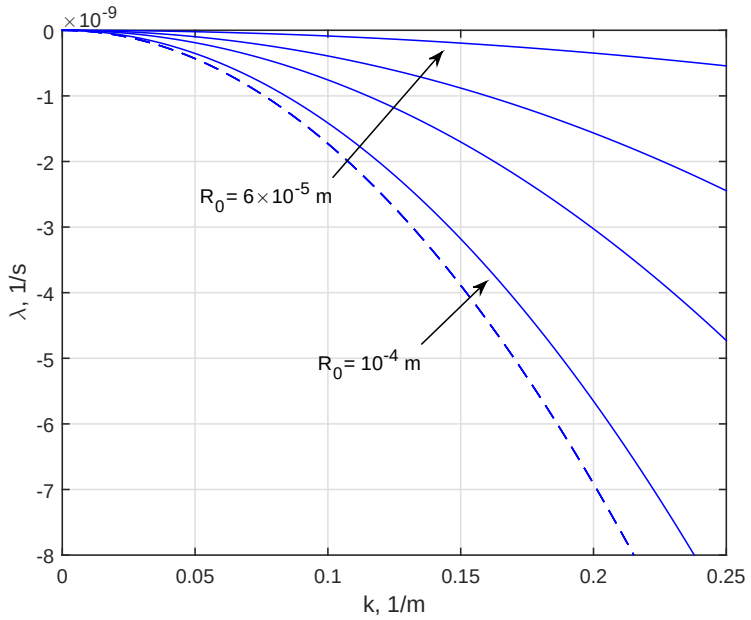

Figure 3.10: The decay rate by formulas (3.49) and (3.51) for variant (b): R_0 varies, $n_0 = 4 \times 10^{10}$.

3.6 Concluding remarks

We studied the effect of the rheology including bubbles on the Frenkel-Biot P1-waves in porous rocks. Using two-segment rheology, we derived the P1-type wave equations with and without the bubbles describing the velocity of the solid matrix in the medium. We compared the linearized versions of the equations in terms of the decay rate $\lambda(k)$ of the Fourier modes. For the both cases with and without the bubbles, the $\lambda(k)$-curve lies entirely below zero. We discovered that $|\lambda(k)|$ increases with the increase of the radius and the number of the bubbles.

Chapter 4

Complex rheology and decay rate for P1 waves in porous granular media with gas bubbles

SUMMARY: We investigate the effect of more complex rheological models for P1-waves, including and excluding the bubbles, in comparison to Chapter 3. For the wave with the bubbles the model consists of three segments representing the solid continuum, fluid continuum and a bubble surrounded by the fluid. We derive the Nikolaevskiy-type equations describing the velocity of the solid matrix in the moving reference system. The equations are linearized to yield the decay rate λ as a function of the wave number k. We compare the $\lambda(k)$-dependence for the cases with and without the bubbles, using typical values of the input mechanical parameters. For the both cases, the $\lambda(k)$-curve lies entirely below zero, which is in line with the notion of the elastic wave being an essentially passive system. We discover that the increase of the radius of the bubbles leads to faster decay, while the increase in the number of the bubbles leads to slower decay of the elastic wave.

4.1 Introduction

This chapter studies the influence of different rheologies with the bubbles, on the wave attenuation in the liquid-saturated porous media. We will use an extended stress-strain relation relative to the model of Nikolaevskiy to take into account the bubbles in modelling the P-type waves.

Liu et al. (1976) demonstrated that rheology based on the scheme often referred to as Generalized Standard Linear Solid (GSLS) helps to better describe measured characteristics of seismic waves in earth continuum. The importance of complex multi-component GSLS was acknowledged by Bohlen (2002) who employed the rheology with many Maxwell bodies connected in parallel. Nikolaevskiy (1989) used complex stress-strain relations in a fluid-saturated grain, where the solid matrix and fluid are in contact. This resulted, in the final analysis, in the nonlinear higher-order partial differential equation of the form

$$\frac{\partial v}{\partial t} + v\frac{\partial v}{\partial x} = \sum_{p=1}^{5} \varepsilon^{p-1} A_{p+1} \frac{\partial^{p+1} v}{\partial x^{p+1}}\,, \tag{4.1}$$

where v is the velocity of the solid matrix, ε is the small parameter reflecting slow evolution of the wave (this is discussed below) and A_{p+1} are the coefficients linked to mechanical parameters of the system. From the standpoint of wave dynamics, the even derivatives in Eq. (4.1) are responsible for the dissipation and odd derivatives for the dispersion effects. Equation (4.1) assumes the form of the Korteweg–de Vries–Burgers equation if the index p goes from just 1 and 2. But with the range of p going further as shown, the equation manifests an extension of this classical equation to include high-order spatial derivatives. As explained below, this extension results from the complex rheology of the system.

Experimental evidence indicates that the presence of gas bubbles changes the characteristics of the wave (Wijngaarden, 1968, 1972; Anderson and Hampton, 1980; Dunin and Nikolaevskiy, 2005). Typically, in rocks saturated with fluids, the P1-wave is

the only observable wave (Nikolaevskiy, 2008). However, the presence of gas, even in small proportion can affect the wave type (Nikolaevskiy and Strunin, 2012), so that, P2-wave may also be visible. Dunin et al. (2006) studied the effect of gas bubbles on linear P1- and P2-waves, and derived the dispersion relation connecting the frequency and wave number. Of special interest was the transformation of the wave type due to the bubbles. They found that the transformation was due to the change in the motion of the liquid in the porous space. Instead of the overflow between the pours incurring large Darcy friction, which is characteristic of the P2-waves, the liquid may be displaced into the volume released when a bubble is compressed. In this case the oscillations of the porous matrix and of the bubbles occur in phase and, as a result, the decay of the P2-wave diminishes due to the reduction in the Darcy friction. As far as the rheology is concerned, Dunin et al. (2006) used a rather simple stress-strain relation, $\sigma = Ee$, in standard notations. Various aspects of the wave propagation in multifluid and bubbly flows were studied in (Brunner and Spetzler, 2001; Collier et al., 2006; Tisato et al., 2015; Papageorgiou and Chapman, 2015). For example, Collier et al. (2006) explored the influence of the gas bubbles on attenuation in volcanic magma, where the bubbles grow not only due to gas expansion, but also due to the exsolution of volatiles, such as water, from the melt into the bubbles. In our present study we do not consider such kind of thermodynamic disequilibrium conditions.

As we mentioned before, the rheological model used in (Nikolaevskiy, 1985, 1989), despite containing several Maxwell bodies, did not include an element representing gas bubble. In the present chapter we include the bubble element into the two-branch rheological model relative to the model of Nikolaevskiy (1985), see Figure 4.1, and then derive and analyze the equation of the type (4.1), where the coefficients A_p depend on the bubble-related parameters. The resulting equation will describe the decay (or attenuation) of the freely propagating seismic wave. We will investigate the influence of the bubble-related parameters, including their radius and concentration,

on the decay rate.

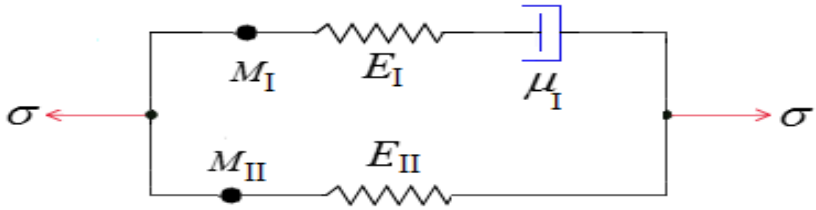

Figure 4.1: Two–branch rheological scheme from (Nikolaevskiy, 1985) .

During its propagation the seismic wave decays due to the viscous friction both within individual phases, e.g. fluid, and between the phases. The decay may be described in terms of the decay rate in time as in (Nikolaevskiy, 1989), or decay rate in space via the attenuation factor as in (Dunin et al., 2006). These descriptions are closely connected and just correspond to different realizations of the wave, that is the wave propagation under different initial and/or boundary conditions. To illustrate this, let us represent a Fourier modes of the linear wave as $\exp(i\xi_1)$, where $\xi_1 = wt + kx$, w is the frequency and k the wave number connected with each other via the dispersion relation. Writing this relation in the form $w = w(k)$ with k being real-valued, we can find the corresponding complex-valued w. Its imaginary part determines how fast the wave decays in time. Physically this situation corresponds to the wave in an unbounded medium, which decays as time goes. Alternatively, one may write down the dispersion relation as $k = k(w)$ and consider the real-valued frequency w as the argument, whereas the wave number k becomes complex-valued. Imaginary part of k governs the decay of the wave in space. From physical standpoint this realization can be associated with the wave which propagates, say, from the surface into underground. The decay of such a wave against the distance is characterized by the attenuation factor.

Importantly, the dynamics of the fluid in porous media may exhibit boundary layers. They form when the frequency of the seismic wave is relatively high. This contrasts the low-frequency waves where the viscous forces dominate throughout the fluid volume so that inertial effects may be neglected. However, at high frequencies the inertial effects dominate in the bulk of the fluid, while the viscous friction concentrates within narrow boundary layers near solid walls due to the no-slip conditions. Allowing for the boundary layers in the analysis significantly affects the frequency dependence of the attenuation of the wave. Namely the low- and high-frequency branches of the attenuation curve become asymmetric. Masson et al. (2006) confirmed this effect by numerical computations of the governing mechanics equations. The model that we use in our present chapter is one-dimensional with all the functions depending on t and one coordinate x along the direction of the wave propagation. Thus, instead of analyzing the structure of the boundary layers, we adopt the simple Newton's law for the momentum exchange between the fluid and the solid, stating proportionality of the viscous friction to the difference between their respective velocities.

In our study of the wave decay we choose to analyze the decay in time, that is the $w = w(k)$ form of the dispersion relation. We will execute a procedure similar to Nikolaevskiy (2008), where one-dimensional (x-dependent) dynamics are considered, and all the functions of interest are decomposed into series in small parameter ε characterizing slow evolution of the wave in space and time. Introducing the running variable ξ and using ε to scale the distance x and time t,

$$\xi = \varepsilon(x - ct)\,, \quad \tau = (\varepsilon^2/2)t\,,$$

we seek the velocity of the solid matrix in the form

$$v = \varepsilon v_1 + \varepsilon^2 v_2 + \dots\,.$$

We will show, in line with Nikolaevskiy (2008), that the complex rheology generates higher-order time derivatives (Nikolaevskiy, 1989). They, in turn, translate into

high-order derivatives in ξ in the resulting equation (4.1) because

$$\frac{\partial}{\partial t} = (\varepsilon^2/2)\frac{\partial}{\partial \tau} - \varepsilon c\frac{\partial}{\partial \xi} \approx -\varepsilon c\frac{\partial}{\partial \xi}\,.$$

Once derived, equation (4.1) gives the dispersion relation, which is the main point of interest in this work. Our focus is on the dissipation controlled by the even x-derivatives. Therefore, we will study a truncated form of equation (4.1),

$$\frac{\partial v}{\partial t} + v\frac{\partial v}{\partial \xi} = A_2\frac{\partial^2 v}{\partial \xi^2} + \varepsilon^2 A_4\frac{\partial^4 v}{\partial \xi^4} + \varepsilon^4 A_6\frac{\partial^6 v}{\partial \xi^6}\,. \tag{4.2}$$

It is convenient to seek the Fourier modes in the form $v \sim exp(\lambda t + ikx)$. Substituting these into Eq. (4.2) gives

$$\lambda = -A_2k^2 + \varepsilon^2 A_4k^4 - \varepsilon^4 A_6k^6 \tag{4.3}$$

with k being the wave number associated with the scaled length ξ. When analyzing Eq. (4.3) we remember that k is not allowed to be too large, otherwise the assumption of the slow variation of the wave in space will be violated. As we noted, the slowness is facilitated by the smallness of ε. Therefore, in Eq. (4.3) the term $\varepsilon^2 A_4k^4$ should be treated just as a correction to the leading term A_2k^2, and the following term $\varepsilon^4 A_6k^6$ as a correction to the term $\varepsilon^2 A_4k^4$. Thus, the value of λ remains negative at all plausible values of the mechanical parameters of the system (such as elastic moduli and viscosities). This reflects the essentially dissipative nature of the seismic wave, or, in other words, the impossibility of self-excitation of motion. In view of the crucial presence of the small parameter ε in equations (4.2) and (4.3) we revise our earlier attempt (Strunin, 2014) to guarantee this important property of the freely propagating seismic wave in the model. In (Strunin, 2014) a popular form of Eq. (4.2) was considered where the small parameter ε was omitted. It was reasoned that the mechanical parameters, of which A_4 and A_6 are composed, should therefore assume special limited values, in order to guarantee that $\lambda < 0$. However, negativity of λ is simply ensured by the smallness of ε, which is the essential part of Eq. (4.2) as explicitly shown.

4.2 Basic equations of one-dimensional dynamics

4.2.1 Conservation of mass and momentum

For a one-dimensional case the momentum and mass balance equations are (Nikolaevskiy, 1990)

$$\begin{gathered}\frac{\partial}{\partial t}(1-m)\rho^{(s)}v+\frac{\partial}{\partial x}(1-m)\rho^{(s)}vv=\frac{\partial}{\partial x}\sigma^{(ef)}-(1-m)\frac{\partial p}{\partial x}-I\,,\\ \frac{\partial}{\partial t}m\rho^{(f)}u+\frac{\partial}{\partial x}m\rho^{(f)}uu=-m\frac{\partial p}{\partial x}+I\,,\\ \frac{\partial}{\partial t}(1-m)\rho^{(s)}+\frac{\partial}{\partial x}(1-m)\rho^{(s)}v=0\,,\\ \frac{\partial}{\partial t}m\rho^{(f)}+\frac{\partial}{\partial x}m\rho^{(f)}u=0\,,\end{gathered}\tag{4.4}$$

where, the subscripts s and f label the solid and gas-liquid mixture respectively, ρ, v, and u are the corresponding densities and mass velocities, m is the porosity, $\sigma^{(ef)}$ is the effective Terzaghi stress, p is the pore pressure, and I is the interfacial viscous force approximated by

$$I=\delta m(v-u),\quad \delta=\frac{\mu^{(f)}m}{\ell}\,,$$

where $\mu^{(f)}$ is the gas-liquid mixture viscosity and ℓ is the intrinsic permeability.

4.2.2 Dynamics of bubbles

The equation of the dynamics of a bubble (Dontsov et al., 1987) has the form

$$R\frac{\partial^2}{\partial t^2}R+\frac{3}{2}\left(\frac{\partial}{\partial t}R\right)^2+\frac{4\mu}{\rho^{(L)}}\left(\frac{1}{R}+\frac{m}{4\ell}R\right)\frac{\partial}{\partial t}R=(p_g-p)/\rho^{(L)}\,,\tag{4.5}$$

where R is the bubble radius, p is the pressure in the liquid, $p_g=p_0(R_0/R)^{\chi}$ is the gas pressure inside the bubble (here $\chi=3\varsigma$, ς is the adiabatic exponent), $\rho^{(L)}$ is the density of the liquid without the bubbles, and μ is the viscosity of the liquid without

the bubbles. The density equations for the solid and liquid without gas are

$$\begin{aligned}\rho^{(s)} &= \rho_0^{(s)}(1-\beta^{(s)}\sigma) = \rho_0^{(s)}\left[1+\beta^{(s)}p-\frac{\beta^{(s)}\sigma^{(ef)}}{1-m}\right] \\ &\approx \rho_0^{(s)}[1+\beta^{(s)}p-\beta^{(s)}\sigma^{(ef)}]\,, \end{aligned} \tag{4.6}$$

$$\rho^{(L)} = \rho_0^{(L)}(1+\beta^{(L)}p)\,. \tag{4.7}$$

The mean density of the gas-liquid mixture is

$$\rho^{(f)} = (1-\phi)\rho^{(L)} + \phi\rho^{(g)}, \tag{4.8}$$

where

$$\phi = (4\pi/3)R^3 n_0\,.$$

Here σ is the true stress, ϕ is the volume gas content and n_0 is the number density of the bubbles per unit volume. In Eq. (4.8) we can neglect the density of the gas $\rho^{(g)}$ due to the low gas content. The change in ϕ is due to the change in the bubble radius R. Then Eq. (4.8) becomes

$$\rho^{(f)} = \rho_0^{(L)}(1+\beta^{(L)}p)\Big(1-\frac{4\pi}{3}R_0^3 n_0\Big)\,. \tag{4.9}$$

Similarly to Dunin et al. (2006) we also assume that the pore pressure p is equal to the pressure in the liquid far from the bubble.

4.2.3 Stress-strain relation

In this section we derive the stress-strain relation for the viscoelastic medium based on the rheological Maxwell-Voigt model, which includes the gas bubble. The model includes two friction elements with viscosities μ_1 and μ_2, three elastic springs with the elastic moduli E_1, E_2, and E_3, and three oscillating masses M_1, M_2, and M_3 as shown in Figure 4.2. The total stress in denoted σ. We also denote the displacements of the elements of the model by e with respective subscripts.

Using the same approach as in Chapters 1 and 3, we derive the following relation between the stress and strain,

$$\begin{aligned}
&\left[E_1\,E_3\,\left(\frac{1}{\mu_1}+\frac{1}{\mu_2}\right)\right]\sigma+(E_3+E_1)\frac{d\sigma}{dt}+M_3\,\frac{d^3\sigma}{dt^3}\\
&=\left[E_1\,E_2\,E_3\left(\frac{1}{\mu_1}+\frac{1}{\mu_2}\right)\right]e+[(E_2+E_1)E_3+E_1E_2]\frac{de}{dt}\\
&+\left[E_1E_3M_2\left(\frac{1}{\mu_1}+\frac{1}{\mu_2}\right)\right]\frac{d^2e}{dt^2}+[((E_2+E_1)M_3+(E_3+E_1)M_2)\\
&+E_3M_1]\,\frac{d^3e}{dt^3}+[(M_2+M_1)M_3]\frac{d^5e}{dt^5}\,.
\end{aligned}\tag{4.10}$$

Generalizing equation (4.10) using similar approach to Nikolaevskiy (2008), we get

$$\sigma^{(ef)}+\eta\sum_{q=1,3}b_q\,\frac{D^q\sigma^{(ef)}}{Dt^q}=E_2e+\beta^{(s)}k_b\,p+\eta\sum_{q=1,2,3,5}a_q\,\frac{D^qe}{Dt^q}\,,\tag{4.11}$$

where $\sigma^{(ef)}$ is the effective stress, k_b is the bulk elastic module of the porous matrix, $\eta=[E_1\,E_3\,(\frac{1}{\mu_1}+\frac{1}{\mu_2})]^{-1}$ and the coefficients a_q and b_q are expressed as

$$a_1=[(E_2+E_1)E_3+E_1E_2]\,,\ a_2=M_2\,,$$

$$a_3=[(E_2+E_1)M_3+(E_3+E_1)M_2+E_3M_1],\ a_5=[(M_2+M_1)M_3]\,,$$

$$b_1=(E_3+E_1)\,,\ b_3=M_3\,.$$

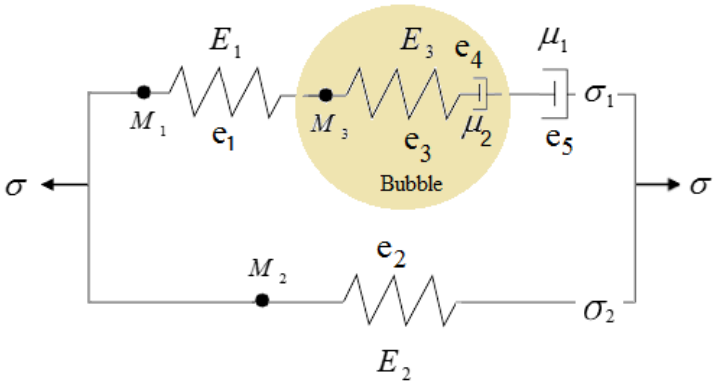

Figure 4.2: Rheological scheme including a gas bubble.

Finally, we add the closing relation between the deformation e and the velocity v of the solid,

$$\frac{De}{Dt} \equiv \frac{\partial e}{\partial t} + v\frac{\partial e}{\partial x} = \frac{\partial v}{\partial x}\,. \tag{4.12}$$

4.3 Elastic waves in saturated media including gas bubbles

Following the approach of Nikolaevskiy (2008), we consider the P1-wave in a porous media under the full saturation. We address the reader to Appendix B, which presents an extract from the paper of Nikolaevskiy (2008). This extract contains five main sections of this paper in full. We believe this is the best way to convey the main idea of his approach.

For p1-waves the mass velocities v and u have the same sign,

$$v = u + O(\varepsilon\, v)\,, \tag{4.13}$$

where ε is the small parameter. The Darcy force has the order as shown,

$$I = \varepsilon^{\gamma}\delta m(v-u) = \varepsilon^{\gamma}\delta m v, \qquad \delta = m\,\mu/k = O(1)\,. \tag{4.14}$$

Describing a weakly non-linear wave we use the running coordinate system with simultaneous scale change,

$$\begin{aligned} &\xi = \varepsilon(x - ct)\,, \qquad \tau = \frac{1}{2}\varepsilon^2\, t\,, \\ &\frac{\partial}{\partial x} = \varepsilon\frac{\partial}{\partial \xi}\,, \qquad \frac{\partial}{\partial t} = \varepsilon\left(\frac{1}{2}\varepsilon\frac{\partial}{\partial \tau} - c\frac{\partial}{\partial \xi}\right)\,. \end{aligned} \tag{4.15}$$

Thus, the constitutive law (4.11) transforms into the following form

$$\begin{aligned} &\sigma^{(ef)} + \eta\sum_{q=1,3} b_q\,\varepsilon^q\left(\frac{1}{2}\varepsilon\frac{\partial}{\partial\tau} + (v-c)\frac{\partial}{\partial\xi}\right)^q \sigma^{(ef)} \\ &= E_2 e + \beta^{(s)} k_b\, p + \eta\sum_{q=1,2,3,5} a_q\,\varepsilon^q\left(\frac{1}{2}\varepsilon\frac{\partial}{\partial\tau} + (v-c)\frac{\partial}{\partial\xi}\right)^q e\,. \end{aligned} \tag{4.16}$$

Now, we seek the unknown functions as power series

$$\begin{aligned} &v = \varepsilon v_1 + \varepsilon^2 v_2 + \dots, && u = \varepsilon u_1 + \varepsilon^2 u_2 + \dots, \\ &\sigma^{ef} = \sigma_0^{(ef)} + \varepsilon\sigma_1^{(ef)} + \varepsilon^2\sigma_2^{(ef)} \dots, && p = p_0 + \varepsilon p_1 + \varepsilon^2 p_2 \dots, \\ &m = m_0 + \varepsilon m_1 + \varepsilon^2 m_2 \dots, && e = e_0 + \varepsilon e_1 + \varepsilon^2 e_2 \dots, \\ &\phi = \phi_0 + \varepsilon\phi_1 + \varepsilon^2\phi_2 \dots, && R = R_0(1 + \varepsilon R_1 + \varepsilon^2 R_2 \dots). \end{aligned} \tag{4.17}$$

4.3.1 First approximation

Using equations (4.17), we collect the linear terms $\sim \varepsilon$ in system (4.4),

$$\begin{aligned} -(1-m_0)\rho_0^{(s)} c\frac{\partial v_1}{\partial \xi} &= \frac{\partial \sigma_1^{(ef)}}{\partial \xi} - (1-m_0)\frac{\partial p_1}{\partial \xi}, \\ -m_0\rho_0^{(f)} c\frac{\partial u_1}{\partial \xi} &= -m_0\frac{\partial p_1}{\partial \xi}, \\ \rho_0^{(s)} c\frac{\partial m_1}{\partial \xi} - (1-m_0)c\frac{\partial \rho_1^{(s)}}{\partial \xi} + (1-m_0)\rho_0^{(s)}\frac{\partial v_1}{\partial \xi} &= -\frac{1}{2}(1-m_0)\frac{\partial \rho_0^{(s)}}{\partial \tau}, \\ -m_0 c\frac{\partial \rho_1^{(f)}}{\partial \xi} - \rho_0^{(f)} c\frac{\partial m_1}{\partial \xi} + m_0\rho_0^{(f)}\frac{\partial u_1}{\partial \xi} &= -\frac{1}{2}m_0\frac{\partial \rho_0^{(f)}}{\partial \tau}. \end{aligned} \tag{4.18}$$

The system (4.18) gives the integrals

$$\begin{aligned} (1-m_0)\rho_0^{(s)}\, c v_1 &= -\sigma_1^{(ef)} + (1-m_0)p_1, \\ m_0\rho_0^{(f)}\, c u_1 &= m_0 p_1, \\ (1-m_0)\rho_0^{(s)} v_1 &= \left((1-m_0)\rho_1^{(s)} - \rho_0^{(s)} m_1\right) c, \\ m_0\rho_0^{(f)} u_1 &= (\rho_0^{(f)} m_1 + m_0\rho_1^{(f)})c. \end{aligned} \tag{4.19}$$

According to (4.6) and (4.9) the terms $\sim \varepsilon$ in the density series are

$$\begin{aligned} \rho_1^{(s)} &= \rho_0^{(s)}\left(\beta^{(s)} p_1 - \frac{\beta^{(s)}\sigma_1^{(ef)}}{(1-m_0)}\right), \\ \rho_1^{(f)} &= \rho_0^{(L)}\left(\beta^{(L)}\kappa_1 p_1 - 4\pi n_0 \kappa_2 R_0^3 R_1\right) \end{aligned} \tag{4.20}$$

and also

$$\rho_0^{(f)} = \kappa_1 \kappa_2 \rho_0^{(L)} \,, \tag{4.21}$$

where

$$\kappa_1 = 1 - \frac{4\pi}{3} R_0^3 n_0 \,,\; \kappa_2 = 1 + \beta^{(L)} p \,.$$

Inserting (4.20) and (4.21) into the last two equations in (4.19) (mass equations) we get

$$(1-m_0)v_1 = [(1-m_0)\beta^{(s)} p_1 - \beta^{(s)} \sigma_1^{(ef)} - m_1]c \,, \tag{4.22}$$

$$m_0 u_1 = \left[m_1 + \frac{m_0 \beta^{(L)} p_1}{\kappa_2} - \frac{4\pi\, n_0 m_0 R_0^3\, R_1}{\kappa_1} \right] c \,. \tag{4.23}$$

The combination of (4.22) and (4.23) gives

$$\begin{aligned} (1-m_0)v_1 + m_0 u_1 = \Bigg[& \frac{\left(\beta + (1-m_0)\beta^{(s)}\beta^{(L)} p_0\right) p_1}{\kappa_2} - \beta^{(s)} \sigma_1^{(ef)} \\ & - \frac{4\pi\, n_0 m_0 R_0^3\, R_1}{\kappa_1} \Bigg] c \,, \end{aligned} \tag{4.24}$$

where $\beta = (1-m_0)\beta^{(s)} + m_0 \beta^{(L)}$. The condition (4.13) means $v_1 = u_1$, therefore equation (4.24) becomes

$$v_1 = \left[\frac{\left(\beta + (1-m_0)\beta^{(s)}\beta^{(L)} p_0\right) p_1}{\kappa_2} - \beta^{(s)} \sigma_1^{(ef)} - \frac{4\pi\, n_0 m_0 R_0^3\, R_1}{\kappa_1} \right] c \,. \tag{4.25}$$

Due to the conditions $v_1 = u_1$, $\rho_0 = (1-m_0)\,\rho_0^{(s)} + m_0\,\rho_0^{(L)}$ and using (4.21), the first two of the momentum equations (4.19) give

$$\rho_0\, c\, v_1 = -\sigma_1^{(ef)} + A p_1 \,, \tag{4.26}$$

where

$$A = (1-m_0) + \frac{m_0}{\kappa_1 \kappa_2} \,.$$

Now, the linear terms $\sim \varepsilon$ in relations (4.12) and (4.16) give

$$\frac{1}{2}\frac{\partial e_0}{\partial \tau} - c\frac{\partial e_1}{\partial \xi} + v_1 \frac{\partial e_0}{\partial \xi} = \frac{\partial v_1}{\partial \xi} \,, \tag{4.27}$$

$$\sigma_1^{(ef)} - E_2\, e_1 - \beta^{(s)}\, k_b p_1 = T\,, \tag{4.28}$$

where

$$T \equiv \eta\Big[\sum_{q=1,2,3,5} a_q\,(-c)^q\,\varepsilon^{q-1}\frac{\partial^q e_0}{\partial\xi^q} + \sum_{q=1,3} b_q\,c^q\,\varepsilon^{q-1}\frac{\partial^q \sigma_0^{(ef)}}{\partial\xi^q}\Big]\,.$$

The linear terms $\sim\varepsilon$ in the bubble equation (4.5) give

$$-\frac{\mu\, c}{\rho_0^{(L)}\kappa_2}\left[\frac{4}{R_0}+\frac{m_0 R_0}{\ell}\right]\frac{\partial R_0}{\partial\xi} = -\frac{1}{\rho_0^{(L)}\kappa_2}(p_0\,\chi\,R_1 + p_1)\,. \tag{4.29}$$

Equations (4.27), (4.28) and (4.29) lead to the integrals

$$e_1 = -\frac{v_1}{c},\quad \sigma_1^{(ef)} = E_2\, e_1 + \beta^{(s)} k_b p_1,\quad p_1 = -p_0\,\chi\,R_1\,. \tag{4.30}$$

The effective stress $\sigma_1^{(ef)}$ in (4.30) can be rewritten as

$$\sigma_1^{(ef)} = -\left[\frac{E_2 v_1}{c} + p_0\,\chi\beta^{(s)} k_b\,R_1\right]\,. \tag{4.31}$$

Substituting (4.31) and the value of p_1 from (4.30) into (4.25), leads to

$$(1-\beta^{(s)}E_2)v_1 + \big(B - k_b\beta^{(s)}\beta^{(s)}\big)p_0\chi R_1 c = 0\,, \tag{4.32}$$

where

$$B = \frac{\big(\beta + (1-m_0)\beta^{(s)}\beta^{(L)}p_0\big)}{\kappa_2} + \frac{4\pi n_0 m_0 R_0^3}{\kappa_1 p_0\chi}\,.$$

Now, from (4.26) and using the value of p_1 from (4.30), we obtain the effective stress as

$$\sigma_1^{(ef)} = -\,(\rho_0\, c v_1 + A)\, p_0\chi R_1\,. \tag{4.33}$$

The combination of (4.31) and (4.33) results in

$$(E_2 - \rho_0\, c^2)v_1 - \big(A - k_b\beta^{(s)}\big)p_0\chi R_1 c = 0\,. \tag{4.34}$$

Equations (4.32) and (4.34) must coincide, therefore

$$\begin{vmatrix} (1-\beta^{(s)}E_2) & (B - k_b\beta^s\beta^s)\,p_0\chi \\ (E_2 - \rho_0\, c^2) & -\big(A - k_b\beta^{(s)}\big)\,p_0\chi \end{vmatrix} = 0\,. \tag{4.35}$$

Equation (4.35) gives the velocity of the wave,

$$c^2 = \frac{(A - k_b\beta^{(s)})Z_1 + E_2}{\rho_0}\,, \tag{4.36}$$

where

$$Z_1 = \frac{1 - \beta^{(s)}E_2}{B - k_b\beta^{(s)}\beta^{(s)}}\,.$$

Thus, all the variables are expressed through any one selected variable, for example, the velocity v_1,

$$\begin{gathered} e_1 = -\frac{v_1}{c}\,,\ \sigma_1^{(ef)} = -(E_2 - k_b\beta^{(s)}Z_1)\frac{v_1}{c}\,,\ p_1 = Z_1\frac{v_1}{c}\,,\ R_1 = -\frac{Z_1}{p_0\chi}\frac{v_1}{c}\,, \\ m_1 = \left[((1-m_0) - k_b\beta^{(s)})\beta^{(s)}Z_1 + \beta^{(s)}E_2 - (1-m_0)\right]\frac{v_1}{c}\,, \\ \rho_1^{(f)} = \rho_0^{(L)}Z_1\left(\beta^{(L)}\kappa_1 + \frac{\kappa_2 4\pi n_0\,R_0^3}{p_0\chi}\right)\frac{v_1}{c}\,, \\ \rho_1^{(s)} = \rho_0^{(s)}\beta^{(s)}\left[Z_1(1 - k_b\beta^{(s)}) + E_2\right]\frac{v_1}{c}\,. \end{gathered} \tag{4.37}$$

4.3.2 Second approximation

Collecting the quadratic terms $\sim \varepsilon^2$ in (4.16), we get

$$\sigma_2^{(ef)} - E_2 e_2 - \beta^{(s)}\,k_b\,p_2 = T\,, \tag{4.38}$$

where

$$T \equiv \eta\Bigg[\sum_{q=1,2,3,5} a_q\,(-c)^q\,\varepsilon^{q-1}\frac{\partial^q e_1}{\partial\xi^q} + \sum_{q=1,3} b_q\,c^q\,\varepsilon^{q-1}\frac{\partial^q\sigma_1^{(ef)}}{\partial\xi^q}\Bigg]\,.$$

Note that here we keep (as Nikolaevskiy did in (Nikolaevskiy, 2008)) the higher powers of ε to represent small corrections to the leading terms. These corrections will eventually translate into small corrections in the derived Nikolaevskiy equation further in this chapter; they will be the object of our study. Thus,

$$\frac{\partial\sigma_2^{(ef)}}{\partial\xi} - E_2\frac{\partial e_2}{\partial\xi} - \beta^{(s)}\,k_b\frac{\partial p_2}{\partial\xi} = \frac{\partial T}{\partial\xi}\,. \tag{4.39}$$

From (4.12) in the order $\sim \varepsilon^2$ we get

$$\frac{\partial}{\partial\xi}(ce_2 + v_2) = F\,,$$

$$F = -\frac{1}{c}\left(\frac{1}{2}\frac{\partial v_1}{\partial\tau} + \frac{\partial v_1 v_1}{\partial\xi}\right). \tag{4.40}$$

Therefore,

$$\frac{\partial e_2}{\partial\xi} = \frac{F}{c} - \frac{1}{c}\frac{\partial v_2}{\partial\xi}\,. \tag{4.41}$$

Substituting (4.41) into (4.39) we obtain,

$$\frac{\partial}{\partial\xi}\left(c\sigma_2^{(ef)} + E_2 v_2 - c\beta^{(s)}\,k_b\,p_2\right) = E_2 F + c\frac{\partial T}{\partial\xi}\,. \tag{4.42}$$

From the momentum equations (4.4) for the solid and liquid, we get

$$(1-m_0)\rho_0^{(s)}\,c\,\frac{\partial v_2}{\partial\xi} + \frac{\partial\sigma_2^{(ef)}}{\partial\xi} - (1-m_0)\frac{\partial p_2}{\partial\xi} = \Sigma_1\,, \tag{4.43}$$

where

$$\Sigma_1 = (1-m_0)\rho_0^{(s)}\left(\frac{1}{2}\frac{\partial v_1}{\partial\tau} + \frac{\partial v_1 v_1}{\partial\xi}\right) - (1-m_0)\rho_1^{(s)}c\frac{\partial v_1}{\partial\xi}$$
$$+m_1\rho_0^{(s)}c\frac{\partial v_1}{\partial\xi} - m_1\frac{\partial p_1}{\partial\xi} + \varepsilon^{\gamma-1}\delta m_0 v_1$$

and

$$m_0\rho_0^{(f)}\,c\,\frac{\partial u_2}{\partial\xi} - m_0\frac{\partial p_2}{\partial\xi} = \Sigma_2\,, \tag{4.44}$$

where

$$\Sigma_2 = m_0\rho_0^{(f)}\left(\frac{1}{2}\frac{\partial u_1}{\partial\tau} + \frac{\partial u_1 u_1}{\partial\xi}\right) - m_0\rho_1^{(f)}c\frac{\partial u_1}{\partial\xi}$$
$$-m_1\rho_0^{(f)}c\frac{\partial u_1}{\partial\xi} + m_1\frac{\partial p_1}{\partial\xi} - \varepsilon^{\gamma-1}\delta m_0 u_1\,.$$

Due to the condition (4.13), the combination of (4.43) with (4.44) gives

$$\rho_0\,c\,\frac{\partial v_2}{\partial\xi} + \frac{\partial\sigma_2^{(ef)}}{\partial\xi} - \frac{\partial p_2}{\partial\xi} = \Sigma\,, \tag{4.45}$$

where $\Sigma = \Sigma_1 + \Sigma_2$, so that

$$\Sigma = \rho_0\left(\frac{1}{2}\frac{\partial v_1}{\partial\tau} + \frac{\partial v_1 v_1}{\partial\xi}\right) - c((1-m_0)\rho_0^{(s)}\beta^{(s)} + m_0\rho_0^{(L)}\beta^{(L)}\kappa_1)\frac{\partial p_1 v_1}{\partial\xi}$$

$$+c\rho_0^{(s)}\beta^{(s)}\frac{\partial\sigma_1^{(ef)}v_1}{\partial\xi}+c\,\rho_0^{(L)}\,4\pi n_0 m_0\kappa_2 R_0^3\frac{\partial R_1 v_1}{\partial\xi}+c(\rho_0^{(s)}-\kappa_1\kappa_2\rho_0^{(L)})\frac{\partial m_1 v_1}{\partial\xi}\,.$$

Equations (4.42) and (4.45) result in

$$\frac{\partial}{\partial\xi}\left[(E_2-\rho_0\,c^2)v_2+(1-\beta^{(s)}\,k_b)c\,p_2\right]=E_2F-c\Sigma+c\frac{\partial T}{\partial\xi}\,. \tag{4.46}$$

From the bubble equation (4.5), in the order $\sim\varepsilon^2$,

$$\begin{gathered}\frac{-\mu\,c}{\rho_0^{(L)}\kappa_2}\left(4+\frac{m_0R_0^2}{\ell}\right)\frac{\partial R_1}{\partial\xi}=\\ \frac{1}{\rho_0^{(L)}\kappa_2}\left[\frac{\beta^{(L)}\,p_0\chi}{\kappa_2}p_1\,R_1+\frac{\beta^{(L)}}{\kappa_2}p_1^2+\frac{p_0\chi(\chi+1)}{2}\,R_1^2-p_0\chi\,R_2-p_2\right]\,.\end{gathered} \tag{4.47}$$

We re-write equation (4.47) as

$$p_2=\Gamma-p_0\chi\,R_2\,, \tag{4.48}$$

where

$$\Gamma=\mu c\left(4+\frac{m_0R_0^2}{\ell}\right)\frac{\partial R_1}{\partial\xi}+\frac{\beta^{(L)}\,p_1}{\kappa_2}(\,p_0\chi\,R_1+p_1)+\frac{p_0\chi(\chi+1)}{2}\,R_1^2\,.$$

Now we substitute the value of p_2 from (4.48) into (4.46) to get

$$\frac{\partial}{\partial\xi}\left[(E_2-\rho_0\,c^2)v_2-(1-\beta^{(s)}\,k_b)p_0\,\chi\,R_2\,c\right]=E_2F-c\Sigma+c\frac{\partial T}{\partial\xi}-c(1-\beta^{(s)}\,k_b)\frac{\partial\Gamma}{\partial\xi}\,. \tag{4.49}$$

In the second order the mass balances (4.4) for the solid and liquid-gas mixture have the form

$$\frac{\partial}{\partial\xi}\Big((1-m_0)v_2-[(1-m_0)\beta^{(s)}p_2-\beta^{(s)}\sigma_2^{(ef)}-m_2]c\Big)=\Lambda^{(s)}/\rho_0^{(s)}\,, \tag{4.50}$$

$$\begin{gathered}\frac{\partial}{\partial\xi}\left(m_0u_2-\left[m_2+\frac{m_0\beta^{(L)}p_2}{\kappa_2}-\frac{4\pi\,m_0\,n_0R_0^3(R_2+R_1^2)}{\kappa_1}\right.\right.\\ \left.\left.+\frac{4\pi\,m_0\,n_0R_0^3\,p_0\,\chi\,\beta^{(L)}R_1^2}{\kappa_1\kappa_2}\right]c\right)=\Lambda^{(L)}/\rho_0^{(L)}\,,\end{gathered} \tag{4.51}$$

where

$$\begin{gathered}\Lambda^{(s)}=\rho_0^{(s)}\frac{1}{2}\frac{\partial}{\partial\tau}\left[(m_1-(1-m_0)\,\beta^{(s)}p_1+\,\beta^{(s)}\sigma_1^{(ef)})\right]\\ +\rho_0^{(s)}\frac{\partial}{\partial\xi}\left[m_1v_1-((1-m_0)p_1+\sigma_1^{(ef)})\beta^{(s)}v_1-c\beta^{(s)}m_1\left(p_1-\frac{\sigma_1^{(ef)}}{(1-m_0)}\right)\right]\,,\end{gathered} \tag{4.52}$$

$$\begin{aligned}\Lambda^{(L)} &= -\rho_0^{(L)}\frac{1}{2}\frac{\partial}{\partial\tau}\left[\kappa_1\left(m_1\kappa_2 + m_0\beta^{(L)}p_1\right) - 4\pi n_0\kappa_2 R_0^3 R_1\right] \\ +\rho_0^{(L)}\frac{\partial}{\partial\xi}&\left[\left(\beta^{(L)}\kappa_1 p_1 - 4\pi n_0\kappa_2 R_0^3 R_1\right)(cm_1 - m_0 u_1)\right] - \kappa_1\kappa_2\rho_0^{(L)}\frac{\partial m_1 u_1}{\partial\xi}\,.\end{aligned} \tag{4.53}$$

The combination of (4.50) and (4.51) gives

$$\begin{aligned}\frac{\partial}{\partial\xi}\Bigg[v_2 - \Bigg(&\frac{(\beta + (1-m_0)\beta^{(s)}\beta^{(L)}p_0)p_2}{\kappa_2} - \beta^{(s)}\sigma_2^{(ef)} - \frac{4\pi\, m_0\, n_0 R_0^3(R_2 + R_1^2)}{\kappa_1} \\ &+\frac{4\pi\, m_0\, n_0 R_0^3\, p_0\,\chi\,\beta^{(L)}R_1^2}{\kappa_1\kappa_2}\Bigg)c\Bigg] = \Lambda\,,\end{aligned} \tag{4.54}$$

where

$$\Lambda \equiv (\Lambda^{(s)}/\rho_0^{(s)}) + (\Lambda^{(L)}/\rho_0^{(L)})\,.$$

From equation (4.42) we have

$$\frac{\partial\sigma_2^{(ef)}}{\partial\xi} = \frac{\partial}{\partial\xi}\left(T + k_b\,\beta^{(s)}\,\Gamma - k_b\beta^{(s)}\,p_0\,\chi\,R_2 - \frac{E_2}{c}v_2\right) + \frac{1}{c}E_2 F\,. \tag{4.55}$$

Now we insert (4.55) and the value of p_2 represented by (4.48), into equation (4.54),

$$\begin{aligned}\frac{\partial}{\partial\xi}&\left[(1 - E_2\beta^{(s)})v_2 - \left(\omega_1 p_0\chi - \frac{4\pi\, m_0 n_0 R_0^3}{\kappa_1}\right)R_2\, c\right] \\ &= \Lambda - \beta^{(s)}E_2 F - c\beta^{(s)}\frac{\partial T}{\partial\xi} - c\omega_1\frac{\partial\Gamma}{\partial\xi} + c\omega_2\frac{\partial R_1^2}{\partial\xi}\,,\end{aligned} \tag{4.56}$$

where

$$\begin{aligned}\omega_1 &= k_b\beta^{(s)}\beta^{(s)} + \frac{(\beta + (1-m_0)\beta^{(s)}\beta^{(L)}p_0)}{\kappa_2}\,, \\ \omega_2 &= \frac{4\pi\, m_0\, n_0 R_0^3\,\beta^{(L)}p_0\,\chi}{\kappa_1\kappa_2} - \frac{4\pi\, m_0\, n_0 R_0^3}{\kappa_1}\,.\end{aligned}$$

The determinant of the left-hand side of the system of equations (4.49) and (4.56) coincides with the determinant of (4.35), which equals zero. A non-zero solution for v_2 exists only if the following compatibility condition takes place,

$$\begin{vmatrix}(E_2 - \rho_0\, c^2) & \frac{\partial}{\partial\xi}\left(E_2 F - c\Sigma + c\frac{\partial T}{\partial\xi} - (1 - \beta^{(s)}\,k_b)c\frac{\partial\Gamma}{\partial\xi}\right) \\ (1 - E_2\beta^{(s)}) & \frac{\partial}{\partial\xi}[\Lambda - \beta^{(s)}E_2 F - c\beta^{(s)}\frac{\partial T}{\partial\xi} - c\omega_1\frac{\partial\Gamma}{\partial\xi} + c\omega_2\frac{\partial R_1^2}{\partial\xi}]\end{vmatrix} = 0 \tag{4.57}$$

(see Appendix C). This is the evolution equation with respect to $v \cong v_1$:

$$cM\frac{\partial \Gamma}{\partial \xi} - cN\frac{\partial T}{\partial \xi} + c\omega_2\psi\frac{\partial R_1^2}{\partial \xi} + \Lambda\psi + c\Sigma(1 - E_2\beta^{(s)}) - E_2FN = 0\,, \tag{4.58}$$

where

$$\psi = (E_2 - \rho_0 c^2)\,,\; M = (1 - \beta^{(s)}\,k_b)(1 - E_2\beta^{(s)}) - \omega_1\psi\,,\; N = (1 - \beta^{(s)}\rho_0\,c^2)\,.$$

Now, we re-write equation (4.58) in terms of v and re-group,

$$\begin{aligned}
&\frac{1}{2}\Big[Y_1 + \psi\Big((1 - \kappa_1\kappa_2)\bar{m}_1 - E_2\beta^{(s)} - \Big(Y_2 + \frac{4\pi\, n_0 R_0^3}{p_0\chi}\Big)Z_1\Big)\Big]\frac{\partial v}{\partial \tau} \\
-&\left[N\eta c^2(a_1 - b_1(E_2 - k_b\beta^{(s)}Z_1)) + \frac{MZ_1\mu c^2}{p_0\chi}\left(4 + \frac{m_0R_0^2}{\ell}\right)\right]\frac{\partial^2 v}{\partial \xi^2} + \varepsilon N\eta c^3 a_2\frac{\partial^3 v}{\partial \xi^3} \\
&-\varepsilon^2 N\eta\, c^4\left[a_3 - b_3(E_2 - k_b\beta^{(s)}Z_1)\right]\frac{\partial^4 v}{\partial \xi^4} - \varepsilon^4 N\eta a_5\, c^6\frac{\partial^6 v}{\partial \xi^6} - [\zeta_1 + \zeta_2]\frac{\partial vv}{\partial \xi} = 0\,,
\end{aligned} \tag{4.59}$$

where

$$\begin{aligned}
\bar{m}_1 &= ((1 - m_0) - k_b\beta^{(s)})\beta^{(s)}Z_1 + \beta^{(s)}E_2 - (1 - m_0)\,, \\
Y_1 &= \big(E_2N + c^2\rho_0(1 - E_2\beta^{(s)})\big)\,,\; Y_2 = m_0(\kappa_1\beta^{(L)} - \beta^{(s)}) + \beta^{(s)}(1 - \beta^{(s)}k_b)\,, \\
\zeta_1 &= \psi\Big(\bar{m}_1 - (1 - m_0)\beta^{(s)}Z_1 + \beta^{(s)}(E_2 - k_b\beta^{(s)}Z_1)(1 - \bar{m}_1) - \beta^{(s)}Z_1\bar{m}_1 \\
&+ \kappa_1\beta^{(L)}Z_1\bar{m}_1 - \kappa_1\kappa_2 + 4\pi\, n_0\kappa_2 R_0^3\frac{Z_1}{p_0\chi}(\bar{m}_1 - m_0) - m_0\kappa_1\beta^{(L)}Z_1 + \omega_2\frac{Z_1^2}{(p_0\chi)^2}\Big)\,, \\
\zeta_2 &= c^2(1 - E_2\beta^{(s)})\Big(\rho_0 - \rho_0\kappa_1\beta Z_1 - \rho_0^{(s)}\beta^{(s)}(E_2 - k_b\beta^{(s)}Z_1) - m_0\kappa_2\rho^{(L)}\frac{Z_1}{p_0\chi} \\
&+ \bar{m}_1(\rho^{(s)} - \kappa_1\kappa_2\rho^{(L)})\Big) + \frac{M(\chi + 1)}{2p_0\chi}Z_1^2 + E_2N\,.
\end{aligned}$$

In short the evolution equation (4.59) can be written as

$$C_1\frac{\partial v}{\partial \tau} - C_2\frac{\partial^2 v}{\partial \xi^2} + \varepsilon C_3\frac{\partial^3 v}{\partial \xi^3} - \varepsilon^2 C_4\frac{\partial^4 v}{\partial \xi^4} - \varepsilon^4 C_6\frac{\partial^6 v}{\partial \xi^6} - \zeta\frac{\partial vv}{\partial \xi} = 0\,, \tag{4.60}$$

where

$$\begin{aligned}
C_1 &= \frac{1}{2}\Big[Y_1 + \psi\Big((1 - \kappa_1\kappa_2)\bar{m}_1 - E_2\beta^{(s)} - \Big(Y_2 + \frac{4\pi\, n_0 R_0^3}{p_0\chi}\Big)Z_1\Big)\Big]\,, \\
C_2 &= \left[N\eta c^2(a_1 - b_1(E_2 - k_b\beta^{(s)}Z_1)) + \frac{MZ_1\mu c^2}{p_0\chi}\left(4 + \frac{m_0R_0^2}{\ell}\right)\right]\,,\; C_3 = N\eta c^3 a_2 \\
C_4 &= N\eta\, c^4(a_3 - b_3(E_2 - k_b\beta^{(s)}Z_1))\,,\; C_6 = N\eta a_5\, c^6\,,\; \zeta = \zeta_1 + \zeta_2\,.
\end{aligned}$$

4.4 Elastic waves in saturated media without gas bubbles

Our goal is to study the effect of inclusion of gas bubbles into the rheological model, on the elastic wave decay. For this purpose we will remove the bubble-representing segment from Figure 4.2 and re-derive the wave equation (note that our rheological model consists of only two branches: one for the solid and the other for the bubble-fluid mixture). This differs from the original Nikolaevskiy model, which includes three parallel branches (Nikolaevskiy, 1989, 2008).

4.4.1 Stress-strain relation

By removing the bubble segment from the rheological model in Figure 4.2 we get Figure 4.3, for which we derive the following stress-strain relation (Nikolaevskiy, 1985),

$$\sigma + \theta \frac{d\sigma}{dt} = E_2 e + (E_1 + E_2)\theta \frac{de}{dt} + M_2 \frac{d^2 e}{dt^2} + (M_1 + M_2)\theta \frac{d^3 e}{dt^3}\,, \tag{4.61}$$

where $\theta = \mu_1 / E_1$. This equation was discussed in detail in Chapter 1.

Hence, the constitutive law (4.61) will written as,

$$\begin{aligned} &\sigma^{(ef)} + b_1\, \varepsilon \left(\frac{1}{2}\varepsilon \frac{\partial}{\partial \tau} + (v - c)\frac{\partial}{\partial \xi} \right) \sigma^{(ef)} \\ &= E_2 e + \beta^{(s)} k_b\, p + \sum_{q=1}^{3} a_q\, \varepsilon^q \left(\frac{1}{2}\varepsilon \frac{\partial}{\partial \tau} + (v - c)\frac{\partial}{\partial \xi} \right)^q e\,, \end{aligned} \tag{4.62}$$

where

$$a_1 = (E_1 + E_2)\,\theta, \quad a_2 = M_2\,, \quad a_3 = (M_1 + M_2)\,\theta\,, \quad b_1 = \theta\,.$$

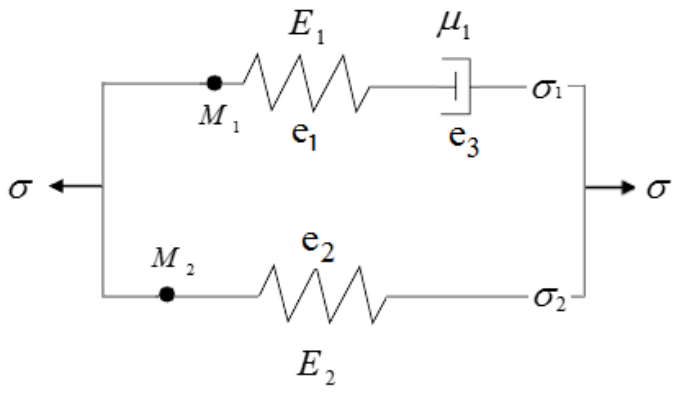

Figure 4.3: Rheological scheme without gas bubble.

Note that the stress-strain relation (4.61) can be obtained directly from the relation (4.10). Assuming $\mu_2 = \infty$ (rigid bar instead of friction piston) and $M_3 = 0$ (no mass) in (4.10), equation (4.61) takes the form

$$(E_1\,E_3)\frac{1}{\mu_1}\,\sigma + (E_3+E_1)\frac{d\sigma}{dt} = (E_1\,E_2\,E_3)\frac{1}{\mu_1}e + [(E_2+E_1)E_3 + E_1E_2]\frac{de}{dt} + E_1\,E_3\,M_2\frac{1}{\mu_1}\frac{d^2e}{dt^2} + [(E_3+E_1)M_2 + E_3M_1]\,\frac{d^3e}{dt^3}\,, \tag{4.63}$$

Now dividing by E_1 and E_3 and assuming $E_3 = \infty$ (rigid bar instead of spring), one gets the same stress-strain relation (4.61)

$$\sigma + \frac{\mu_1}{E_1}\frac{d\sigma}{dt} = E_2e + (E_2+E_1)\frac{\mu_1}{E_1}\frac{de}{dt} + M_2\frac{d^2e}{dt^2} + (M_1+M_2)\frac{\mu_1}{E_1}\frac{d^3e}{dt^3}\,. \tag{4.64}$$

4.4.2 First approximation for the system without gas bubbles

The first approximations for the momentum and mass-balance equations without gas bubbles are the same as for the system (4.4). As for the density equations, the

solid density remains unchanged but for gas-liquid mixture we neglect the volume gas content ϕ in equation (4.8),

$$\rho^{(f)} = \rho^{(L)} = \rho_0^{(L)}(1 + \beta^{(L)}p)\,. \tag{4.65}$$

The first approximation of (4.65) is

$$\rho_1^{(L)} = \rho_0^{(L)}\beta^{(L)}p_1\,. \tag{4.66}$$

Inserting this into the mass equation for the fluid (4.19), we get

$$m_0 u_1 = \left[m_1 + m_0\beta^{(L)}p_1\right] c\,. \tag{4.67}$$

Now, the combination of (4.22) and (4.67) yields

$$(1 - m_0)v_1 + n_0 u_1 = \left[(1 - m_0)\beta^{(s)}p_1 - \beta^{(s)}\sigma_1^{(ef)} + m_0\beta^{(L)}p_1\right] c\,. \tag{4.68}$$

Due to the condition (4.13), equation (4.68) becomes

$$v_1 = \left[(1 - m_0)\beta^{(s)}p_1 - \beta^{(s)}\sigma_1^{(ef)} + m_0\beta^{(L)}p_1\right] c\,. \tag{4.69}$$

After we apply the conditions

$$v_1 = u_1, \quad \rho_0 = (1 - m_0)\,\rho_0^{(s)} + m_0\,\rho_0^{(L)}$$

the first two equations in (4.19) give

$$\rho_0\, c\, v_1 = -\sigma_1^{(ef)} + p_1\,. \tag{4.70}$$

The first approximation of relation (4.62) is

$$\sigma_1^{(ef)} - E_2\, e_1 - \beta^{(s)}\, k_b p_1 = \sum_{q=1}^{3} a_q\,(-c)^q\,\varepsilon^{q-1}\frac{\partial^q e_0}{\partial\xi^q} + \, b_1\, c\frac{\partial\sigma_0^{(ef)}}{\partial\xi}\,. \tag{4.71}$$

Equations (4.71) and (4.27) result in the integral

$$\sigma_1^{ef} = -\frac{E_2 v_1}{c} + \beta^{(s)}k_b p_1\,. \tag{4.72}$$

Substituting (4.72) into (4.69), we get

$$(1-\beta^{(s)}E_2)v_1 = c(1-m_0)\beta^{(s)}\,p_1 + c\,m_0\beta^{(L)}p_1 - \beta^{(s)}\beta^{(s)}k_b\,c\,p_1\,. \tag{4.73}$$

As $\beta = (1-m_0)\beta^{(s)} + m_0\beta^{(L)}$, equation (4.73) becomes

$$(1-\beta^{(s)}E_2)v_1 = (\beta - \beta^{(s)}\beta^{(s)}k_b)c\,p_1\,. \tag{4.74}$$

From (4.70) we obtain

$$\sigma_1^{(ef)} = p_1 - \rho_0\,c\,v_1\,. \tag{4.75}$$

Therefore, the combination of (4.75) with (4.72) yields

$$(\rho_0\,c^2 - E_2)v_1 = (1-\beta^{(s)}k_b)c\,p_1\,. \tag{4.76}$$

The determinant of the system of equations (4.74) and (4.76) gives the wave velocity c,

$$\begin{vmatrix} (1-\beta^{(s)}E_2) & -(\beta - \beta^{(s)}\beta^{(s)}k_b) \\ (\rho_0\,c^2 - E_2) & -(1-\beta^{(s)}k_b) \end{vmatrix} = 0\,. \tag{4.77}$$

Thus,

$$c^2 = \frac{E_2 + Z_2(1-\beta^{(s)}k_b)}{\rho_0}\,, \tag{4.78}$$

where

$$Z_2 = \frac{(1-\beta^{(s)}E_2)}{(\beta - \beta^{(s)}\beta^{(s)}k_b)}\,.$$

Again we can express all the variables through the velocity v_1,

$$\begin{gathered} e_1 = -\frac{v_1}{c}, \quad \rho_1^{(s)} = \rho^{(s)}\beta^{(s)}[Z_2(1-\beta^{(s)}k_b) + E_2]\frac{v_1}{c}, \quad \rho_1^{(L)} = \rho^{(L)}\beta^{(L)}Z_2\frac{v_1}{c}\,, \\ p_1 = Z_2\frac{v_1}{c}, \quad m_1 = [(1-m_0)\beta^{(s)}Z_2 + \beta^{(s)}(E_2 - \beta^{(s)}k_bZ_2) - (1-m_0)]\frac{v_1}{c}\,, \\ \sigma_1^{(ef)} = -(E_2 - \beta^{(s)}k_bZ_2)\frac{v_1}{c}\,. \end{gathered} \tag{4.79}$$

4.4.3 Second approximation for the system without gas bubbles

In the second approximation for the system without the bubbles we again arrive at an equation of the form (4.46), except the formulas for Σ and T are changed,

$$\frac{\partial}{\partial\xi}\left[(E_2-\rho_0\,c^2)v_2+(1-\beta^{(s)}\,k_b)c\,p_2\right]=E_2F-c\Sigma+c\frac{\partial T}{\partial\xi}\,, \tag{4.80}$$

where

$$\Sigma=\rho_0\Big(\frac{1}{2}\frac{\partial v_1}{\partial\tau}+\frac{\partial v_1v_1}{\partial\xi}\Big)-c\rho_0\beta\frac{\partial p_1v_1}{\partial\xi}+c\rho_0^{(s)}\beta^{(s)}\frac{\partial\sigma_1^{(ef)}v_1}{\partial\xi}+c(\rho_0^{(s)}-\rho_0^{(L)})\frac{\partial m_1v_1}{\partial\xi}\,,$$

$$T=\sum_{q=1}^{3}a_q\,(-c)^q\,\varepsilon^{q-1}\frac{\partial^q e_1}{\partial\xi^q}+\,b_1\,c\frac{\partial\sigma_1^{(ef)}}{\partial\xi}\,.$$

The second approximation of the mass balance for the sold is the same as (4.50), while for the fluid it takes the form

$$\frac{\partial}{\partial\xi}\Big[m_0u_2-(m_2+m_0\beta^{(L)}p_2)c\Big]=\Lambda^{(L)}/\rho_0^{(L)}\,, \tag{4.81}$$

where

$$\Lambda^{(L)}=-\frac{1}{2}\rho_0^{(L)}\frac{\partial}{\partial\tau}\left[m_1+m_0\beta^{(L)}p_1\right]+\rho_0^{(L)}\frac{\partial}{\partial\xi}\left[cm_1\beta^{(L)}p_1-m_0\beta^{(L)}p_1u_1-m_1u_1\right]\,.$$

The combination of (4.50) and (4.81) results in

$$\frac{\partial}{\partial\xi}\Big[v_2-(\beta p_2-\beta^{(s)}\sigma_2^{(ef)})c\Big]=\Lambda\,, \tag{4.82}$$

where

$$\Lambda=(\Lambda^{(s)}/\rho_0^{(s)})+(\Lambda^{(L)}/\rho_0^{(L)})\,.$$

From (4.42) we find

$$\frac{\partial\sigma_2^{(ef)}}{\partial\xi}=\frac{\partial}{\partial\xi}\Big(T+k_b\,\beta^{(s)}\,p_2-\frac{E_2}{c}v_2\Big)+\frac{1}{c}E_2F\,. \tag{4.83}$$

Substituting (4.83) into (4.82) we get

$$\frac{\partial}{\partial\xi}\left[(1-E_2\beta^{(s)})v_2-(\beta-\beta^{(s)}\beta^{(s)})c\,p_2\right]=\Lambda-\beta^{(s)}E_2F-c\beta^{(s)}\frac{\partial T}{\partial\xi}\,. \tag{4.84}$$

In analogy to (4.57), the compatibility condition for the system of equations (4.80), (4.84) has the form

$$\begin{vmatrix} (E_2 - \rho_0\, c^2) & \frac{\partial}{\partial\xi}(E_2 F - c\Sigma + c\frac{\partial T}{\partial\xi}) \\ (1 - E_2\beta^{(s)}) & \frac{\partial}{\partial\xi}(\Lambda - \beta^{(s)} E_2 F - c\beta^{(s)}\frac{\partial T}{\partial\xi}) \end{vmatrix} = 0\,. \tag{4.85}$$

Then the evolution equation for $v \cong v_1$ is

$$\Lambda\psi - cN\frac{\partial T}{\partial\xi} + c\Sigma(1 - E_2\beta^{(s)}) - E_2 F N = 0\,. \tag{4.86}$$

Rearranging, we arrive at

$$\begin{aligned} c^2\rho_0(1 - E_2\beta^{(s)})\frac{\partial v}{\partial\tau} - Nc^2(a_1 - b_1(E_2 - \beta^{(s)}k_b Z_2))\frac{\partial^2 v}{\partial\xi^2} + \varepsilon N\, a_2\, c^3\frac{\partial^3 v}{\partial\xi^3} \\ -\varepsilon^2 N a_3 c^4\frac{\partial^4 v}{\partial\xi^4} + [G_1 + G_2]\frac{\partial vv}{\partial\xi} = 0\,, \end{aligned} \tag{4.87}$$

where

$$\begin{aligned} \hat{m}_1 &= (1 - m_0)\beta^{(s)} Z_2 + \beta^{(s)}(E_2 - \beta^{(s)}k_b Z_2) - (1 - m_0)\,, \\ G_1 &= \psi\Big(- ((1 - m_0) + \hat{m}_1)\beta^{(s)} Z_2 - \beta^{(s)}(E_2 - \beta^{(s)}k_b Z_2)\Big(1 + \frac{\hat{m}_1}{(1 - m_0)}\Big) \\ &\qquad + \beta^{(L)} Z_2\hat{m}_1 - m_0\beta^{(L)} Z_2\Big)\,, \\ G_2 &= \Big(c^2(1 - E_2\beta^{(s)})\left(\rho_0 - \rho_0\beta Z_2 - \rho^{(s)}\beta^{(s)}(E_2 - \beta^{(s)}k_b Z_2) + \hat{m}_1(\rho^{(s)} - \rho^{(L)})\right) \\ &\qquad + E_2(1 - \beta^{(s)}\rho_0\, c^2)\Big)\,. \end{aligned}$$

Finally, we re-write the evolution equation (4.87) as

$$D_1\frac{\partial v}{\partial\tau} - D_2\frac{\partial^2 v}{\partial\xi^2} + \varepsilon D_3\frac{\partial^3 v}{\partial\xi^3} - \varepsilon^2 D_4\frac{\partial^4 v}{\partial\xi^4} + G\frac{\partial vv}{\partial\xi} = 0\,, \tag{4.88}$$

where

$$D_1 = c^2\rho_0(1 - E_2\beta^{(s)})\,,\ D_2 = Nc^2(a_1 - b_1(E_2 - \beta^{(s)}k_b Z_2))\,,\ D_3 = N\, a_2\, c^3\,,$$

$$D_4 = Na_3c^4\,,\ G = G_1 + G_2\,.$$

We remark that for the wave propagating to the left, that is with $\xi = \varepsilon(x + ct)$, one obtains (as we checked) the same equation (4.88).

4.5 Linearized model

In this section we investigate the linearized versions of the model with and without the bubbles, that is (4.60) and (4.88). Our particular interest is its dissipative part responsible for decay of the wave.

4.5.1 Evaluation of the parameters and the wave velocity

From (Nikolaevskiy, 1985; Carcione, 1998; Smeulders, 2005; Dunin et al., 2006; Mikhailov, 2010; Nikolaevskiy, 2016; Sutton and Biblarz, 2017), the values of the parameters are: densities, $\rho_0^{(L)} = 1000\,\mathrm{kg/m^3}$ for water, $\rho^{(g)} = 2\,\mathrm{kg/m^3}$ for gas, $\rho_0^{(s)} = 2500\,\mathrm{kg/m^3}$ for solid; porosity $m_0 = 0.25$; bulk modulus $k_b = 1.7 \times 10^9\,\mathrm{Pa}$ for matrix, $k_b = 30 \times 10^9\,\mathrm{Pa}$ for solid; compressibility $\beta^{(L)} = 2 \times 10^{-9}\,\mathrm{Pa^{-1}}$ for water, $\beta^{(L)} = 2.4 \times 10^{-6}\,\mathrm{Pa^{-1}}$ for gas, $\beta^{(s)} = 2 \times 10^{-10}\,\mathrm{Pa^{-1}}$ for solid; steady pressure $p_0 = 10^5\,\mathrm{Pa}$; bubble radius $R_0 = 5 \times 10^{-5}\,\mathrm{m}$; volume gas content $\phi_0 = 10^{-3}$; viscosities $\mu_1 = 10^{-3}\,\mathrm{Pa{\cdot}s}$ for water, $\mu_2 = 2 \times 10^{-5}\,\mathrm{Pa{\cdot}s}$ for gas; adiabatic exponent $\zeta = 1.4$, and permeability $\ell = 2 \times 10^{-11}\,\mathrm{m^2}$. Using the data from (Nikolaevskiy, 1985; Nikolaevskiy and Stepanova, 2005; Nikolaevskiy and Strunin, 2012; Nikolaevskiy, 2016), the values of the parameters of the rheological model in Figure 4.2 are

$$M_1 = \rho^{(L)}\, L_s^2 = 10^{-2}\,\mathrm{kg/m}\,,\; M_2 = \rho^{(s)}\, L_s^2 = 0.02\,\mathrm{kg/m}\,,$$

$$M_3 = \rho^{(g)}\, L_s^2 = 2 \times 10^{-6}\,\mathrm{kg/m}$$

and

$$(a) \quad E_1 = 1/\beta^{(L)} = 4 \times 10^5\,\mathrm{Pa}\,,\; E_2 = c^2\rho_0 = 2 \times 10^7\,\mathrm{Pa}\,,\; E_3 = 3\chi\, p_0 = 4 \times 10^7\,\mathrm{Pa}\,,$$

where we used, just for the purpose of evaluating of E_i and M_i, the typical velocity $c \sim 100\,\mathrm{m/s}$ and the linear size of the oscillator $L_s = 0.3\,\mathrm{cm}$ from (Nikolaevskiy, 1985; Vilchinska et al., 1985). Note that the above values of E_i are known only

approximately. With this in mind, in the present study we also explore other the values of E_i that are considerably different from variant (a).

$$(b) \quad E_1 = 5 \times 10^5 \,\mathrm{Pa}\,, \quad E_2 = 5 \times 10^8 \,\mathrm{Pa}\,, \quad E_3 = 5 \times 10^4 \,\mathrm{Pa}\,,$$

$$(c) \quad E_1 = 6 \times 10^5 \,\mathrm{Pa}\,, \quad E_2 = 2 \times 10^9 \,\mathrm{Pa}\,, \quad E_3 = 5 \times 10^3 \,\mathrm{Pa}\,.$$

The reason for this choice is that the two different rheological models that we use (for the wave with and without the bubbles), give close values of λ when we put $R_0 = 0$ and $n_0 = 0$.

Now we apply the formulas for the wave velocity (4.36) and (4.78) to show that they give reasonable orders of magnitude. For variant (a) formula (4.36) for the wave with the bubbles gives $c \approx 577\,\mathrm{m/s}$, and formula (4.78) for the wave without the bubbles gives $c \approx 2100\,\mathrm{m/s}$. For variant (b) the wave with the bubbles has the velocity $c \approx 726\,\mathrm{m/s}$ and the wave without the bubbles the velocity $c \approx 2000\,\mathrm{m/s}$. For variant (c) the wave with the bubbles has $c \approx 1100\,\mathrm{m/s}$, and the wave without the bubbles $c \approx 1800\,\mathrm{m/s}$. This illustrates, in line with the previous studies, that the bubbles may result in considerable change of the wave velocity. However, our main interest in this study is the dissipation rate of the wave, which we explore in the next section.

4.5.2 Dispersion (dissipation) relation

Analysing the linearized model, we are interested in the influence of the bubbles on the wave dissipation. This effect is controlled by the even derivatives, so we truncate the linearized equation (4.60) to the form

$$\frac{\partial v}{\partial \tau} = \frac{C_2}{C_1}\frac{\partial^2 v}{\partial \xi^2} + \varepsilon^2 \frac{C_4}{C_1}\frac{\partial^4 v}{\partial \xi^4} + \varepsilon^4 \frac{C_6}{C_1}\frac{\partial^6 v}{\partial \xi^6}\,. \tag{4.89}$$

For the Fourier modes $v \sim \exp(\lambda t + ikx)$, we get the dissipation relation

$$\lambda(k) = -\frac{C_2}{C_1}k^2 + \varepsilon^2 \frac{C_4}{C_1}k^4 - \varepsilon^4 \frac{C_6}{C_1}k^6\,, \tag{4.90}$$

where λ is the decay rate and k is the wave number. In the case without the bubbles the linearized form of equation (4.88) is

$$\frac{\partial v}{\partial \tau} = \frac{D_2}{D_1}\frac{\partial^2 v}{\partial \xi^2} + \varepsilon^2 \frac{D_4}{D_1}\frac{\partial^4 v}{\partial \xi^4}\,. \tag{4.91}$$

(we again consider only even derivatives). Then the dissipation relation is

$$\lambda(k) = -\frac{D_2}{D_1}k^2 + \varepsilon^2 \frac{D_4}{D_1}k^4\,. \tag{4.92}$$

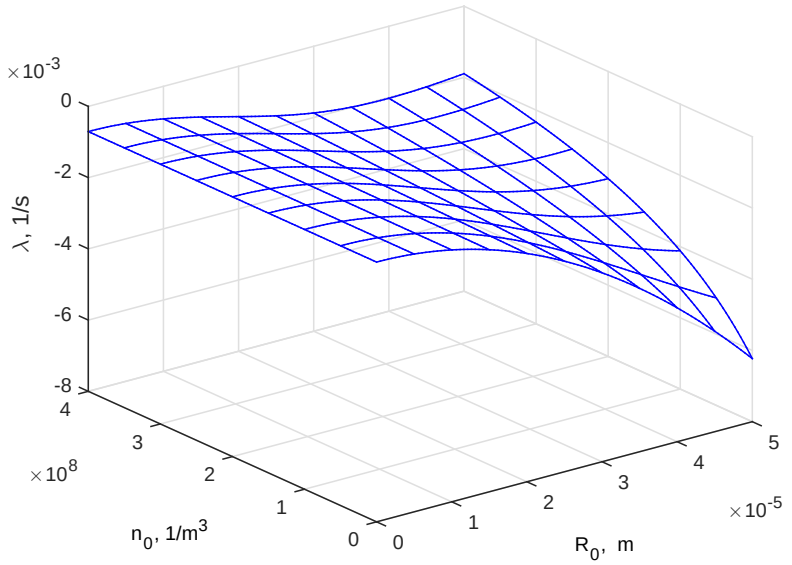

Figure 4.4: The decay rate by formula (4.90) for variant (a), $k_* = 0.25\ 1/\mathrm{m}$.

Figure 4.4 shows the decay rate by formula (4.90) at fixed $k_* = 0.25$ 1/m (Nikolaevskiy, 1989) against R_0 and n_0. See that the increase in R_0 significantly affects the decay rate and makes its absolute value larger due to the bubbles increasing their role through the pressure $p_1 = -p_0\,\chi\,R_1$. As for n_0, one should disregard the region of small n_0 in Figure 4.4 since the equations of continuum mechanics in the form adopted in the model become invalid when there are too few bubbles. This is because one can no longer assume that every fluid particle contains its own bubble (as suggested by equation (4.5)) because this would imply that the fluid particles are no longer small and, hence, the continuum mechanics description fails.

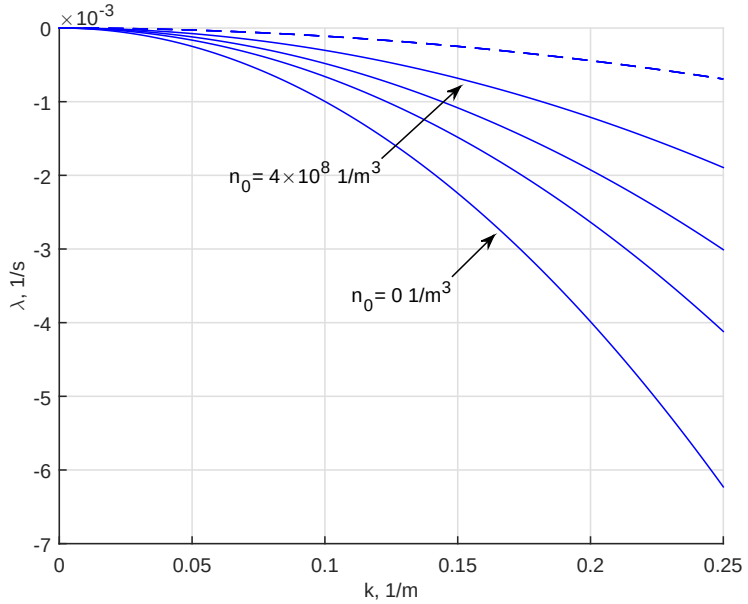

Figure 4.5: The decay rate by formulas (4.90) and (4.92) for variant (a): n_0 varies, $R_0 = 5 \times 10^{-5}$.

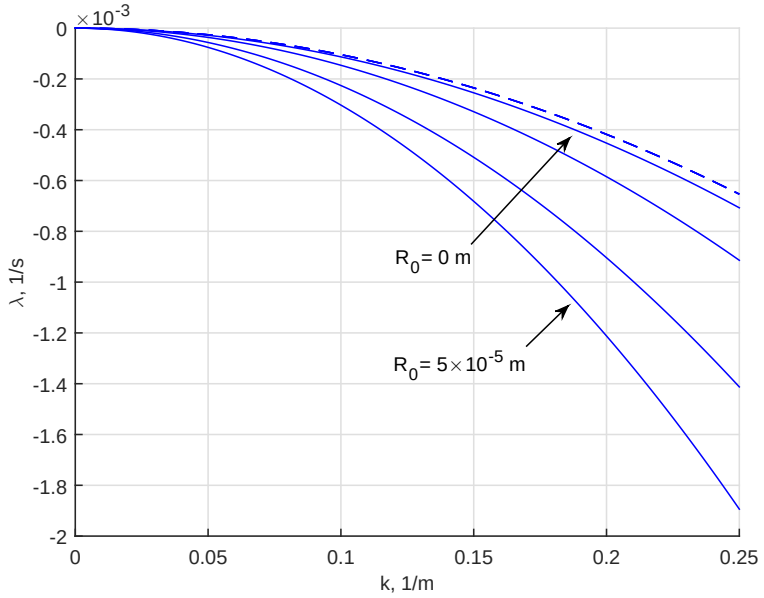

Figure 4.6: The decay rate by formulas (4.90) and (4.92) for variant (a): R_0 varies, $n_0 = 4 \times 10^8$.

Figures 4.5 and 4.6 compare the dispersion curves of the wave with the bubbles and the wave without the bubbles. The dashed line describes the case without the bubbles and the solid lines correspond to the wave with the bubbles. Figure 4.5 is for varying n_0 and fixed R_0. Figure 4.6 is for varying R_0 and fixed n_0 . The decay rate depends on the number and radius of the bubbles. We note that this result agrees with the conception discussed in (Strunin, 2014; Strunin and Ali, 2016) about the passive nature of the freely propagating elastic wave. Similar results are obtained for variants (b) and (c) as shown in Figures 4.7–4.12.

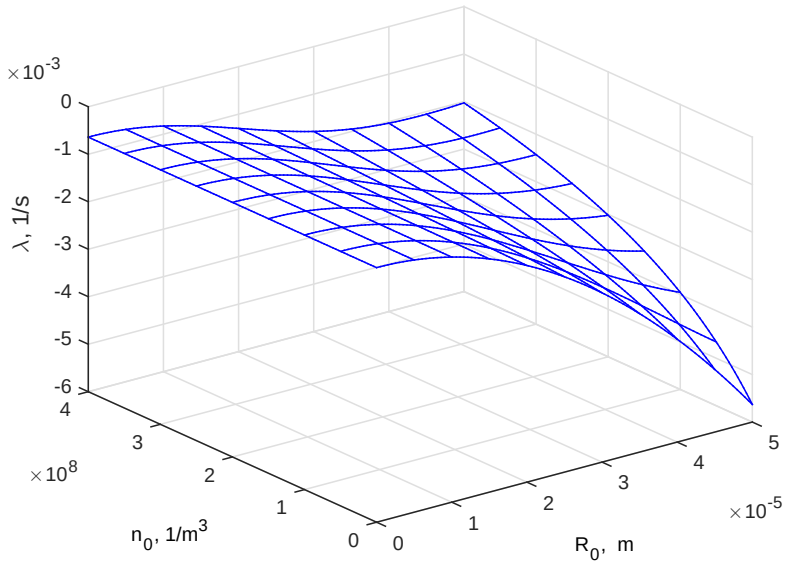

Figure 4.7: The decay rate by formula (4.90) for variant (b), $k_* = 0.25\ \ 1/\mathrm{m}$.

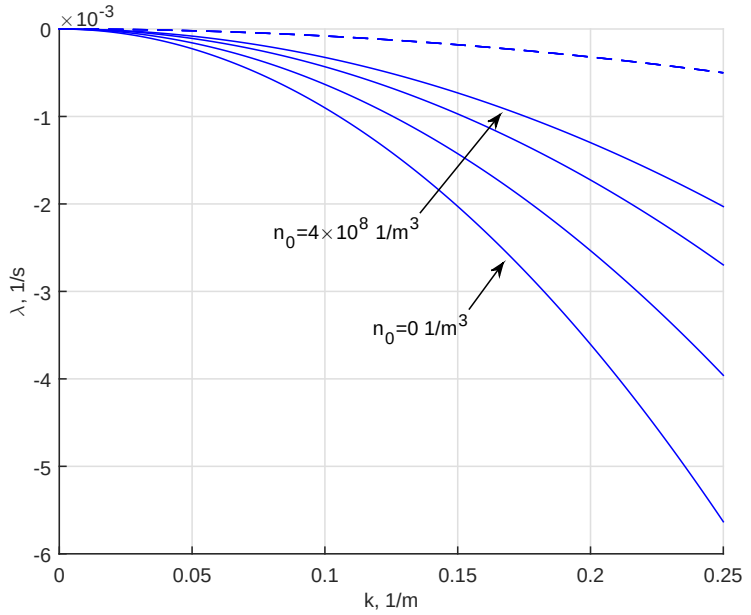

Figure 4.8: The decay rate by formulas (4.90) and (4.92) for variant (b): n_0 varies, $R_0 = 5 \times 10^{-5}$.

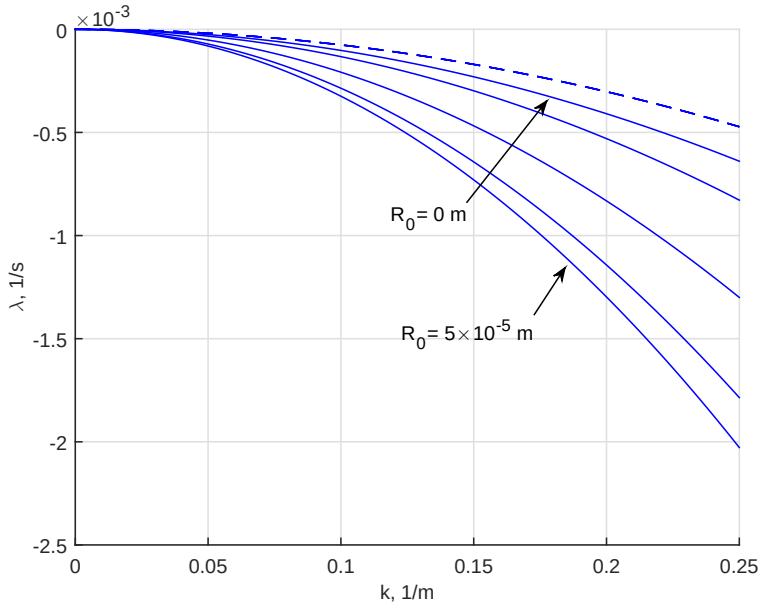

Figure 4.9: The decay rate by formulas (4.90) and (4.92) for variant (b): R_0 varies, $n_0 = 4 \times 10^8$.

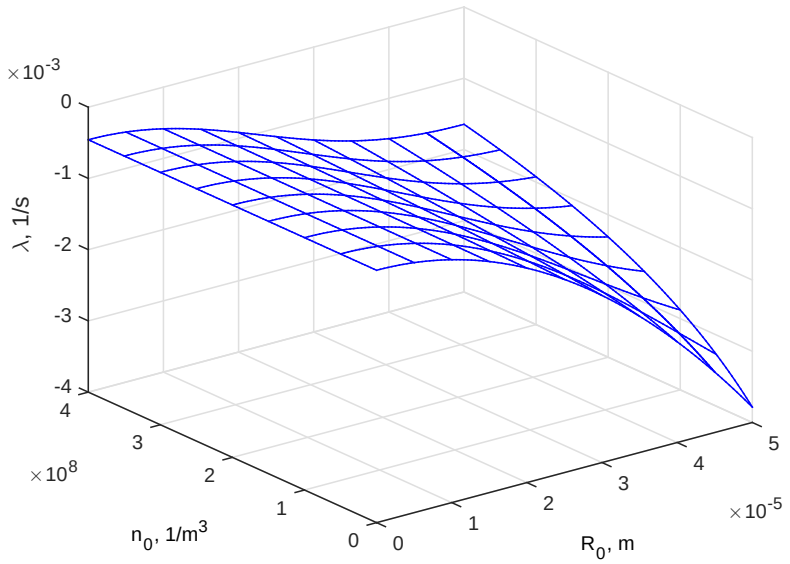

Figure 4.10: The decay rate by formula (4.90) for variant (c), for $k_* = 0.25\ 1/\mathrm{m}$.

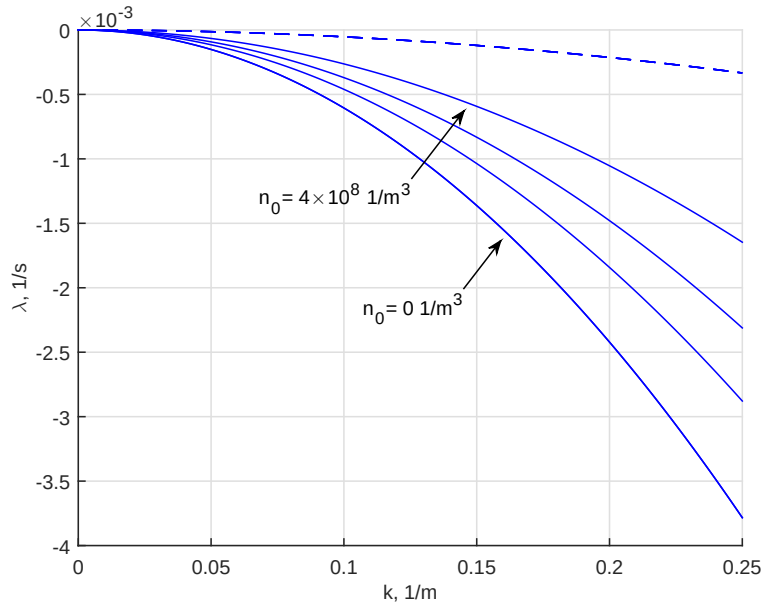

Figure 4.11: The decay rate by formulas (4.90) and (4.92) for variant (c): n_0 varies, $R_0 = 5 \times 10^{-5}$.

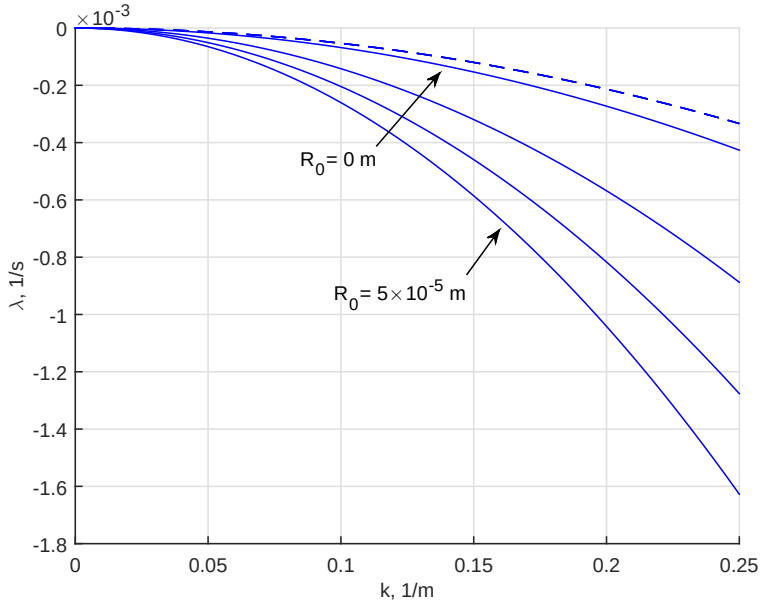

Figure 4.12: The decay rate by formulas (4.90) and (4.92) for variant (c): R_0 varies, $n_0 = 4 \times 10^8$.

For a different $k_* = 0.52$ 1/m (Beresnev and Nikolaevskiy, 1993), the results are similar, see Figures 4.13–4.15.

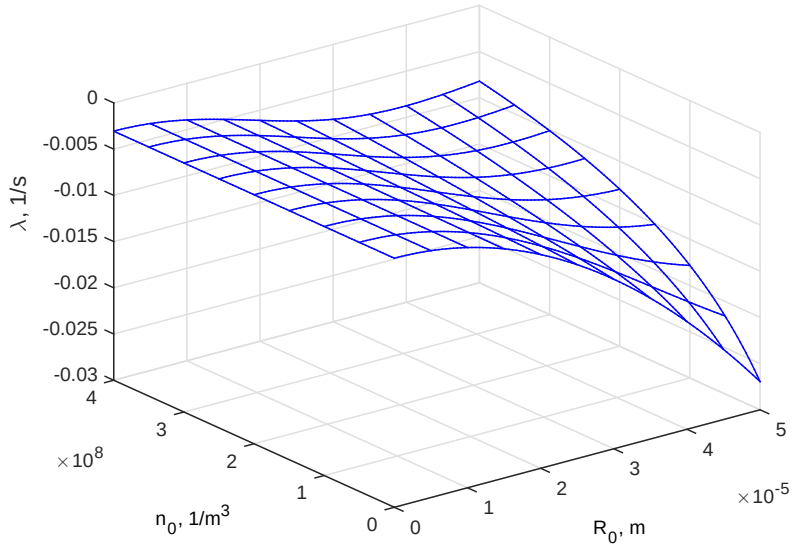

Figure 4.13: The decay rate by formula (4.90) for variant (a), $k_* = 0.52$ 1/m .

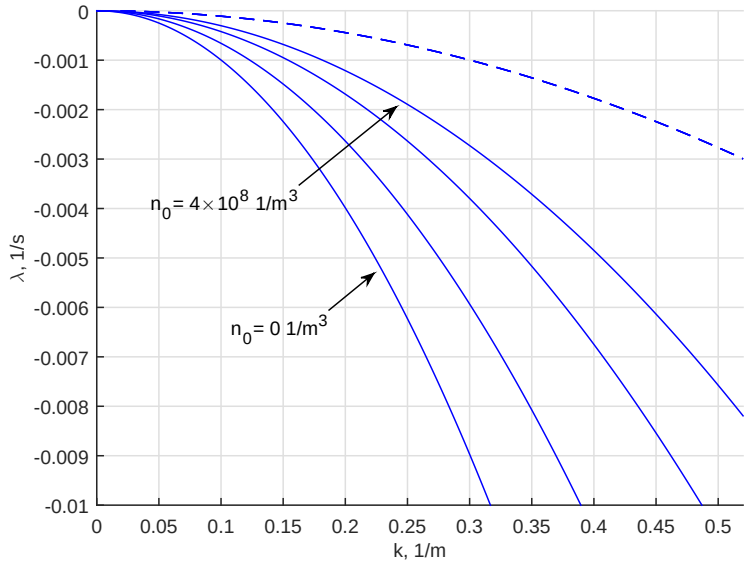

Figure 4.14: The decay rate by formulas (4.90) and (4.92) for variant (a): n_0 varies, $R_0 = 5 \times 10^{-5}$.

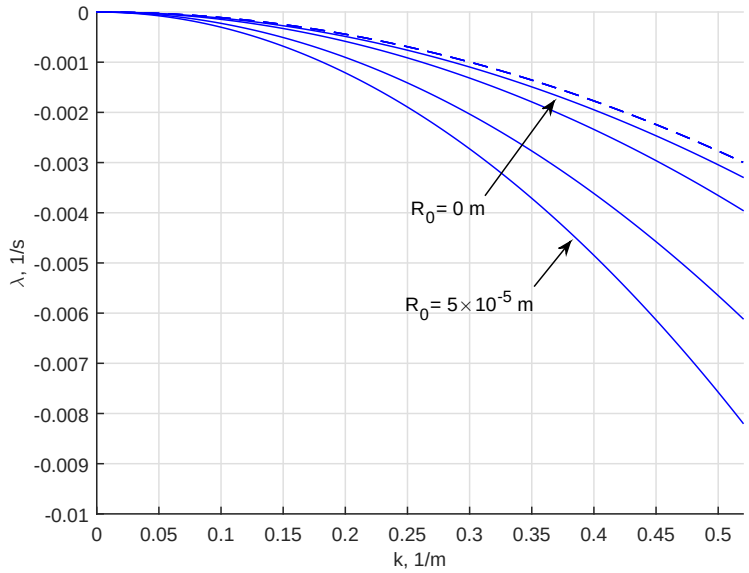

Figure 4.15: The decay rate by formulas (4.90) and (4.92) for variant (a): R_0 varies, $n_0 = 4 \times 10^8$.

4.6 Concluding remarks

We studied the effect of rheology with and without gas bubbles and of the bubble dynamics on the dissipation of elastic waves in porous solids. The Frenkel-Biot waves of P1 type are analysed in the fluid-saturated environment. Using the three-segment rheological model (with the bubbles) and two-segment model (without the bubbles), we derived the Nikolaevskiy-type equations for the velocity of the solid matrix. We compared the linearized versions of the equations in terms of the decay rate $\lambda(k)$ of the Fourier modes. For the both cases – with and without the bubbles – the $\lambda(k)$-curve lies entirely below the zero. We found out that $|\lambda(k)|$ increases with the increase of the radius of the bubbles but decreases with the increase of the number of the bubbles. The decrease manifests the opposite trend to the one observed in Chapter 3. We are inclined to consider the trend obtained in the current chapter as more realistic because of the more complete structure of the bubble element used in the rheological model.

Chapter 5

Evaluating the influence of parameters on the decay rate

SUMMARY: In this chapter, we evaluate the effect of the mechanical parameters on decay rates for the bubble-including equations derived in Chapters 3 and 4.

$$C_1\frac{\partial v}{\partial \tau} - C_2\frac{\partial^2 v}{\partial \xi^2} + \varepsilon C_3\frac{\partial^3 v}{\partial \xi^3} - \varepsilon^2 C_4\frac{\partial^4 v}{\partial \xi^4} - \varepsilon^4 C_6\frac{\partial^6 v}{\partial \xi^6} - \zeta\frac{\partial v v}{\partial \xi} = 0\,. \tag{5.1}$$

$$A_1\frac{\partial v}{\partial \tau} + A_2\frac{\partial^2 v}{\partial \xi^2} + A_N\frac{\partial v v}{\partial \xi} = 0\,. \tag{5.2}$$

5.1 Introduction

In this section, we are mainly interested in testing the effect produced by different values of mechanical parameters on the decay rate. Note that magnitudes of some of these parameters are well known, for example viscosities μ_i, while other parameters such as the masses M_i are known quite poorly. Let us re-write the dispersion relation for equation (5.1) as

$$\lambda(k) = -\frac{C_2}{C_1}k^2 + \varepsilon^2\frac{C_4}{C_1}k^4 - \varepsilon^4\frac{C_6}{C_1}k^6\,. \tag{5.3}$$

5.2 Influence of the rheological parameters

All the parameters participating in our model have their respective ranges of variation. We expect that this variation may exert influence on the wave decay rate. In this section we focus on the parameters of the rheological model in Figure 5.1. While the magnitudes of the viscosities μ_1 and μ_2 are well known from literature, the parameters M_1, M_2, M_3, E_1, E_2, E_3 can only be roughly estimated by the order of magnitude.

We choose to represent our numerical results by 3D plots of the decay rate against the radius of the bubbles R_0 and their number (concentration) n_0. The values of μ_1, and μ_2 are given in Table 5.1. As for the values of M_i and E_i, we considered their reference magnitudes specified in chapter 4 and let them vary from these magnitudes by some orders lower and higher, see Table 5.2.

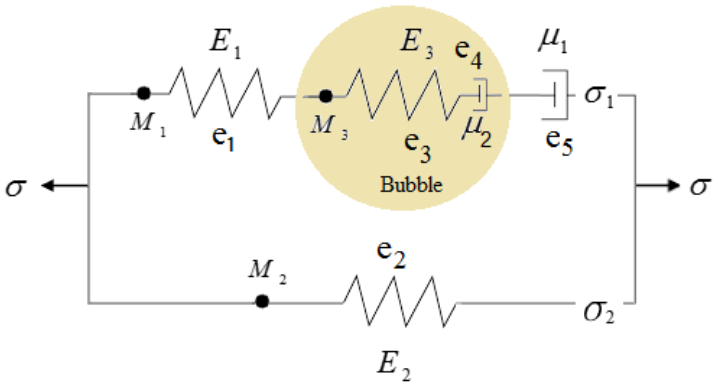

Figure 5.1: Rheological scheme including a gas bubble.

	μ_1, Pa·s	μ_2, Pa·s
1	5×10^{-3}	2×10^{-7}
2	5×10^{-3}	2×10^{-4}
3	10^{-2}	2×10^{-4}
4	10^{-2}	2×10^{-7}

Table 5.1: The values of μ_1, and μ_2 .

	E_1, Pa	E_2, Pa	E_3, Pa	M_1, kg/m	M_2, kg/m	M_3, kg/m
1	4×10^5	2×10^7	5×10^7	10^{-3}	10^{-3}	10^{-6}
2	4×10^5	2×10^9	5×10^7	10^{-3}	10^{-1}	10^{-6}
3	4×10^7	2×10^9	5×10^7	10^{-1}	10^{-1}	10^{-6}
4	4×10^7	2×10^7	5×10^7	10^{-1}	10^{-3}	10^{-6}
5	4×10^5	2×10^7	5×10^3	10^{-3}	10^{-3}	10^{-4}
6	4×10^5	2×10^9	5×10^3	10^{-3}	10^{-1}	10^{-4}
7	4×10^7	2×10^7	5×10^3	10^{-1}	10^{-3}	10^{-4}
8	4×10^7	2×10^9	5×10^3	10^{-1}	10^{-1}	10^{-4}
9	5×10^5	25×10^6	5×10^7	10^{-3}	10^{-2}	5×10^{-6}
10	5×10^5	25×10^8	5×10^7	10^{-3}	5×10^{-2}	5×10^{-6}
11	5×10^8	25×10^8	5×10^7	10^{-2}	5×10^{-2}	5×10^{-6}
12	5×10^8	25×10^6	5×10^7	10^{-2}	10^{-2}	5×10^{-6}
13	5×10^5	25×10^6	5×10^3	10^{-3}	10^{-2}	5×10^{-7}
14	5×10^5	25×10^8	5×10^3	10^{-3}	5×10^{-2}	5×10^{-7}
15	5×10^8	25×10^6	5×10^3	10^{-2}	10^{-2}	5×10^{-7}
16	5×10^8	25×10^8	5×10^3	10^{-2}	5×10^{-2}	5×10^{-7}

Table 5.2: The values of E_1, E_2, E_3, M_1, M_2, and M_3 .

The 16 rows of Table 5.2 and 4 rows of Table 5.1 give $16 \times 4 = 64$ possible graphs. However, some of these graphs are almost identical as we commented in figure captions. Figures 5.2–5.4 represent the results of using the parameter values given in Tables 5.1 and 5.2 in the formula (5.3).

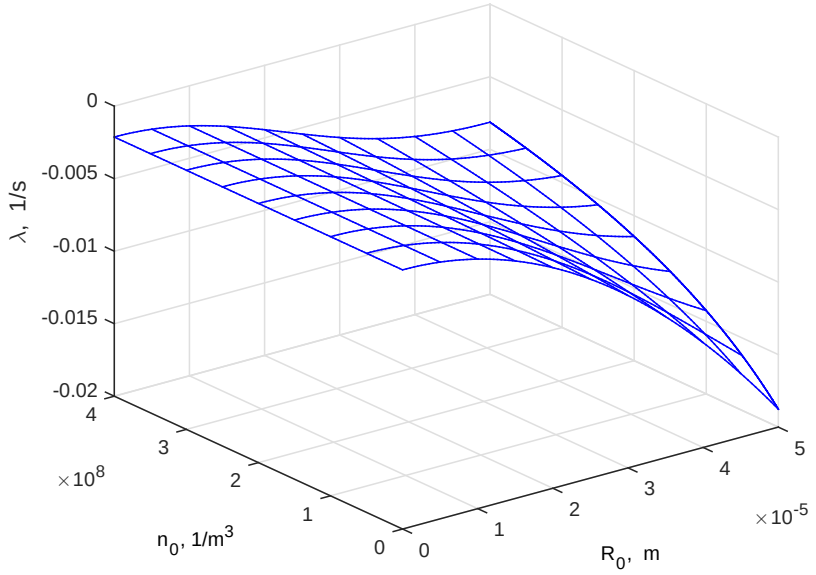

Figure 5.2: The decay rate by formula (5.3) for rows 2 of Tables 5.1 and 5.2, $k_* = 0.25$ 1/m .

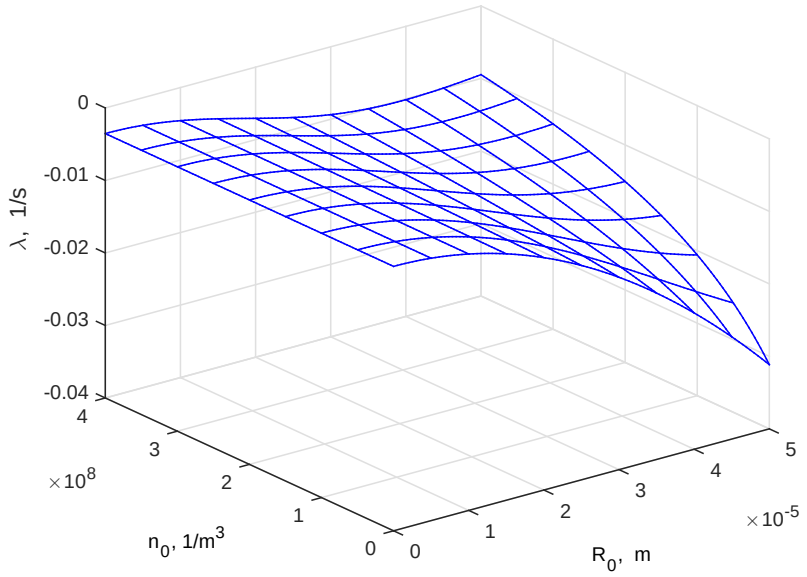

Figure 5.3: The decay rate by formula (5.3) for row 4 of Table 5.1 and row 10 of Table 5.2, $k_* = 0.25\ \ 1/\mathrm{m}$.

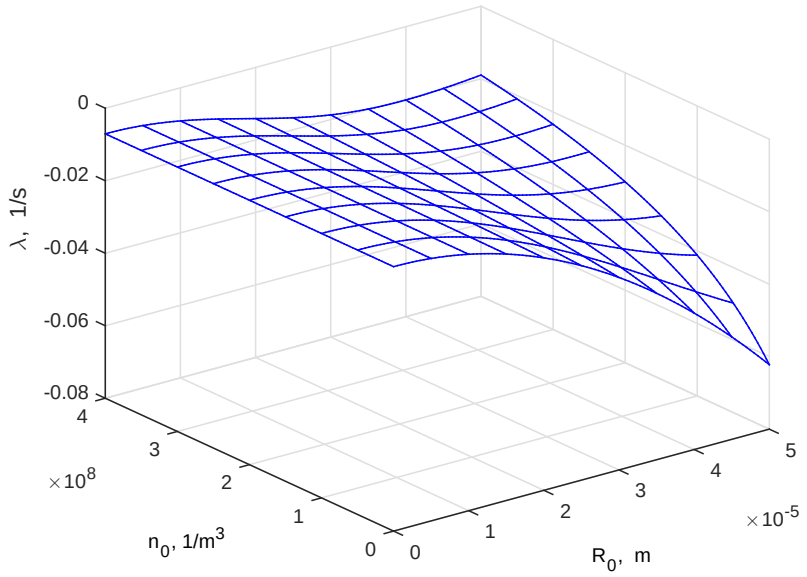

Figure 5.4: The decay rate by formula (5.3) for row 3 of Table 5.1 and row 7 of Table 5.2, $k_* = 0.25\ \ 1/\mathrm{m}$.

Furthermore, when we increased the values of n_0 to $n_0 = (4, 8) \times 10^{10}\, 1/m^3$ and R_0 to $R_0 = 10^{-4}\, m$, we obtained similar results as shown in Figures 5.5–5.14.

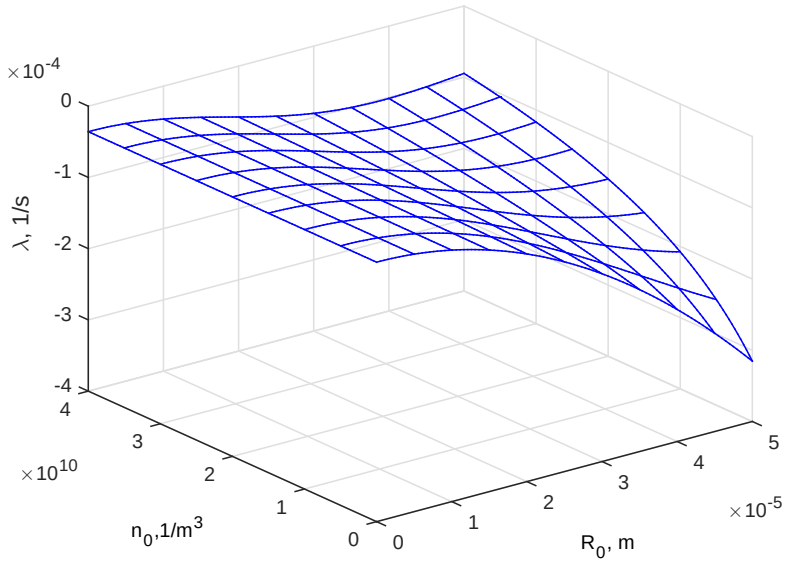

Figure 5.5: The decay rate by formula (5.3) for rows 1 of Tables 5.1 and 5.2, $k_* = 0.25$ 1/m .

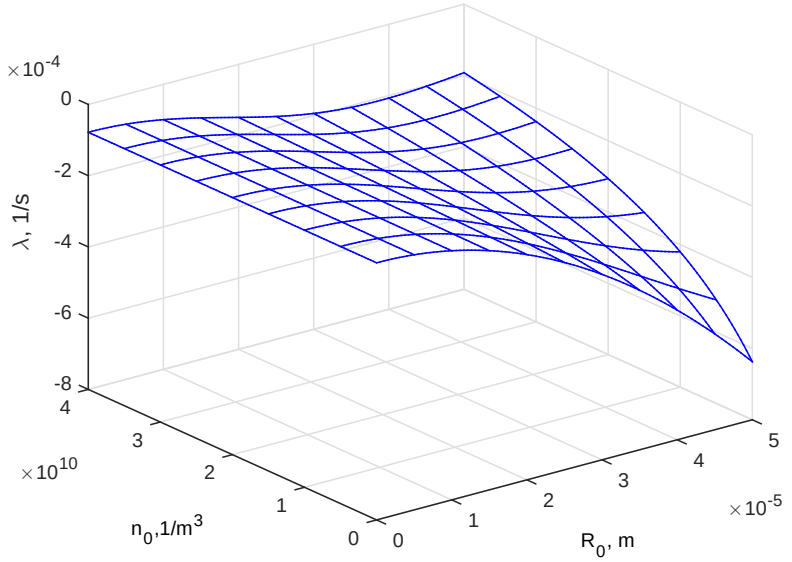

Figure 5.6: The decay rate by formula (5.3) for row 4 of Table 5.1 and row 13 of Table 5.2, $k_* = 0.25$ 1/m .

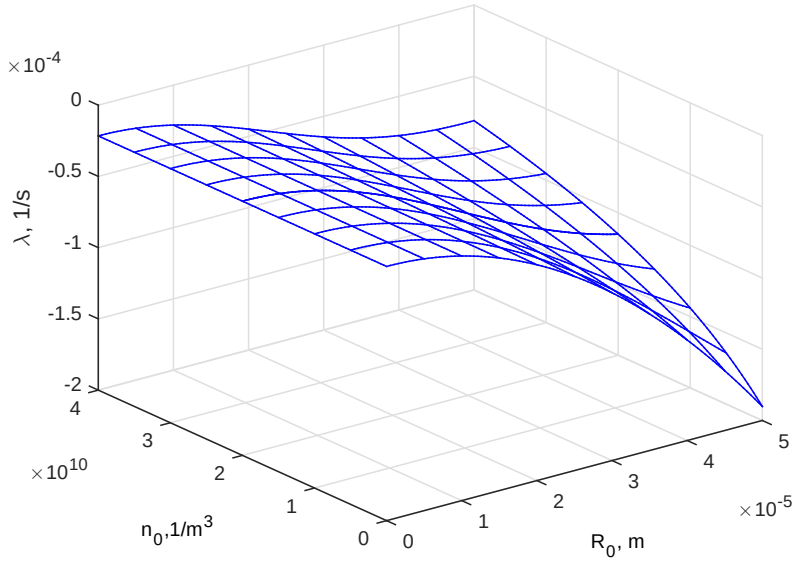

Figure 5.7: The decay rate by formula (5.3) for row 1 of Table 5.1 and row 3 of Table 5.2, $k_* = 0.25$ 1/m .

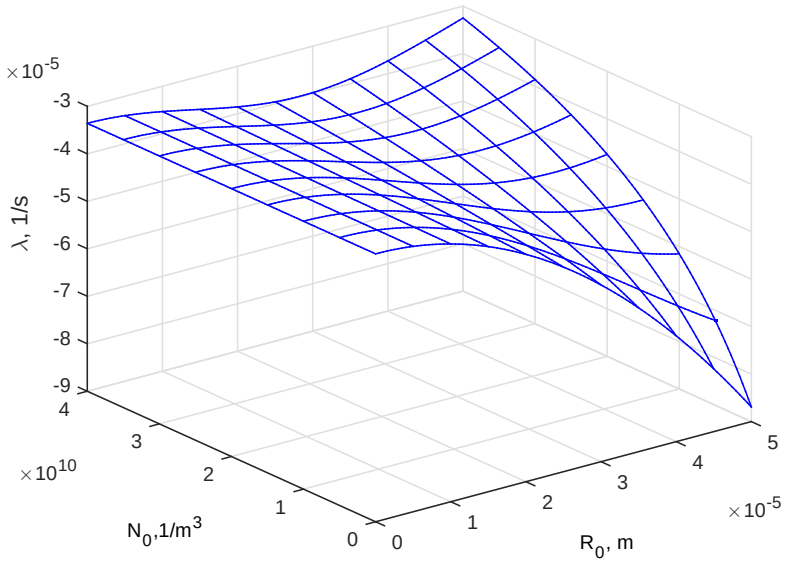

Figure 5.8: The decay rate by formula (5.3) for row 3 of Table 5.1 and row 8 of Table 5.2, $k_* = 0.25$ 1/m .

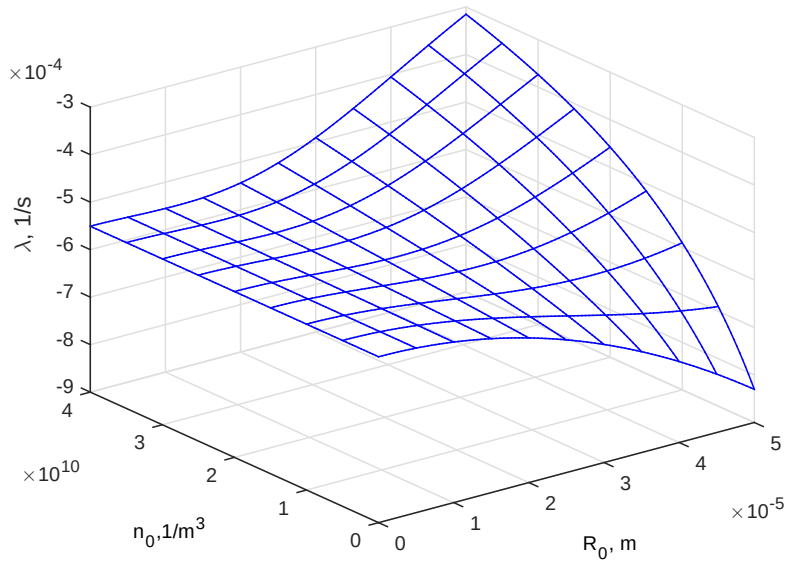

Figure 5.9: The decay rate by formula (5.3) for row 2 of Table 5.1 and row 5 of Table 5.2, $k_* = 0.25\ \ 1/\mathrm{m}$.

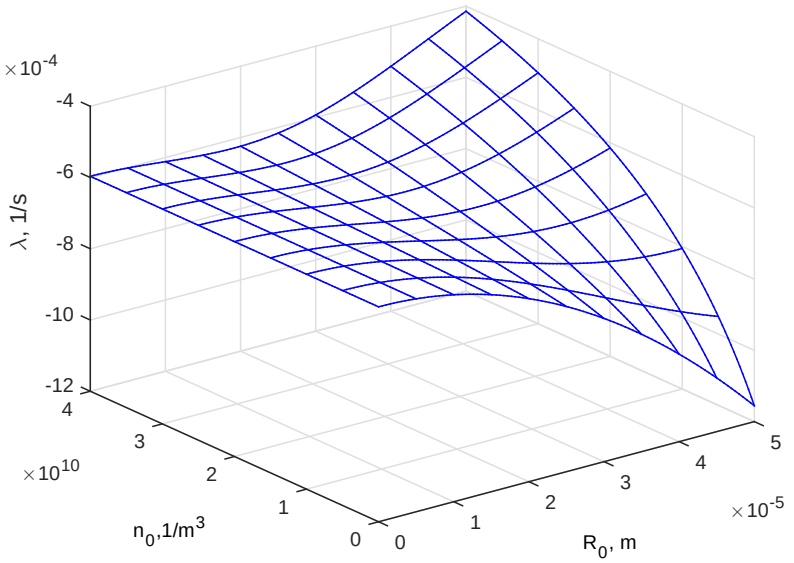

Figure 5.10: The decay rate by formula (5.3) for row 3 of Table 5.1 and row 15 of Table 5.2, $k_* = 0.25\ \ 1/\mathrm{m}$.

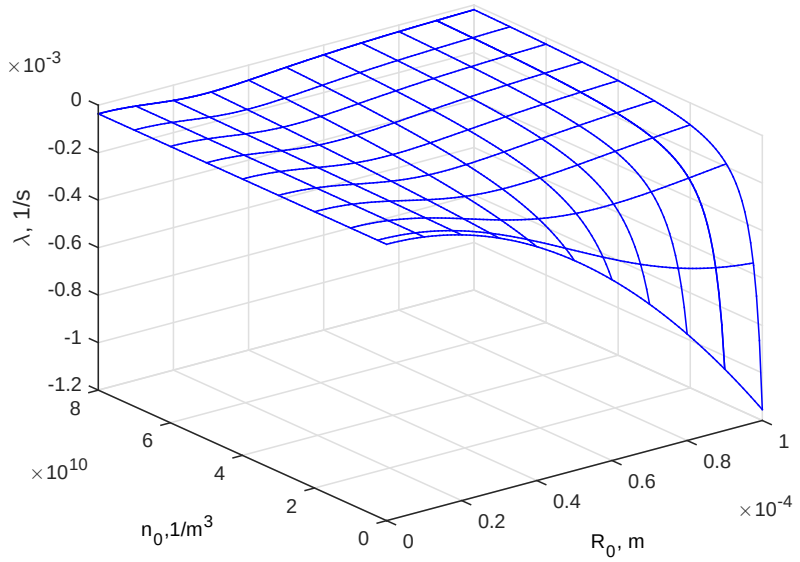

Figure 5.11: The decay rate by formula (5.3) for rows 1 of Tables 5.1 and 5.2, $k_* = 0.25$ 1/m .

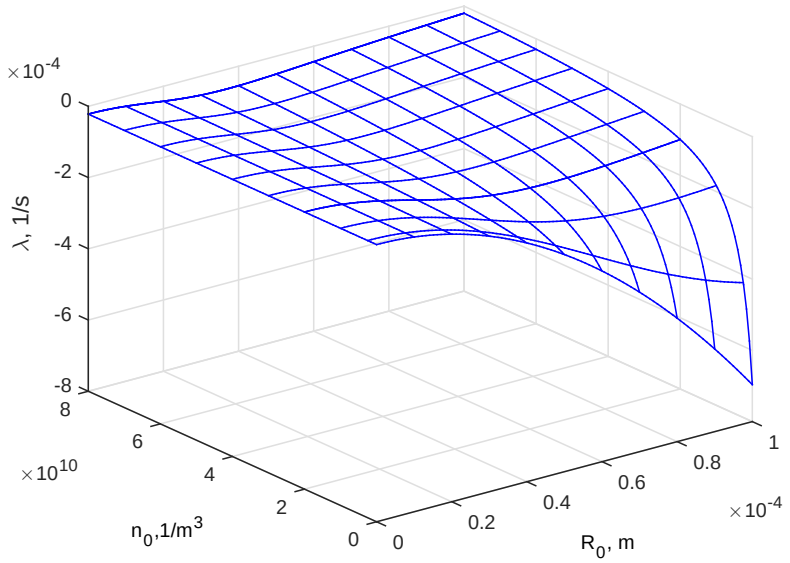

Figure 5.12: The decay rate by formula (5.3) for row 1 of Table 5.1 and row 3 of Table 5.2, $k_* = 0.25$ 1/m .

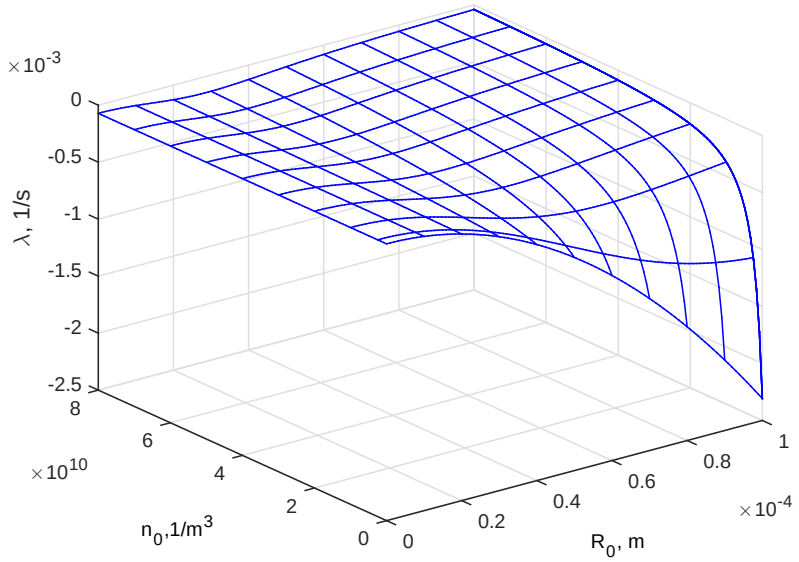

Figure 5.13: The decay rate by formula (5.3) for row 4 of Table 5.1 and row 8 of Table 5.2, $k_* = 0.25\ \ 1/\mathrm{m}$.

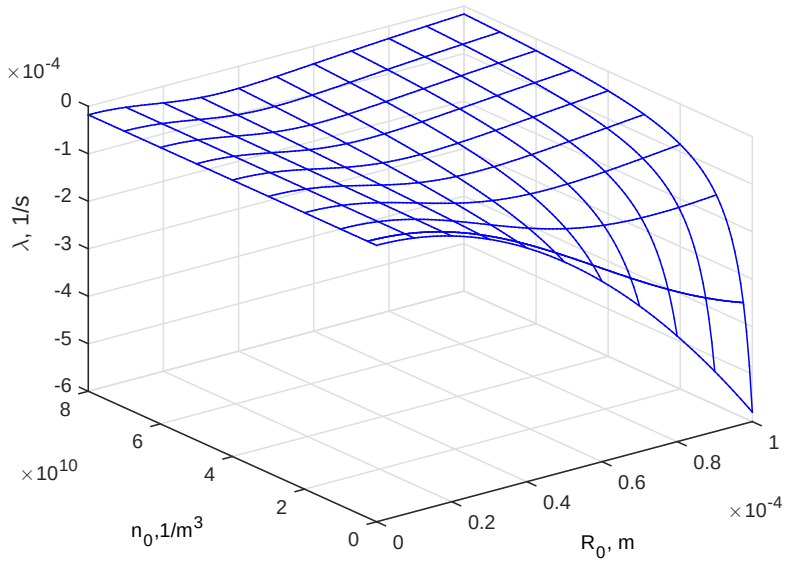

Figure 5.14: The decay rate by formula (5.3) for row 1 of Table 5.1 and row 15 of Table 5.2, $k_* = 0.25\ \ 1/\mathrm{m}$.

As is seen in some figures, for example Figure 5.9, the decay rate λ gets less negative for large values of n_0 and R_0. The results of our computations for Figure 5.9 are shown in Table 5.3. Observe from the table that the value of the wave velocity c becomes complex in the region of large n_0 and R_0. Therefore, we consider the corresponding values of λ non-physical.

λ	-5.5×10^{-4}	-5.6×10^{-4}	-5.7×10^{-4}	-5.2×10^{-4}	-3×10^{-4}	-5×10^{-6}	-9×10^{-8}
n_0	0	10^{10}	2×10^{10}	3×10^{10}	4×10^{10}	4×10^{11}	4×10^{12}
R_0	0	10^{-5}	2×10^{-5}	3×10^{-5}	5×10^{-5}	8×10^{-5}	10^{-4}
c	739	738	732	704	578	137	0+25i

Table 5.3: Numerical data for Figure 5.9 .

At different values of parameters E_i, M_i, μ_i, for example those corresponding to Figure 5.10, the velocity always remains real-valued as shown in Table 5.4. Thus, at relatively small values of n_0 we always observe a finite region of k for which $\lambda < 0$. At large values of n_0 of the order $n_0 \sim 10^{12}$ the rate $\lambda > 0$ at all k. This indicates that our model is not applicable to such extreme amounts of bubbles (for the given values of E_i, M_i, etc.).

λ	-6×10^{-4}	-6.2×10^{-4}	-6.5×10^{-4}	-6.3×10^{-4}	-4×10^{-4}	-7×10^{-6}	3×10^{-7}
n_0	0	10^{10}	2×10^{10}	3×10^{10}	4×10^{10}	4×10^{11}	4×10^{12}
R_0	0	10^{-5}	2×10^{-5}	3×10^{-5}	5×10^{-5}	8×10^{-5}	10^{-4}
c	740	739	733	705	580	145	42

Table 5.4: Numerical data for Figure 5.10 .

Generally speaking, this result leads to a further possible direction of research, which is to determine the area(s) of values of the parameters E_i, M_i, p_0, k_b, etc. where the model produces physically acceptable result of $\lambda < 0$. One would need to study the 8+ dimension parametric space formed by the parameters E_i, M_i, p_0, k_b, etc. Such an investigation is beyond the scope of this thesis. In our work we determined

some of the acceptable values of the parameters, they are given in Tables 5.1 and 5.2, excluding rows 5, 8 and 15 of Table 5.2. We emphasize that the acceptable values of the parameters are not exceptional isolated values (similar to eigenvalues) but belong to finite-size cloud(s) of acceptable values in the parametric space.

Now let us discuss the parametric dependencies for equation (5.2). We re-write the corresponding dispersion relation as

$$\lambda(k) = \frac{A_2}{A_1} k^2 \,. \tag{5.4}$$

Figures 5.15–5.21 show the results of using the parameter values given in Tables 5.1 and 5.2 in the formula (5.4).

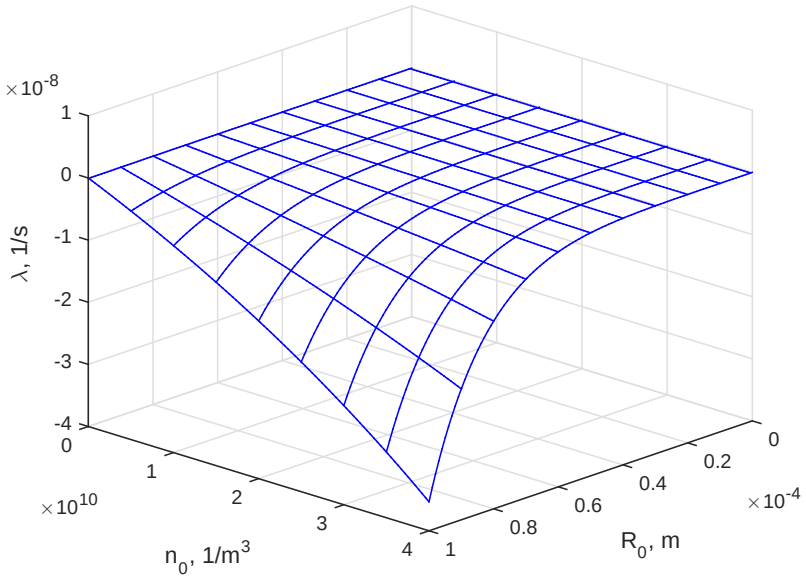

Figure 5.15: The decay rate by formula (5.4) for rows 1 of Tables 5.1 and 5.2, $k_* = 0.25$ 1/m .

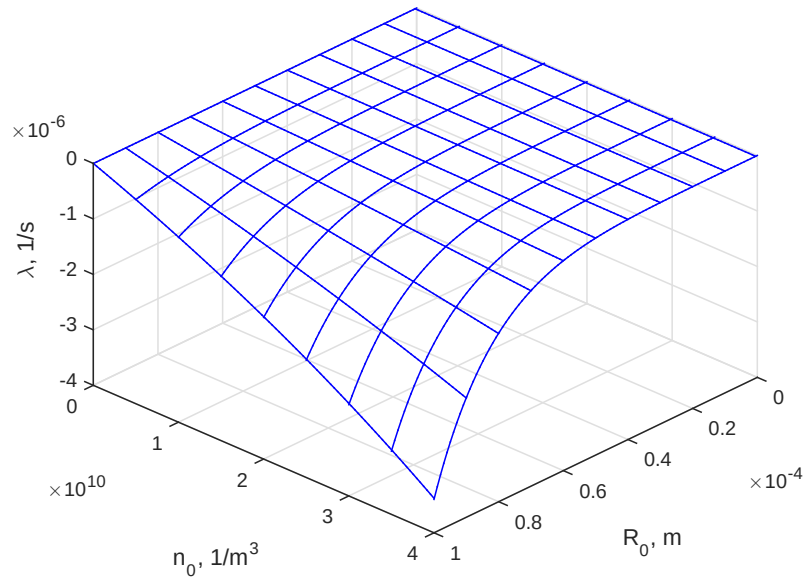

Figure 5.16: The decay rate by formula (5.4) for row 1 of Table 5.1 and row 2 of Table 5.2, $k_* = 0.25\ \ 1/\mathrm{m}$.

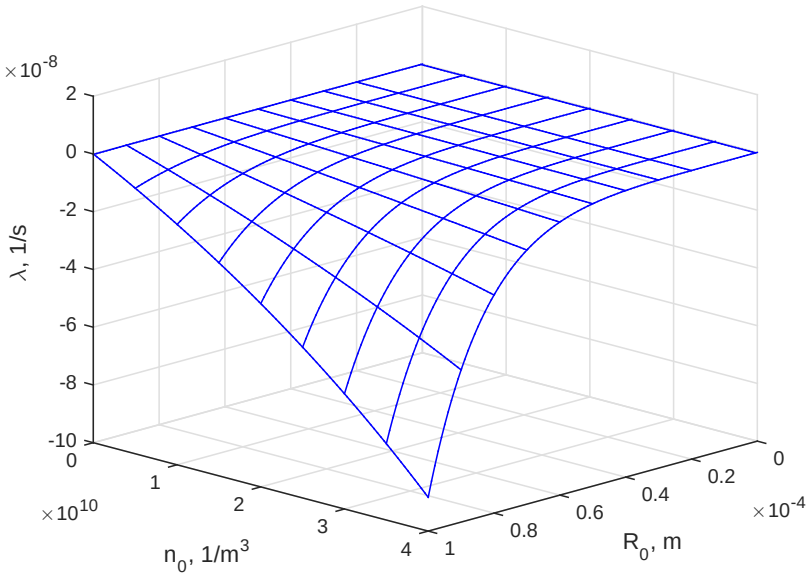

Figure 5.17: The decay rate by formula (5.4) for row 2 of Table 5.1 and row 9 of Table 5.2, $k_* = 0.25\ \ 1/\mathrm{m}$.

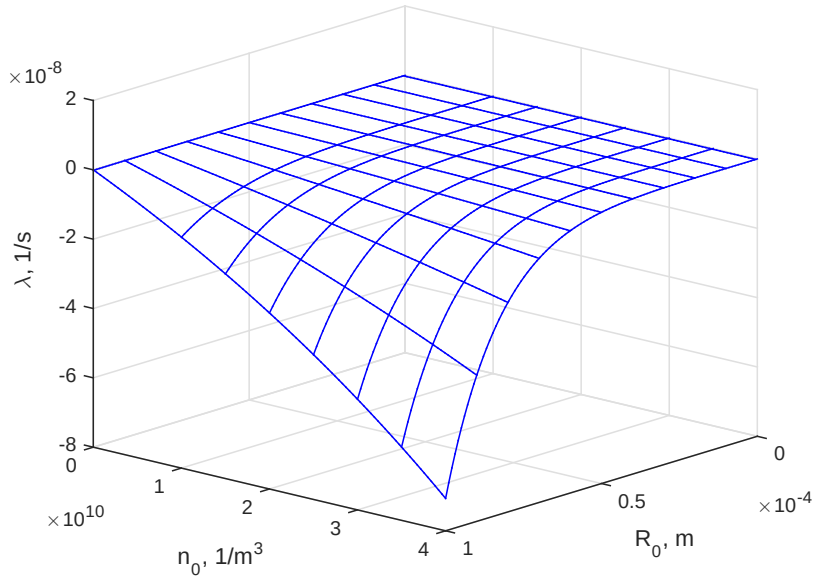

Figure 5.18: The decay rate by formula (5.4) for row 2 of Table 5.1 and row 4 of Table 5.2, $k_* = 0.25\ \ 1/\mathrm{m}$.

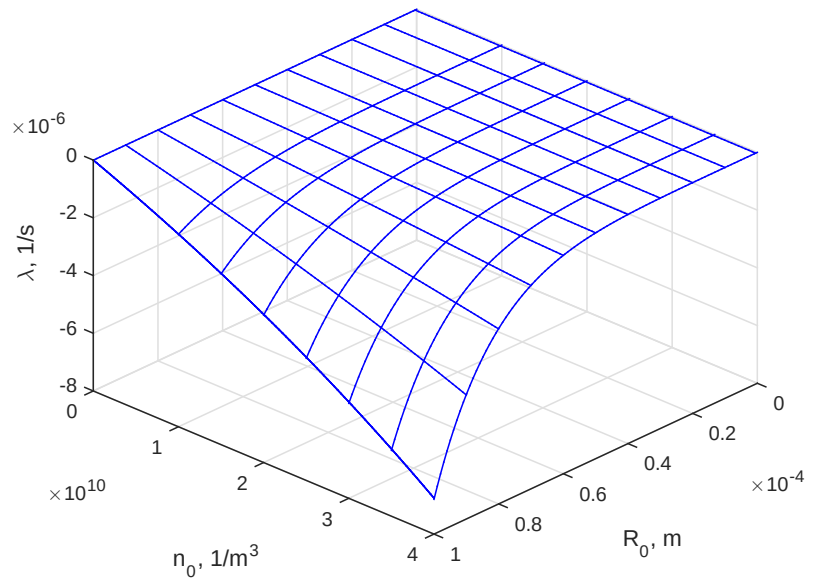

Figure 5.19: The decay rate by formula (5.4) for row 2 of Table 5.1 and row 3 of Table 5.2, $k_* = 0.25\ \ 1/\mathrm{m}$.

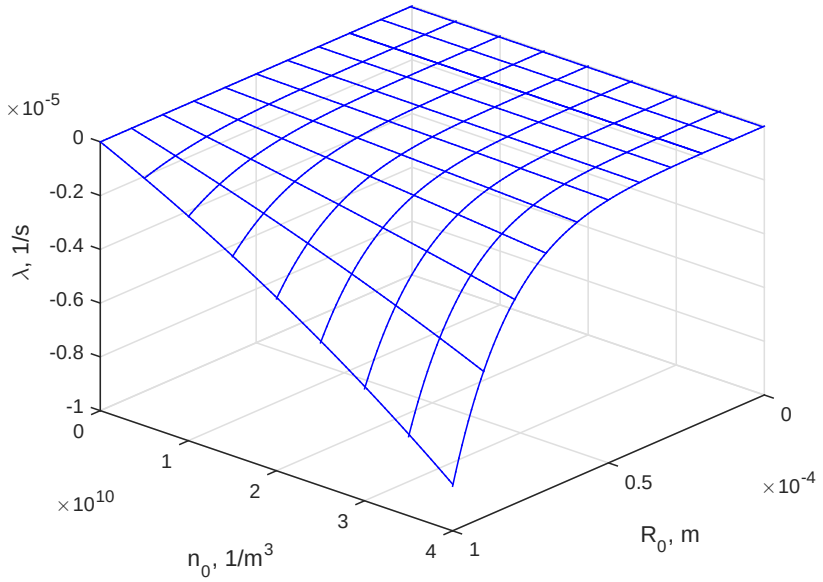

Figure 5.20: The decay rate by formula (5.4) for row 2 of Table 5.1 and row 11 of Table 5.2, $k_* = 0.25\ \ 1/\mathrm{m}$.

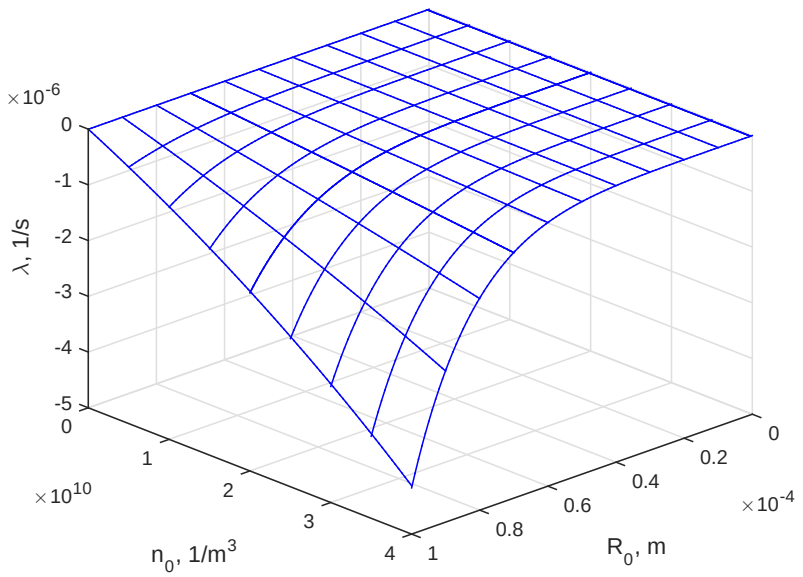

Figure 5.21: The decay rate by formula (5.4) for row 1 of Table 5.1 and row 16 of Table 5.2, $k_* = 0.25\ \ 1/\mathrm{m}$.

Moreover, when we increased the values of n_0 further to $n_0 = 8 \times 10^{10}\, 1/m^3$, we obtained similar results, see, for example, Figures 5.22–5.24.

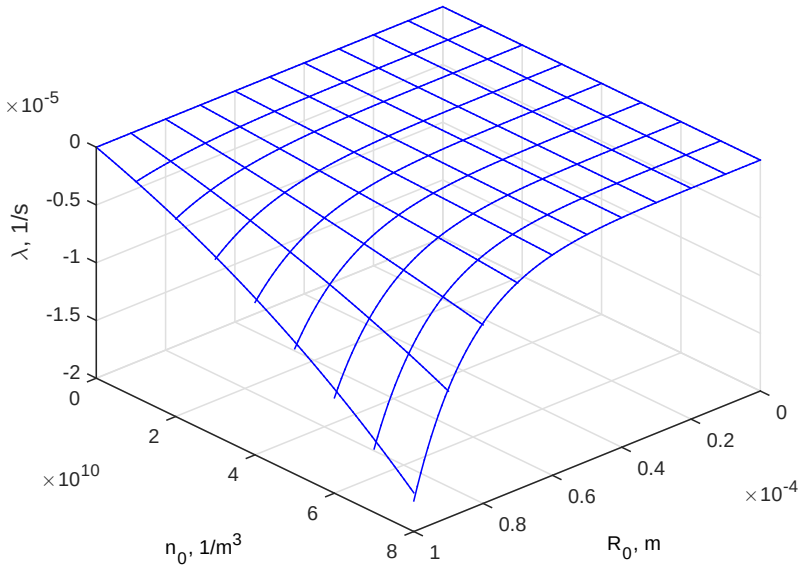

Figure 5.22: The decay rate by formula (5.4) for rows 3 of Tables 5.1 and 5.2, $k_* = 0.25$ 1/m .

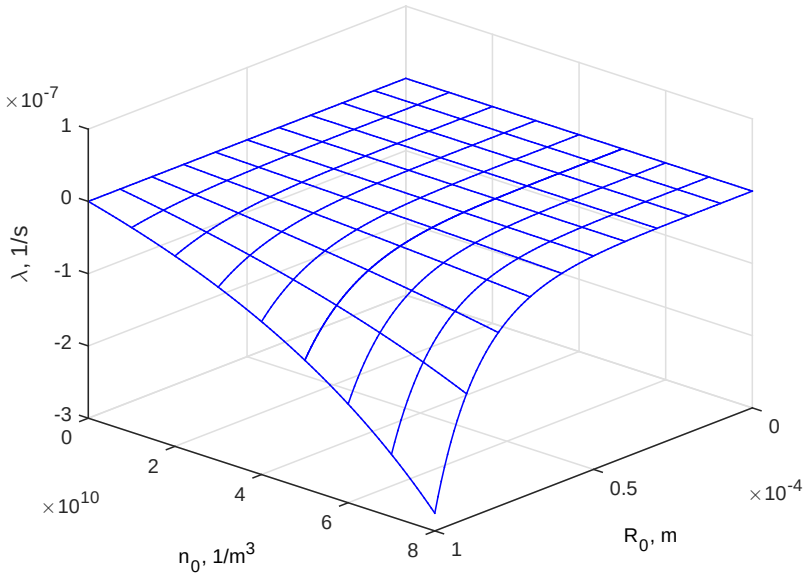

Figure 5.23: The decay rate by formula (5.4) for row 3 of Table 5.1 and row 15 of Table 5.2, $k_* = 0.25$ 1/m .

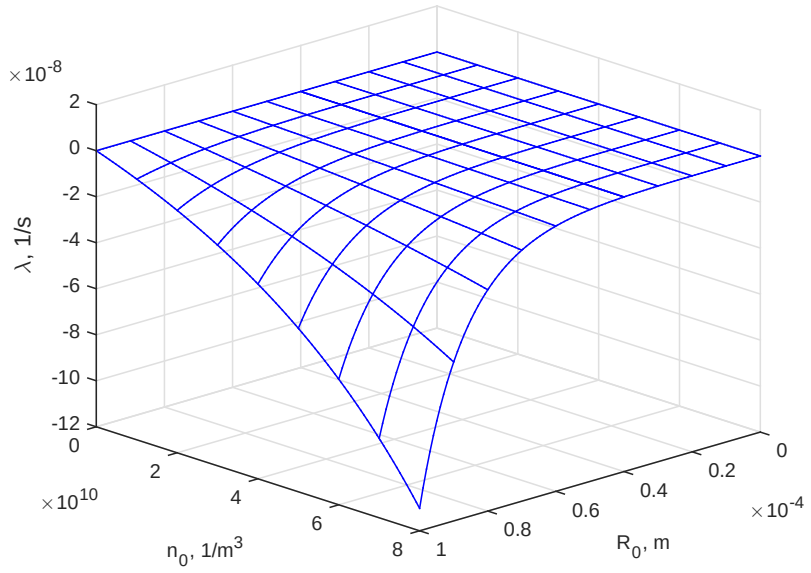

Figure 5.24: The decay rate by formula (5.4) for row 1 of Table 5.1 and row 5 of Table 5.2, $k_* = 0.25\ 1/\mathrm{m}$.

5.3 Influence of other parameters

In this section we aim to determine the effect of the parameters beyond the rheological model, for example porosity m_0, on the decay rate. We consider nine parameters that can have an effect on the decay rate: pressure p_0, porosity m_0, bulk moduli k_b, compressibility $\beta^{(s)}$ for solid, compressibility $\beta^{(L)}$ for liquid, density, $\rho_0^{(s)}$ for solid, density, $\rho_0^{(L)}$ for liquid, permeability ℓ and adiabatic exponent ζ. For each of these parameters we choose the range of variation about its literature values. Furthermore, sometimes our strategy to determine the boundaries of these ranges depends on the behaviour of λ, for example, if λ shows very small change against the parameters, we stopped varying them. Figures 5.25–5.33 show that each of the above parameters can impact significantly on the wave decay rate.

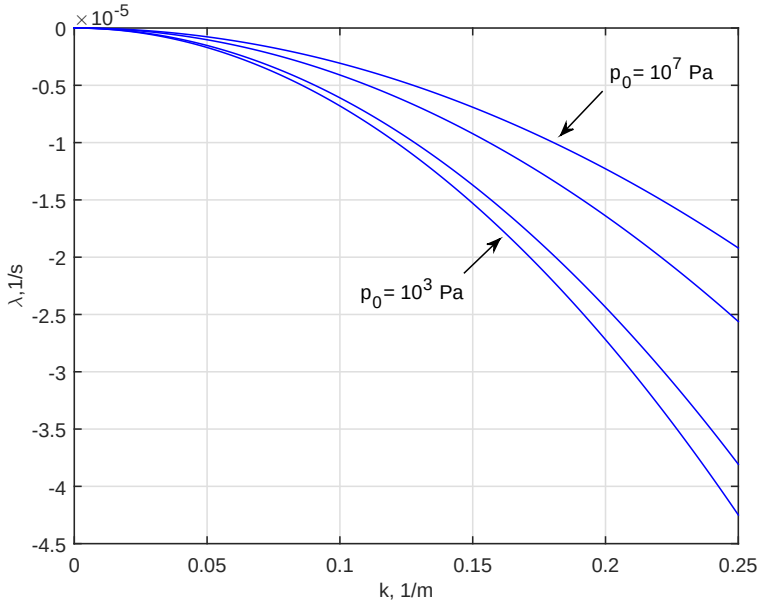

Figure 5.25: The attenuation curves by formula (5.3) for different values of p_0, $k_* = 0.25\ 1/\mathrm{m}$.

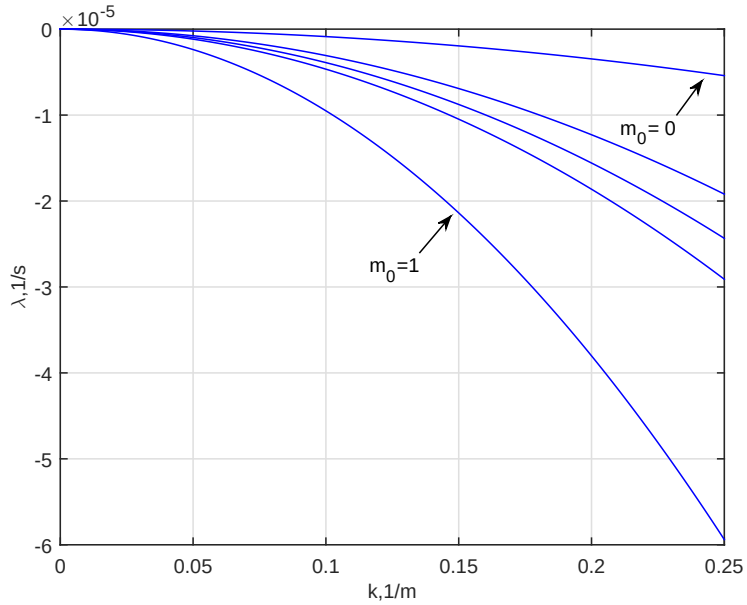

Figure 5.26: The attenuation curves by formula (5.3) for different values of m_0, $k_* = 0.25\ 1/\mathrm{m}$.

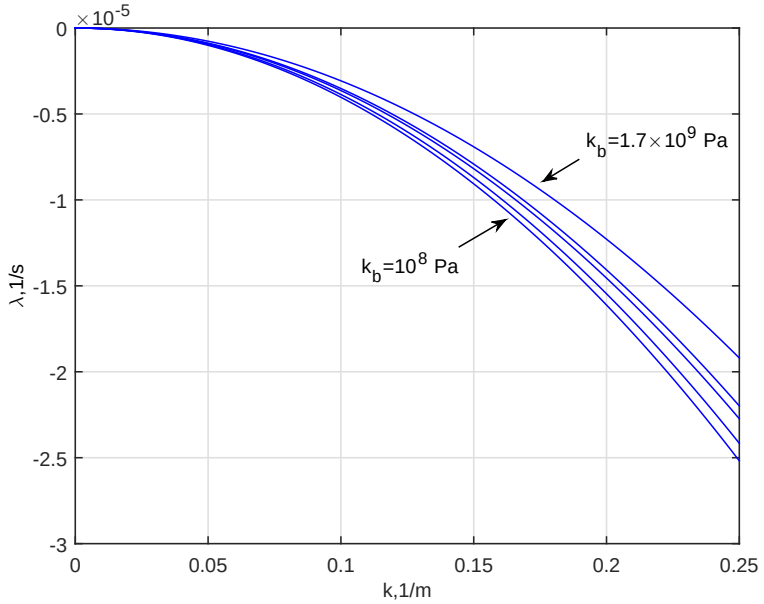

Figure 5.27: The attenuation curves by formula (5.3) for different values of k_b, $k_* = 0.25\ 1/\mathrm{m}$.

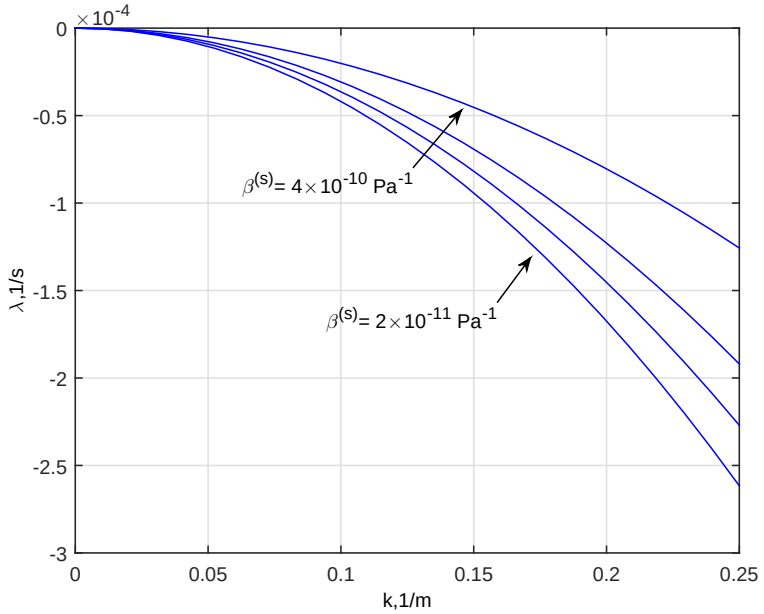

Figure 5.28: The attenuation curves by formula (5.3) for different values of $\beta^{(s)}$, $k_* = 0.25\ 1/\mathrm{m}$.

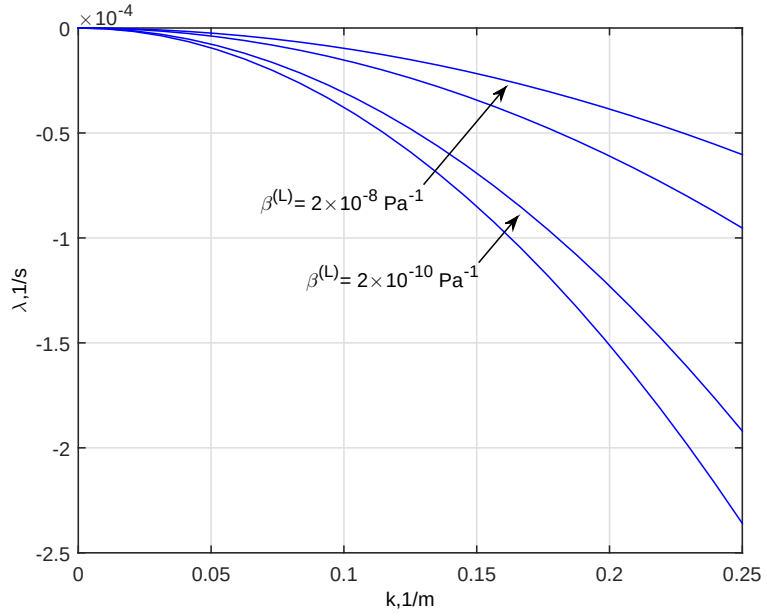

Figure 5.29: The attenuation curves by formula (5.3) for different values of $\beta^{(L)}$, $k_* = 0.25\ \ 1/\mathrm{m}$.

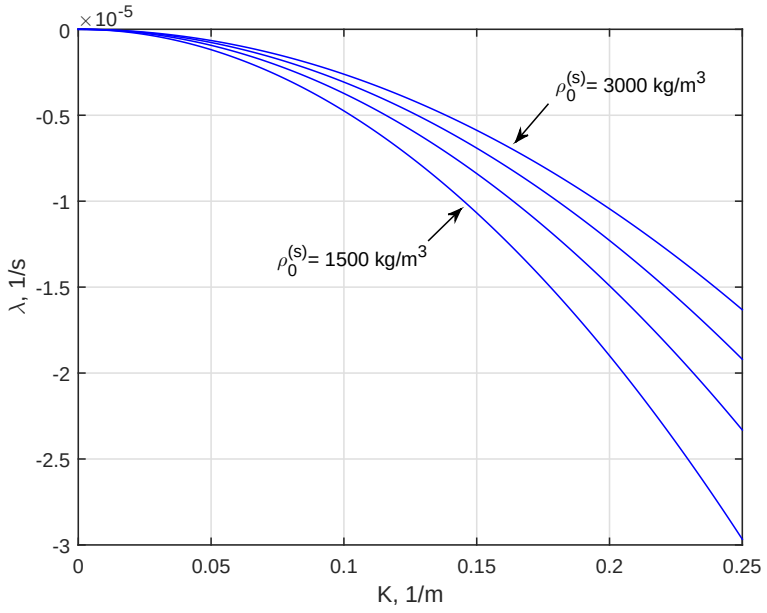

Figure 5.30: The attenuation curves by formula (5.3) for different values of $\rho_0^{(s)}$, $k_* = 0.25\ \ 1/\mathrm{m}$.

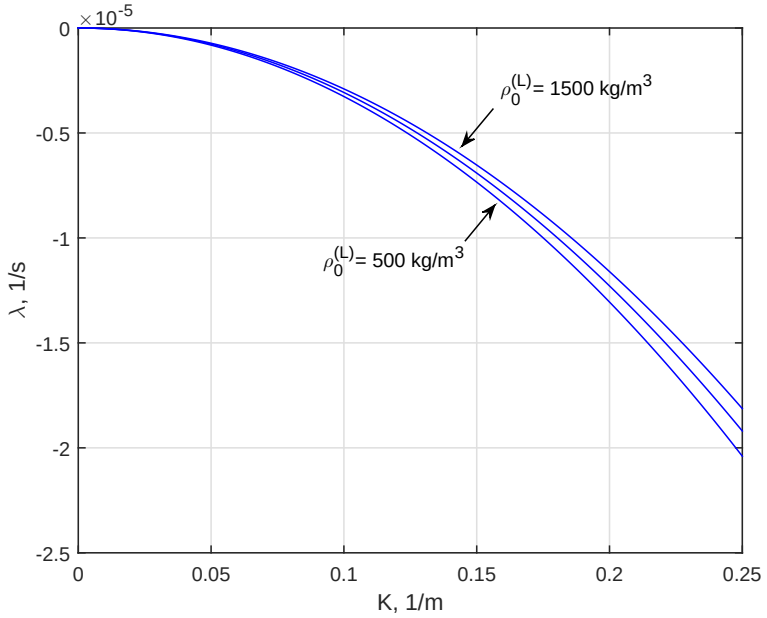

Figure 5.31: The attenuation curves by formula (5.3) for different values of $\rho_0^{(L)}$, $k_* = 0.25$ 1/m .

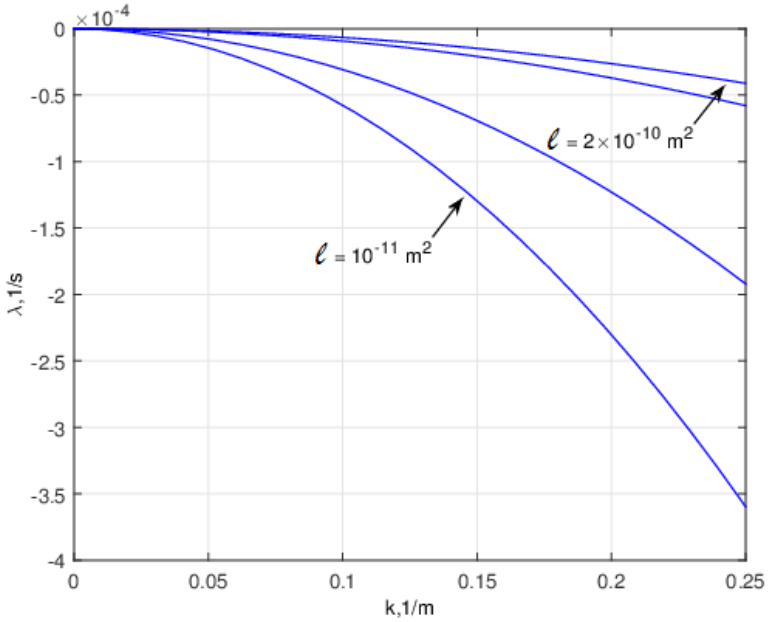

Figure 5.32: The attenuation curves by formula (5.3) for different values of ℓ, $k_* = 0.25$ 1/m .

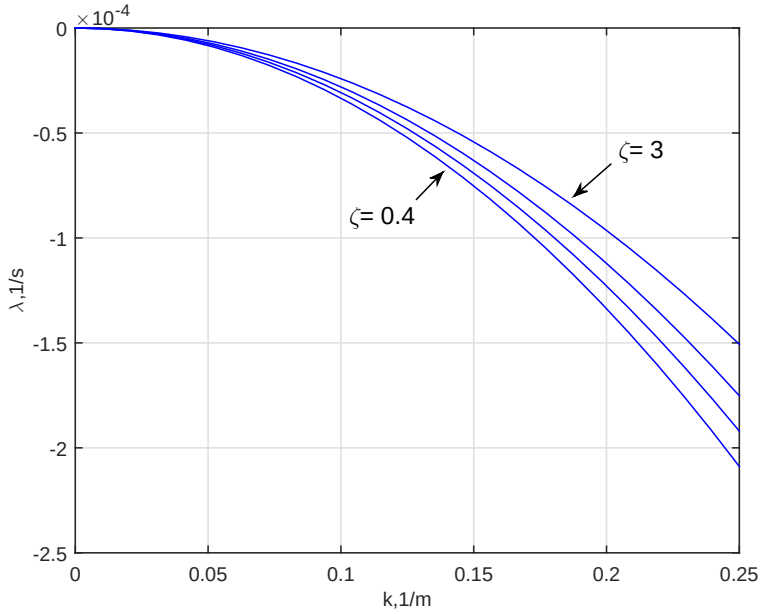

Figure 5.33: The attenuation curves by formula (5.3) for different values of ζ, $k_* = 0.25$ 1/m .

5.4 Concluding remarks

We investigated the effect of the parameter values on the decay rate of the wave with the bubbles. We grouped the parameters as

(a) relevant to the rheological model and

(b) other parameters, and investigated their effect separately.

Chapter 6

Nonlinear dynamics of neutral modes in elastic waves in granular media

SUMMARY: We analyse a model equation describing the dynamics of seismic waves featuring a neutrally stable short-wavelength mode. The system is modelled by the Nikolaevskiy equation relevant to certain type of elastic waves, reaction-diffusion systems and convection. Due to the nonlinear coupling between the time-dependent Fourier modes, the system exhibits asymptotically slow evolution towards either zero or non-zero steady state depending on the initial condition and the neutral wave number. Using the centre manifold technique, we derive the decay law of the system. Then the results are confirmed by the computations of the dynamical system for the Fourier modes.

6.1 Introduction

The Nikolaevskiy equation has been originally derived for seismic waves in granular rocks aiming, in particular, to explain the experimentally detected dominant frequencies (Nikolaevskiy, 1989). The effect of dominant frequencies manifests the formation of waves characterized by special – dominating – frequency as a result of general mechanical impact on soils or rocks (Nikolaevskiy, 1996). This effect has been experimentally found in marine sands (Vilchinska and Nikolaevskiy, 1984) as well as weak soils and fragmented rocks (Guschin, 1998). Prior to these studies, the term "dominant frequency" has been used in (Biot, 1965) and we used it in this project in the same sense as it normally appears in the engineering literature. Generally the Nikolaevskiy equation includes two groups of terms: the dispersion terms and dissipation/excitation terms, with the latter group being responsible for the growth or decay of the patterns. In this chapter we focus on the effects of dissipation/excitation, so for simplicity we consider the Nikolaevskiy equation in the form

$$\frac{\partial v}{\partial t} = A\frac{\partial^2 v}{\partial x^2} + C\frac{\partial^4 v}{\partial x^4} + F\frac{\partial^6 v}{\partial x^6} + Gv\frac{\partial v}{\partial x}\,, \tag{6.1}$$

where the coefficient A provides the effect of dissipation, C is responsible for self-excitation, F represents higher-order dissipation, and G transfers energy from the excitation to dissipation (note that for reaction-diffusion systems the dispersion terms are not part of the equation in the first place). We want to rewrite Eq. (6.1) in terms of the derivative, $v = \partial u/\partial x$.

We get

$$\frac{\partial^2 u}{\partial t \partial x} = \frac{\partial}{\partial x}\left[A\frac{\partial^2 u}{\partial x^2} + C\frac{\partial^4 u}{\partial x^4} + F\frac{\partial^6 u}{\partial x^6}\right] + G\frac{\partial u}{\partial x}\frac{\partial^2 u}{\partial x^2}\,, \tag{6.2}$$

Integrating Eq. (6.2) on x, we obtain

$$\frac{\partial u}{\partial t} = A\frac{\partial^2 u}{\partial x^2} + C\frac{\partial^4 u}{\partial x^4} + F\frac{\partial^6 u}{\partial x^6} + G\left(\frac{\partial u}{\partial x}\right)^2 + E\,, \tag{6.3}$$

where E is the constant of integration and G is a new constant incorporating $1/2$.

Eq. (6.3) contains only one independent parameter (plus parameter E discussed later).

Indeed, let us define the new function U by

$$u = aU\,. \tag{6.4}$$

We also define a new coordinate X and new time T by

$$\begin{aligned} x &= bX\,, \\ t &= cT\,. \end{aligned} \tag{6.5}$$

Now, substituting Eq. (6.4) and Eq. (6.5) into Eq. (6.3) we get

$$\begin{aligned} \frac{\partial u}{\partial t} &= \frac{\partial u}{\partial U}\frac{\partial U}{\partial T}\frac{\partial T}{\partial t} = \frac{a}{c}\frac{\partial U}{\partial T}\,, \\ \frac{\partial u}{\partial x} &= \frac{\partial u}{\partial U}\frac{\partial U}{\partial X}\frac{\partial X}{\partial x} = \frac{a}{b}\frac{\partial U}{\partial X}\,, \\ \frac{\partial^2 u}{\partial x^2} &= \frac{\partial}{\partial x}\Big(\frac{\partial u}{\partial x}\Big) = \frac{1}{b}\frac{\partial}{\partial x}\Big(\frac{a}{b}\frac{\partial U}{\partial X}\Big) = \frac{a}{b^2}\frac{\partial^2 U}{\partial X^2}\,, \end{aligned}$$

In the similar way

$$\begin{aligned} \frac{\partial^4 u}{\partial x^4} &= \frac{a}{b^4}\frac{\partial^4 U}{\partial X^4}\,, \\ \frac{\partial^6 u}{\partial x^6} &= \frac{a}{b^6}\frac{\partial^6 U}{\partial X^6}\,, \end{aligned}$$

Thus, Eq. (6.3) becomes

$$\frac{a}{c}\frac{\partial U}{\partial T} = A\frac{a}{b^2}\frac{\partial^2 U}{\partial (X)^2} + C\frac{a}{b^4}\frac{\partial^4 U}{\partial (X)^4} + F\frac{a}{b^6}\frac{\partial^6 U}{\partial (X)^6} + \frac{a^2}{b^2}G\left(\frac{\partial U}{\partial X}\right)^2 + E\,,$$

$$\frac{\partial U}{\partial T} = A\frac{c}{b^2}\frac{\partial^2 U}{\partial X^2} + C\frac{c}{b^4}\frac{\partial^4 U}{\partial X^4} + F\frac{c}{b^6}\frac{\partial^6 U}{\partial X^6} + G\frac{ac}{b^2}\left(\frac{\partial U}{\partial X}\right)^2 + E\,,$$

Now we choose the a, b, c such that

$$A\frac{c}{b^2} = 1\,, \quad F\frac{c}{b^6} = 1\,, \quad G\frac{ac}{b^2} = 1\,,$$

giving

$$a = \frac{A}{G}\,, \quad b = \left(\frac{F}{A}\right)^{\frac{1}{4}} \quad \text{and} \quad c = \frac{F^{\frac{1}{2}}}{A^{\frac{3}{2}}}\,.$$

Therefore, we come to the equation with only one free parameter, α,

$$\frac{\partial u}{\partial t} = \frac{\partial^2 u}{\partial x^2} + \alpha\frac{\partial^4 u}{\partial x^4} + \frac{\partial^6 u}{\partial x^6} + \left(\frac{\partial u}{\partial x}\right)^2 + E\,, \tag{6.6}$$

where $\alpha = CA^{-1/2}F^{-1/2}$. In the context of elastic waves v represents the velocity in the reference frame moving with the wave. In the context of reaction-diffusion systems u stands for the phase of oscillations of chemical concentration and $E = 0$ (for these systems the transition $u \to u + Et$ eliminates E anyway). When $\alpha > 2$ the curve representing the increment of a small perturbation $\sim e^{\lambda t}$ against the wave number is partly located above zero, see the dashed line in Figure 6.1. By the original

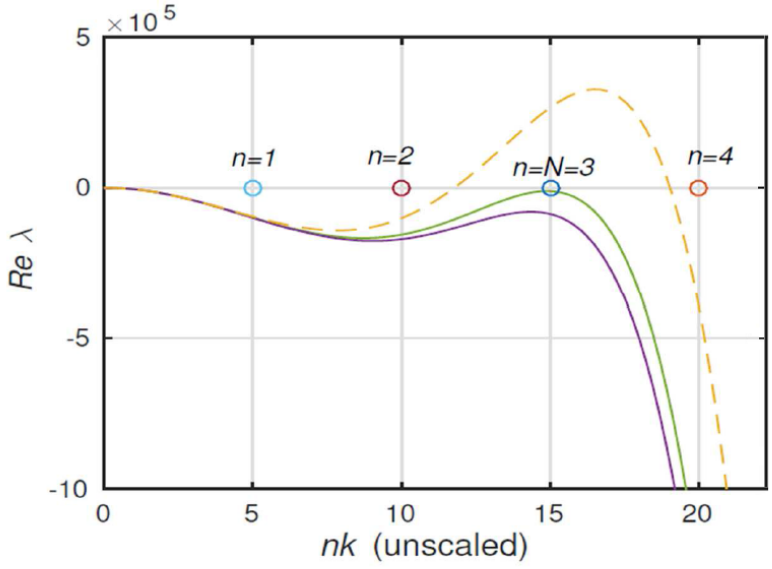

Figure 6.1: The increment versus wave number for an active system (dashed line) and passive system (the mode with $N = 3$ is shown as neutral as an example).

idea of Nikolaevskiy, the wave number k_* corresponding to the maximum growth rate of the perturbation translates into the dominant seismic frequency $v = ck_*$, where c is the average wave velocity. However, as Strunin (2014) argued in the recent paper,

for a passive system such as elastic wave the self-excitation is prohibited because of the absence of internal energy sources. In other words, rocks cannot self-start moving from rest (that is from the state $v(x;0) = 0$ or $u(x;0) = const$). We refer to Strunin (2014) for a more detailed discussion, but note here that the absence of internal sources of energy is obvious from the schematic representation of a grain of material constituting the medium, see Figure 6.2. This rheological model was utilized in (Nikolaevskiy, 1989; Beresnev and Nikolaevskiy, 1993) to derive the rheological stress-strain relation. The element consists of oscillator masses M and M_1 , springs E, E_1 and E_* and friction pistons.

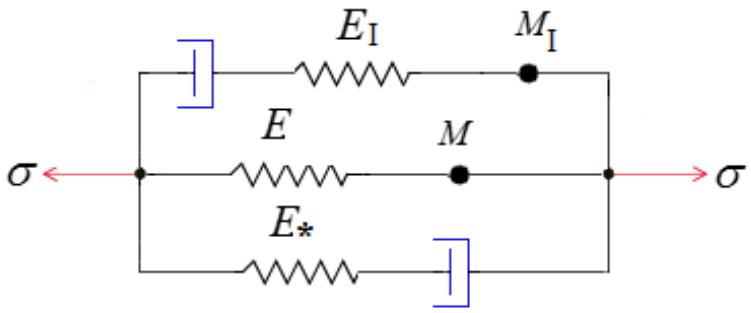

Figure 6.2: Rheological scheme representing a single grain (Nikolaevskiy, 1989) .

However, in application to systems where the capacity for the internal energy supply does exist, the self-excitation is possible. This is the case, for example, for reaction-diffusion systems, where the energy is internally generated by reactions (Strunin, 2009). These arguments do not imply that the dominant frequency cannot be explained within the Nikolaevskiy equation, but, in our view, the interpretation of such frequency needs to be modified. The dominant frequency mode is the one that exhibits slowest decay relative to the other modes, rather than fastest growth. Such a mode would survive for longer period of time in comparison to the other modes, and thus would dominate in the spectrum. Accordingly, the increment curve should lie entirely below zero as shown by the solid lines in Figure 6.1. Although the decaying

dynamics may be less interesting compared to nontrivial pattern formation in systems with self-excitation (such as stationary or chaotic patterns in reaction-diffusion systems), they still deserve attention. This makes the question on how the decay progresses in time particularly important.

6.2 Evolution on the centre manifold

Upon adopting periodic boundary condition, we expand the function $u(x,t)$ into the Fourier series

$$u(x,t) = \sum_{n=\infty}^{\infty} A_n(t) e^{inkx}\,, \tag{6.7}$$

Here $A_{-n} = A_n^*$ to ensure that u is real-valued.

The choice of periodic boundary condition (Strunin, 2014) originates from our previous analysis where we used the imaginable closed-loop configuration of the medium (which, however, may be artificially created in a laboratory experiment). Using this configuration, it is easy to realize the impossibility for a self-supporting elastic wave to run in circles along the loop for ever (effectively presenting a perpetuum mobile). We also note that, for the elastic waves, the original equation is written in terms of the velocity v, not u, see Eq. (6.1). Therefore the adopted condition of periodicity of u is a more strict condition than periodicity of v: generally, the function u is allowed to be non-periodic. So we limit the scope of our study by the most simple situation of u-periodic regimes (in this case the other neutral mode, $k = 0$, will not participate in the analysis of ODEs below). Substituting Eq. (6.7) into Eq. (6.6) we obtain

$$\frac{dA_n}{dt} = [-(nk)^2 + \alpha(nk)^4 - (nk)^6]A_n - k^2 \sum_{m=-\infty}^{\infty} A_{n-m}A_m m(n-m)\,. \tag{6.8}$$

For the linearised equation (6.8), the modes behave as $A_n \sim e^{\lambda_n t}$ with

$$\lambda_n = -(nk)^2 + \alpha(nk)^4 - (nk)^6\,.$$

Consider the limiting case of $\alpha = 2$, when one of the modes is only neutrally stable. The increment curve touches zero level when $nk = 1$. Therefore, if such a neutral mode is chosen to be the N-th Fourier mode, then the basic wave number is

$$k = 1/N\,. \tag{6.9}$$

Thus, under the linearised version of the model, we have one neutral mode and discrete set of exponentially decaying modes. This situation is ideally suitable for treatment by the centre manifold technique; it will allow us to asymptotically describe the decaying dynamics at large times. Taking into account the nonlinear interplay between the modes, we expect the system to eventually approach an asymptotic stage when the exponentially fast dynamics, driven by the linear terms, are replaced by slow evolution driven by the nonlinear coupling. Inserting $\alpha = 2$ and Eq. (6.9) into Eq. (6.8) gives

$$\frac{dA_n}{dt} = \left[-\left(\frac{n}{N}\right)^2 + 2\left(\frac{n}{N}\right)^4 - \left(\frac{n}{N}\right)^6\right] A_n - \left(\frac{1}{N}\right)^2 \sum_{m=-\infty}^{\infty} A_{n-m} A_m m(n-m)\,. \tag{6.10}$$

We begin asymptotic analysis with the case when the neutral mode is the first, $N = 1$.

6.3 Centre manifold approach

Using $N = 1$ in Eq. (6.10), see Figure 6.3, and restricting attention to a few leading modes, we get

$$\begin{aligned}
\frac{dA_1}{dt} &= \qquad\quad 4A_2A_1^* + 12A_3A_2^* + \dots\,,\\
\frac{dA_2}{dt} &= -36A_2 - A_1^2 + 6A_3A_1^* + \dots\,,\\
\frac{dA_3}{dt} &= -576A_3 - 4A_1A_2 + \dots\,,\\
&\dots
\end{aligned} \tag{6.11}$$

The centre manifold theory states (Carr, 2012) that the modes which experience a stage of exponential decay caused by the linear terms (in case of system (6.11) these modes are A_2 and A_3), drop onto a surface, or manifold, where they then evolve slowly. On the manifold the fast modes become connected to the neutral mode by stiff algebraic expressions. As a consequence, these modes depend on time not independently but via the neutral mode. We seek the modes A_2 and A_3 in the form of power series in A_1 and A_1^*,

$$\begin{aligned} A_2 &= a_1 A_1 + b_1 A_1^* \\ &+ a_2 A_1 A_1^* + m_2 A_1^2 + n_2 A_1^{*2} \\ &+ a_3 A_1^2 A_1^* + b_3 A_1^{*2} A_1 + g_3 A_1^3 + h_3 A_1^{*3} \\ &+ w_4 A_1^4 + x_4 A_1^3 A_1^* + y_4 A_1^2 A_1^{*2} + z_4 A_1 A_1^{*3} + l_4 A_1^{*4} + \dots , \end{aligned} \tag{6.12}$$

$$\begin{aligned} A_3 &= p_1 A_1 + q_1 A_1^* \\ &+ p_2 A_1 A_1^* + f_2 A_1^2 + k_2 A_1^{*2} \\ &+ p_3 A_1^2 A_1^* + q_3 A_1^{*2} A_1 + v_3 A_1^3 + y_3 A_1^{*3} + \dots . \end{aligned} \tag{6.13}$$

We substitute Eq. (6.12) and Eq. (6.13) into the A_2- and A_3-equations of system (6.11) simultaneously replacing dA_1/dt by its expression from the first equation of system (6.11). Collecting same powers in A_1 and A_1^* and their products with the help of computer algebra, see Appendix A, we obtain equations for the coefficients of the series Eq. (6.12) and Eq. (6.13). They lead to

$$\begin{aligned} m_2 &= -\frac{1}{36}, \quad v_3 = -\frac{4}{576} m_2 = \frac{1}{5184}, \\ x_4 &= \frac{6v_3 - 8m_2^2}{36} = -\frac{13}{93312}, \quad \dots . \end{aligned} \tag{6.14}$$

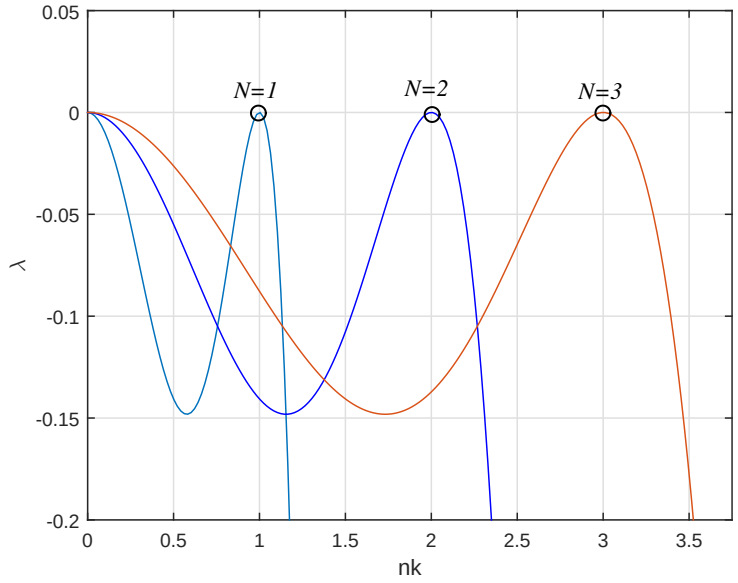

Figure 6.3: The neutral modes $N = 1, 2$, and 3 of Eq. (6.10) .

Note that the structure of the power series appears to be (the coefficients are omitted)

$$
\begin{aligned}
A_2 &\sim A_1^2 + A_1^4 + A_1^6 + \dots , \\
A_3 &\sim \quad A_1^3 + A_1^5 + A_1^7 + \dots , \\
A_4 &\sim \qquad A_1^4 + A_1^6 + A_1^8 + \dots , \\
&\dots
\end{aligned}
$$

Based on Eq. (6.14) and system (6.11), the slow evolution on the manifold, up to the 5-th order, is given by

$$
\begin{aligned}
\frac{dA_1}{dt} &= 4(m_2 A_1^2 + x_4 A_1^3 A_1^* + \dots)A_1^* + 12(v_3 A_1^3 + \dots)(m_2 A_1^{*2} + \dots) = \\
&= -\frac{1}{9} A_1^2 A_1^* - \frac{29}{46656} A_1^3 \left(A_1^*\right)^2 + \dots .
\end{aligned}
\tag{6.15}
$$

A simple approximation can be derived if we retain only the leading term in

Eq. (6.15),

$$\frac{dA_1}{dt} = -\frac{1}{9}A_1^2 A_1^* \,. \tag{6.16}$$

For the real and imaginary parts defined by $A_1 = Z + iY$ we get the system

$$\begin{aligned} \frac{dZ}{dt} &= -\frac{1}{9}\left(Z^3 + ZY^2\right) \,, \\ \frac{dY}{dt} &= -\frac{1}{9}\left(Z^2 Y + Y^3\right) \,. \end{aligned} \tag{6.17}$$

It is easy to figure out that Eq. (6.17) has the solution

$$Z = \frac{Z_0}{\sqrt{t}} \,, \quad Y = \frac{Y_0}{\sqrt{t}} \,. \tag{6.18}$$

Further, inserting Eq. (6.18) into Eq. (6.17) we establish that Z_0, Y_0 are connected by

$$Z_0^2 + Y_0^2 = \frac{9}{2} \,. \tag{6.19}$$

The individual values of Z_0 and Y_0 depend on a specific trajectory governed by system (6.11).

An example of a numerical solution of the 3-component system (6.11) using the solver of Roberts (1998), is given in Figures 6.4 and 6.5. On the vertical axis we plot the imaginary and real parts multiplied by $\sqrt{t}$. This way we can show the asymptotic stage ($t \to \infty$) more vividly as the curve goes horizontally over a longer range relative to the early stage of the dynamics. By comparison, the traditional log-log plot would give a much shorter horizontal stretch of the asymptotic stage, which interests us. We remind that the $1/\sqrt{t}$ regime is asymptotic, therefore the early stage in Figure 6.4 is to be ignored. Therefore the settling of the curves on constant levels proves that each one is eventually proportional to $1/\sqrt{t}$. An inspection of the settled levels of Re A_1 and Im A_1 confirms that they satisfy the prediction Eq. (6.19).

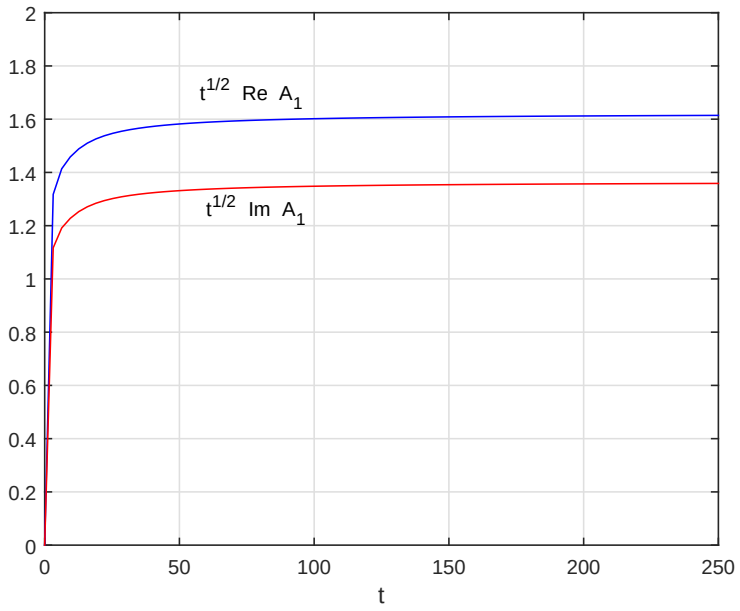

Figure 6.4: Settling of the inverse-square-root law for the neutral mode $N = 1$ from (6.11); the initial condition $A_1 = A_2 = A_3 = 1 + i$.

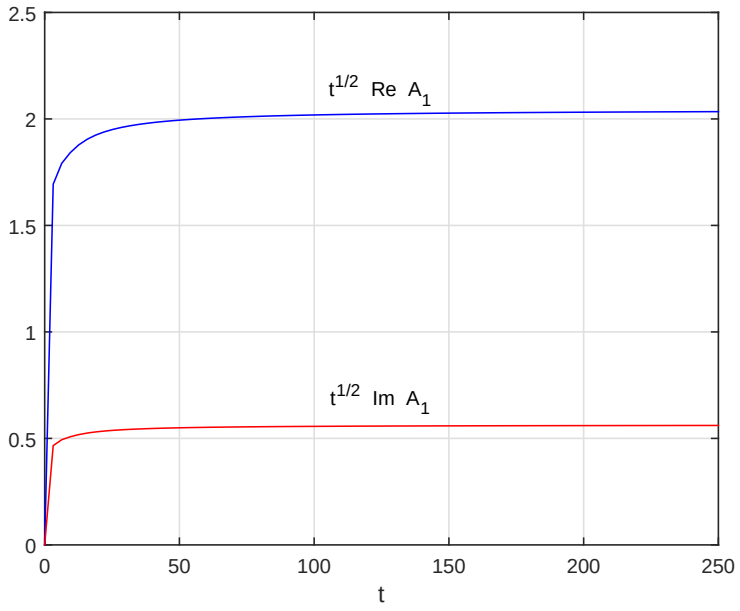

Figure 6.5: Settling of the inverse-square-root law for the neutral mode $N = 1$ from (6.11); the initial condition $A_1 = 1.5 + 0.4i$, $A_2 = 0.5 + 0.4i$, $A_3 = 0.5 + 0.3i$.

Now assume that the neutral mode is the second, $N = 2$. Using $N = 2$ and $n = 1, 2, 3, 4$ in Eq. (6.10), see Figure 6.3, we obtain

$$\begin{aligned}
\frac{dA_1}{dt} &= -\frac{9}{64}A_1 + 6A_4A_3^* + 3A_3A_2^* + A_2A_1^* + \dots\,, \\
\frac{dA_2}{dt} &= \qquad\qquad 4A_4A_2^* + \frac{3}{2}A_3A_1^* - \frac{1}{4}A_1^2 + \dots\,, \\
\frac{dA_3}{dt} &= -\frac{255}{64}A_3 + 2A_4A_1^* - A_1A_2 + \dots\,, \\
\frac{dA_4}{dt} &= -36A_4 - \frac{3}{2}A_1A_3 - A_2^2 + \dots\,, \\
&\dots
\end{aligned} \tag{6.20}$$

The modes A_1, A_3 and A_4 are sought in the form of power series in A_2 and A_2^*, leading to the centre manifolds

$$A_1 = 0\,, \quad A_3 = 0\,, \quad A_4 = -\frac{1}{36}A_2^2 - \frac{1}{5832}A_2^3A_2^* + \dots\,.$$

This results in the slow motion on the manifold according to

$$\frac{dA_2}{dt} = -\frac{1}{9}A_2^2A_2^* - \frac{1}{1458}A_2^3A_2^{*2} + \dots\,. \tag{6.21}$$

In the leading order, Eq. (6.21) has the same form as Eq. (6.16), so that the neutral mode decays as inverse square root of time. This is confirmed by the numerical solution of system (6.20), see Figures 6.6 and 6.7. Figures 6.8 and 6.9 show the exponential decay of A_1 and A_3 towards their respective centre manifolds $A_1 = 0$ and $A_3 = 0$.

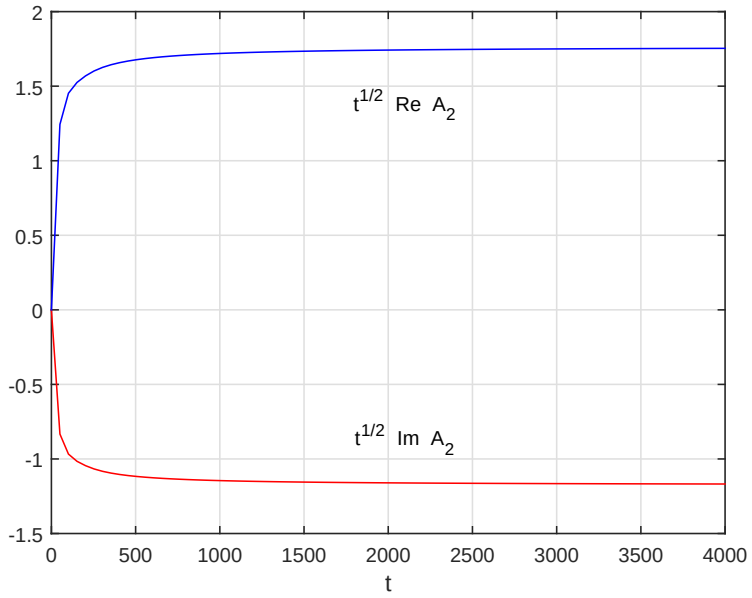

Figure 6.6: Settling of the inverse square-root law for the neutral mode $N = 2$ from (6.20); the initial condition $A_1 = A_2 = A_3 = A_4 = 1 + i$.

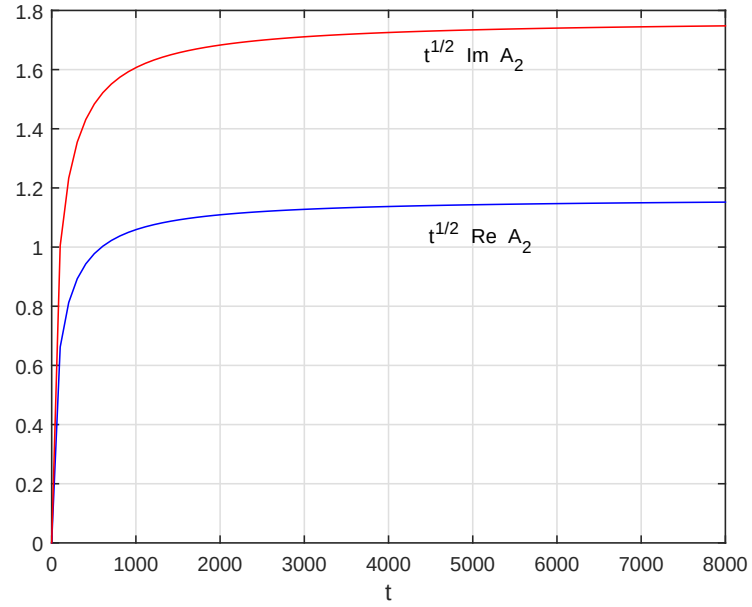

Figure 6.7: Settling of the inverse square-root law for the neutral mode $N = 2$ from (6.20); the initial condition $A_1 = A_2 = A_3 = A_4 = 0.4 + 0.4i$.

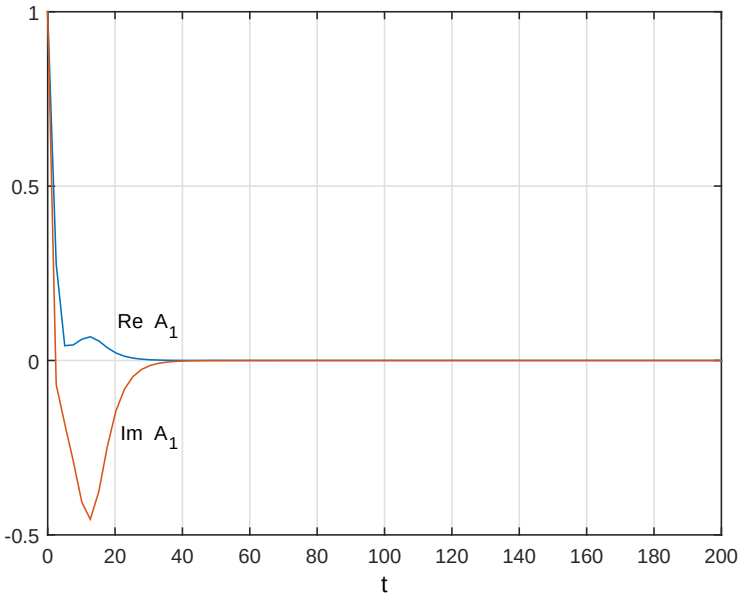

Figure 6.8: The exponential decay (asymptotically) of A_1 for the case $N = 2$.

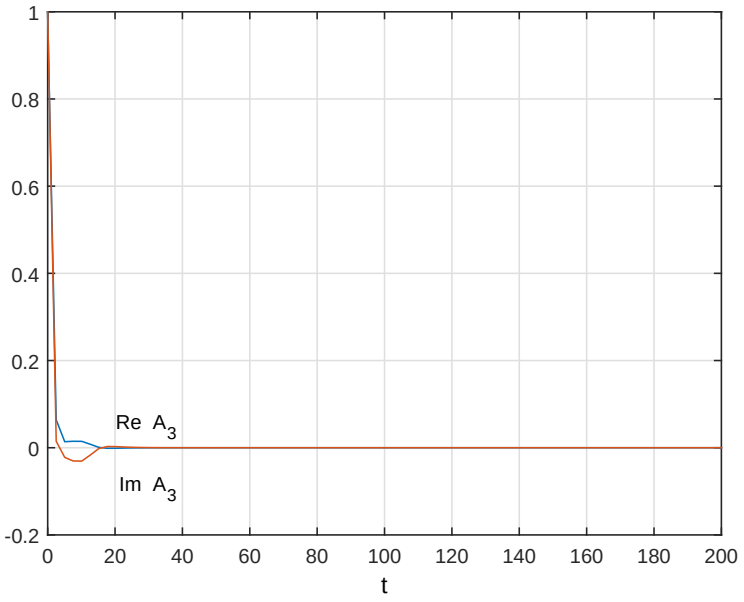

Figure 6.9: The exponential decay (asymptotically) of A_3 for the case $N = 2$.

For the case of the neutral mode with $N = 3$, see Figure 6.3, Eq. (6.10) gives the

system of equations

$$\begin{aligned}
\frac{dA_1}{dt} &= -\frac{64}{729}A_1 + \frac{8}{3}A_4A_3^* + \frac{4}{3}A_3A_2^* + \frac{4}{9}A_2A_1^* + \frac{40}{9}A_5A_4^* + \frac{60}{9}A_6A_5^* + \dots\,, \\
\frac{dA_2}{dt} &= -\frac{100}{729}A_2 + \frac{16}{9}A_4A_2^* + \frac{3}{2}A_3A_1^* - \frac{1}{9}A_1^2 + \frac{10}{3}A_5A_3^* + \frac{48}{9}A_6A_4^* + \dots\,, \\
\frac{dA_3}{dt} &= \qquad\qquad \frac{8}{9}A_4A_1^* - \frac{4}{9}A_1A_2 + \frac{20}{9}A_5A_2^* + 4A_6A_3^* + \dots\,, \\
\frac{dA_4}{dt} &= -\frac{784}{729}A_4 - \frac{3}{2}A_1A_3 - \frac{4}{9}A_2^2 + \frac{10}{3}A_5A_1^* + \frac{24}{9}A_6A_2^* + \dots\,, \\
\frac{dA_5}{dt} &= -\frac{6400}{729}A_5 - \frac{8}{9}A_1A_4 - \frac{4}{3}A_2A_3 + \frac{12}{9}A_6A_1^* + \dots\,, \\
\frac{dA_6}{dt} &= -36A_6 - \frac{10}{9}A_1A_5 - \frac{16}{9}A_2A_4 - A_3^2 + \dots\,, \\
&\dots
\end{aligned} \tag{6.22}$$

Executing the same process in system (6.22) we find the centre manifolds

$$A_1 = 0\,, \quad A_2 = 0\,, \quad A_4 = 0\,, \quad A_5 = 0\,, \quad A_6 = -\frac{1}{36}A_3^2 + \dots\,. \tag{6.23}$$

Then, the slow motion of the neutral mode on the centre manifold is governed by

$$\frac{dA_3}{dt} = -\frac{1}{9}A_3^2A_3^* + \dots\,. \tag{6.24}$$

The numerical solutions of system (6.22), shown in Figures 6.10 and 6.11. In addition, Figures 6.12 and 6.13 show the exponential decay of A_1, A_2, A_4 and A_5 towards their respective centre manifolds $A_1 = 0$, $A_2 = 0$, $A_4 = 0$ and $A_5 = 0$.

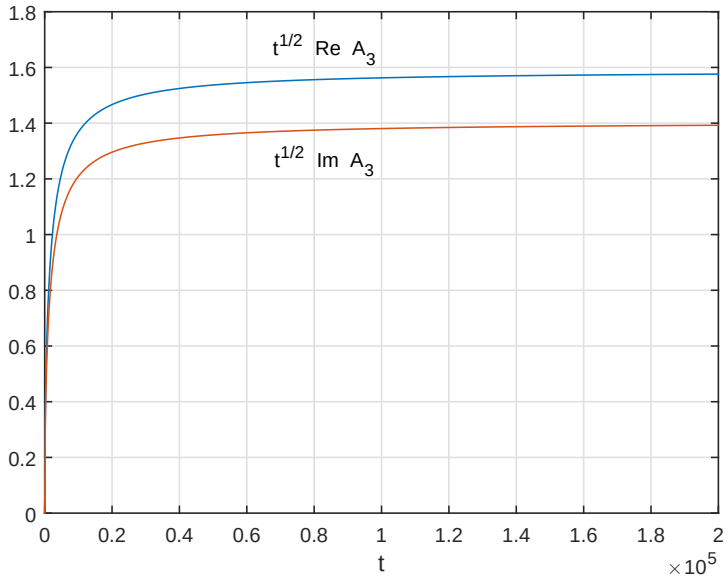

Figure 6.10: Settling of the inverse-square-root law for the neutral mode $N = 3$ from (6.22); the initial condition $A_1 = A_2 = A_3 = A_4 = A_5 = A_6 = 1 + i$.

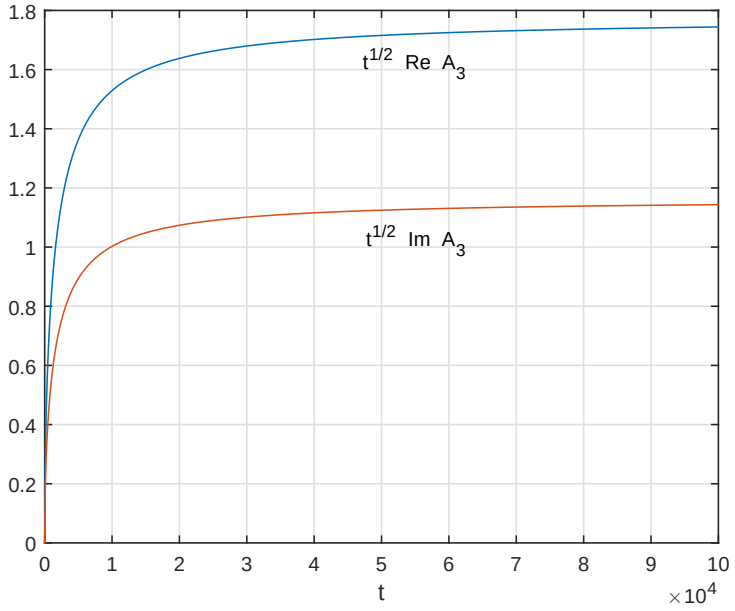

Figure 6.11: Settling of the inverse-square-root law for the neutral mode $N = 3$ from (6.22); the initial condition $A_1 = A_2 = A_3 = A_4 = A_5 = A_6 = 0.05 + 0.04i$.

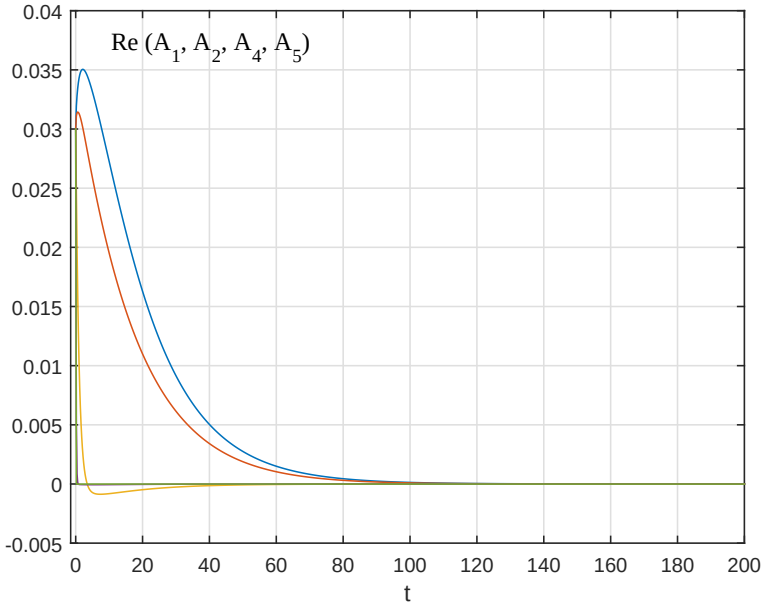

Figure 6.12: The exponential decay (asymptotically) of real parts of A_1, A_2, A_4 and A_5 for the case $N = 3$.

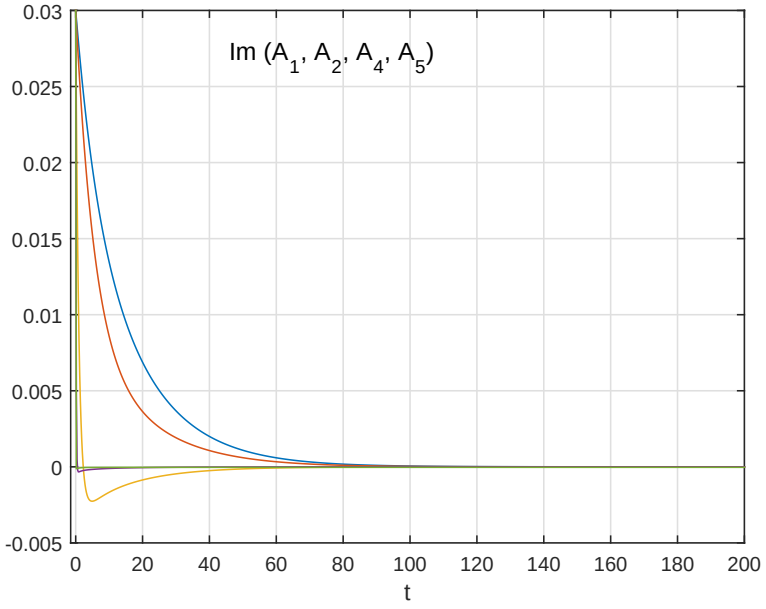

Figure 6.13: The exponential decay (asymptotically) of imaginary parts of A_1, A_2, A_4 and A_5 for the case $N = 3$.

In the numerical experiments with the neutral modes $N = 2$ and $N = 3$ we also found non-zero steady states as illustrated by Figures 6.14–6.19. From the experiments, for all such states $(\mathrm{Re}A_2)^2 + (\mathrm{Im}A_2)^2 \approx 0.025$ for the neutral mode $N = 2$ and $(\mathrm{Re}A_3)^2 + (\mathrm{Im}A_3)^2 \approx 37$ for the neutral mode $N = 3$.

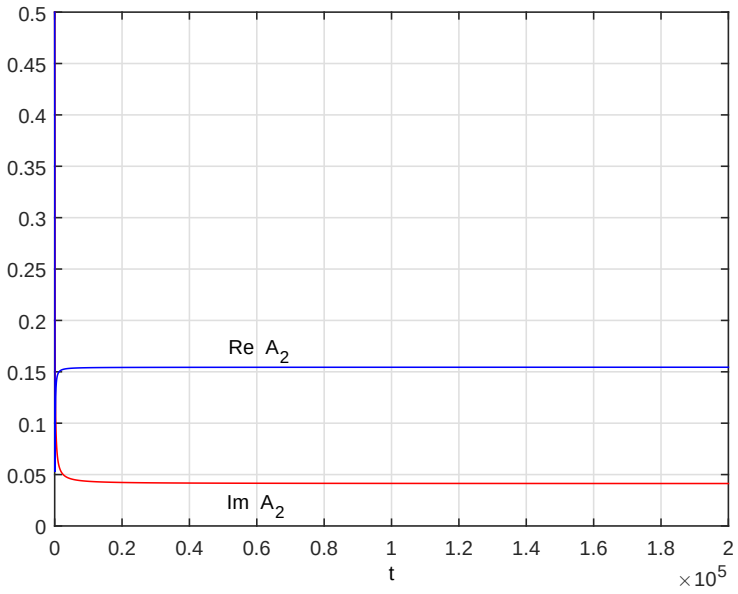

Figure 6.14: The stationary solution for the case $N = 2$ with the initial condition $A_1 = A_2 = A_3 = A_4 = 0.5 + 0.5i$.

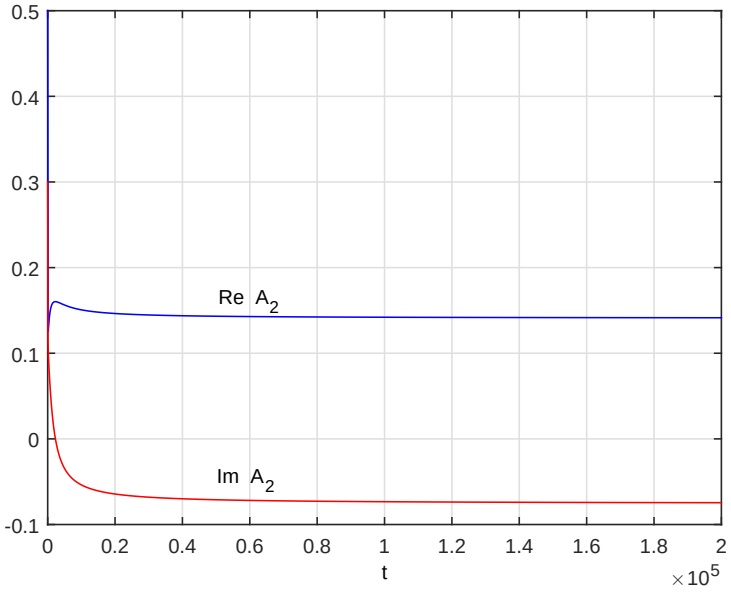

Figure 6.15: The stationary solution for the case $N = 2$ with the initial condition $A_1 = 0.6 + 0.15i$, $A_2 = 0.5 + 0.3i$, $A_3 = 0.3 + 0.4i$, $A_4 = 0.2 + 0.1i$.

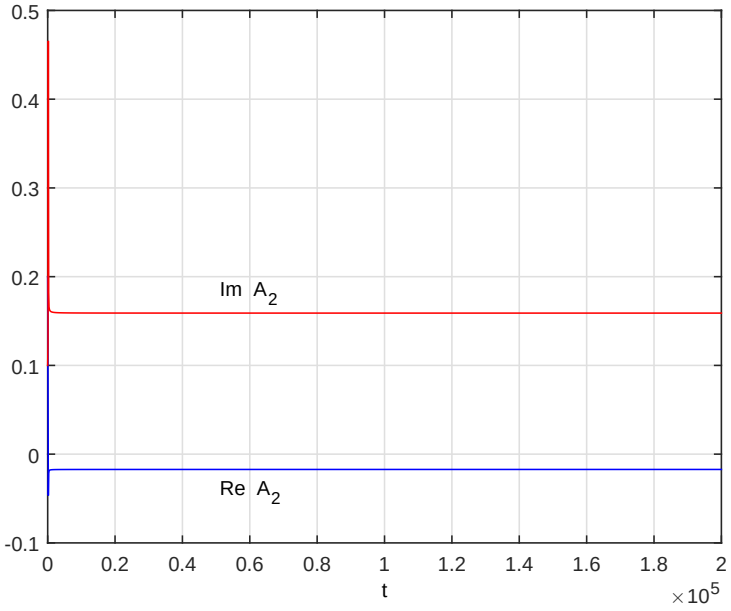

Figure 6.16: The stationary solution for the case $N = 2$ with the initial condition $A_1 = A_2 = A_3 = A_4 = 0.2 + 0.1i$.

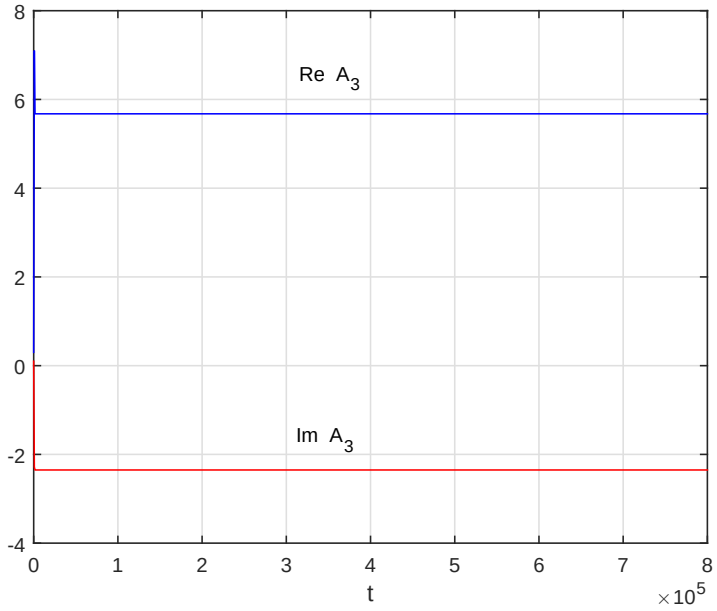

Figure 6.17: The stationary solution for the case $N = 3$ with the initial condition $A_1 = A_3 = A_5 = 0.3 + 0.1i$, $A_2 = A_4 = A_6 = 0.4 + 0.2i$.

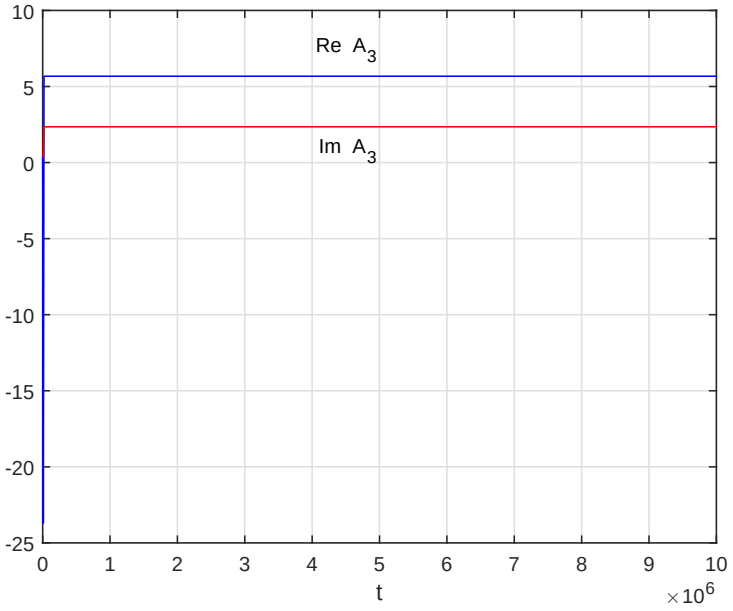

Figure 6.18: The stationary solution for the case $N = 3$ with the initial condition $A_1 = A_2 = A_3 = A_4 = A_5 = A_6 = 0.4 + 0.4i$.

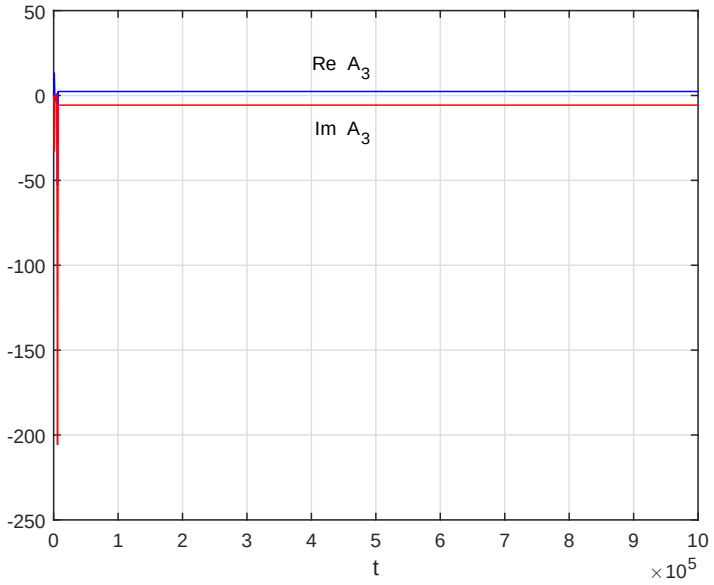

Figure 6.19: The stationary solution for the case $N = 3$ with the initial condition $A_1 = A_2 = A_3 = A_4 = A_5 = A_6 = 0.3 + 0.2i$.

6.4 Concluding remarks

Seismic waves in granular rocks (as well as certain type of reaction-diffusion systems and fluid systems with convection) are described by the Nikolaevskiy equation resulting in the spectrum with dominant frequency/wave number. In the work (Strunin, 2014) such frequency was interpreted as the one belonging to the mode showing slowest decay rather than fastest growth as usually assumed. In the present chapter we investigated the critical case when this mode is neutrally stable. This is the border case separating the impossible situation with self–excited modes and the realistic case of exponentially decaying modes studied in the previous chapters. Depending on the initial conditions and the neutral wave number the system approaches either zero or non-zero steady state. The decaying regime was investigated using the centre manifold technique, revealing the inverse-square-root asymptotic of the solution in time. The results are confirmed by computations of the dynamical system for the time-dependent Fourier modes.

Chapter 7

Conclusions and suggestions for future work

SUMMARY: In this chapter, the main conclusions drawn from this study are summarised. Then, suggestions for further work are presented in the next section.

7.1 Conclusions

In this thesis, we explored the elastic wave propagation in fluid-saturated porous media with bubbles. The thesis consists of the following chapters. Chapter 1 presented the literature review and motivation. Chapter 2 gave general concepts from dynamics. In Chapter 3, we used an extended stress-strain equation relative to the linear standard solid model to take into account the bubbles. Using two–segment rheology, we derived the Frenkel-Biot P1 wave equations for the velocity of the solid matrix, with and without the bubbles. The linearized versions of the equations are compared in terms of the decay rate $\lambda(k)$ of the Fourier modes. For the both cases, the $\lambda(k)$-curve lies entirely below zero. We found that with the increase of the radius and the number of the bubbles the decay rate increases.

In Chapter 4, we investigated how various rheological models, including and excluding the bubbles, affect the linear P1-waves. An extended viscoelastic model relative to the model of Nikolaevskiy (1985) is used. The rheological model for the wave with the bubbles consisted of three segments representing the solid continuum, fluid continuum and a bubble surrounded by the fluid. Using these rheological models, we derived the Nikolaevskiy type equations. The linearized versions of the equations are analysed in terms of the decay rate $\lambda(k)$. The $\lambda(k)$-curve always lies below zero level. We found out that $|\lambda(k)|$ increases with the increase of the radius of the bubbles but decreases with the increase of the number of the bubbles. The decrease manifests the opposite trend to the one observed in Chapter 3. We are inclined to consider the trend obtained in the current chapter as more realistic because of the more complete structure of the bubble element used in the rheological model.

In Chapter 5, we evaluated the influence on the decay rate by the rheological parameters and other parameters of the medium such as pressure and porosity. Each of them has an appreciable effect on the decay rate, as detailed in the thesis. We discovered that the model gives complex wave velocity and/or wave growth, which indicates limitations of the model applicability at extremely large amounts of bubbles. However, we calculated some of acceptable values of the parameters. They belong to finite-size cloud(s) of acceptable values in the multi-dimensional parametric space.

In Chapter 6 we used the centre manifold theory to describe the dynamics of the elastic wave for the special case when there is one neutral mode. Depending on the initial conditions and the neutral wave number k, the system either decays on the centre manifold or approaches non-zero steady state. An asymptotic inverse square-root law for the decay is derived and confirmed numerically by direct computations of the system for the Fourier modes.

7.2 Suggestions for future work

Considering even more elaborated rheological model can be a potential area of future work. In the present thesis we included the bubble into the two-branch rheological model relative to the model of Nikolaevskiy (1985) and then derived and analyzed the wave equations. Instead of using the two-branch model one may consider the three-branch model, see Figure 7.1. This model would give a more complicated constitutive law, which could be interesting to consider.

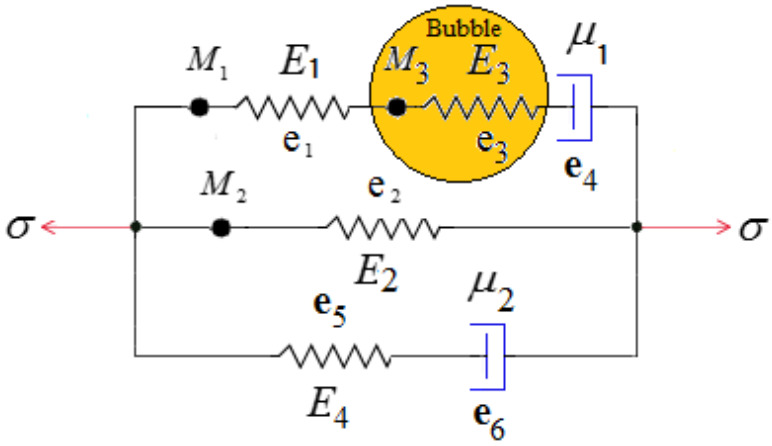

Figure 7.1: Three–branch rheological scheme including a gas bubble.

Another possible future direction is to determine the area(s) of values of the parameters E_i, M_i, p_0, k_b, etc. where the model produces physically acceptable result of $\lambda < 0$. One would need to study the 8+ dimension parametric space formed by the parameters E_i, M_i, p_0, k_b, etc.

References

Agreste, S., Oliveri, F. and Ricciardello, A. (2019), 'Propagation of seismic waves in a continuum modeled as a granular material', *Meccanica* pp. 1–11.

Ali, A. and Strunin, D. V. (2019), 'The role of rheology in modelling elastic waves with gas bubbles in granular fluid-saturated media', *Journal of Mechanics of Materials and Structures* **14**(1), 1–24.

Anderson, A. L. and Hampton, L. D. (1980), 'Acoustics of gas-bearing sediments i. background', *The Journal of the Acoustical Society of America* **67**(6), 1865–1889.

Andronov, A. A., Vitt, A. A. and Khaikin, S. E. (2013), *Theory of Oscillators: Adiwes International Series in Physics*, Vol. 4, Elsevier.

Auriault, J. (1980), 'Dynamic behaviour of a porous medium saturated by a newtonian fluid', *International Journal of Engineering Science* **18**(6), 775–785.

Banks, H. T., Hu, S. and Kenz, Z. R. (2011), 'A brief review of elasticity and viscoelasticity for solids', *Advances in Applied Mathematics and Mechanics* **3**(1), 1–51.

Bedford, A. and Drumheller, D. S. (1994), *Introduction to elastic wave propagation*.

Beresnev, I. A. (2013), 'Compressional-wave propagation in porous media saturated with two fluids', *Geophysics* **79**(1), L1–L11.

Beresnev, I. A. (2016), 'Does biots theory have predictive power?', *Pure and Applied Geophysics* **173**(8), 2671–2686.

Beresnev, I. and Nikolaevskiy, V. (1993), 'A model for nonlinear seismic waves in a medium with instability', *Physica D: Nonlinear Phenomena* **66**(1), 1–6.

Bernoff, A. J. (1994), 'Finite amplitude convection between stress-free boundaries; ginzburg–landau equations and modulation theory', *European Journal of Applied Mathematics* **5**(03), 267–282.

Berryman, J. G. (1981), 'Elastic wave propagation in fluid-saturated porous media', *The Journal of the Acoustical Society of America* **69**(2), 416–424.

Biot, M. A. (1956*a*), 'Theory of propagation of elastic waves in a fluid-saturated porous solid. i. low-frequency range', *The Journal of the acoustical Society of america* **28**(2), 168–178.

Biot, M. A. (1956*b*), 'Theory of propagation of elastic waves in a fluid-saturated porous solid. ii. higher frequency range', *the Journal of the Acoustical Society of America* **28**(2), 179–191.

Biot, M. A. (1962*a*), 'Generalized theory of acoustic propagation in porous dissipative media', *The Journal of the Acoustical Society of America* **34**(9A), 1254–1264.

Biot, M. A. (1962*b*), 'Mechanics of deformation and acoustic propagation in porous media', *Journal of applied physics* **33**(4), 1482–1498.

Biot, M. A. (1965), *Mechanics of incremental deformations: theory of elasticity and viscoelasticity of initially stressed solids and fluids, including thermodynamic foundations and applications to finite strain*, Wiley.

Bohlen, T. (2002), 'Parallel 3-d viscoelastic finite difference seismic modelling', *Computers and Geosciences* **28**(8), 887–899.

Borisov, A. B. and Zverev, V. V. (2016), *Nonlinear Dynamics: Non-integrable Systems and Chaotic Dynamics*, Vol. 36, Walter de Gruyter GmbH and Co KG.

Brunner, W. and Spetzler, H. (2001), 'Observations of time-dependent meniscus behavior with implications for seismic attenuation in three-phase systems', *Geophysical research letters* **28**(9), 1867–1870.

Buckingham, M. J. (1999), 'Theory of compressional and transverse wave propagation in consolidated porous media', *The Journal of the Acoustical Society of America* **106**(2), 575–581.

Burridge, R. and Keller, J. B. (1981), 'Poroelasticity equations derived from microstructure', *The Journal of the Acoustical Society of America* **70**(4), 1140–1146.

Carcione, J. M. (1998), 'Viscoelastic effective rheologies for modelling wave propagation in porous media', *Geophysical prospecting* **46**(3), 249–270.

Carr, J. (2012), *Applications of centre manifold theory*, Vol. 35, Springer Science and Business Media.

Cheng, A. H. D. (2014), 'Fundamentals of poroelasticity', *Analysis and Design Methods: Comprehensive Rock Engineering: Principles, Practice and Projects* **2**, 113.

Ciarletta, M., Straughan, B. and Tibullo, V. (2018), 'Acceleration waves in a nonlinear biot theory of porous media', *International Journal of Non-Linear Mechanics* **103**, 23–26.

Cimellaro, G. P. and Marasco, S. (2018), Energy dissipation, *in* 'Introduction to Dynamics of Structures and Earthquake Engineering', Springer, pp. 161–172.

Collier, L., Neuberg, J., Lensky, N., Lyakhovsky, V. and Navon, O. (2006), 'Attenuation in gas-charged magma', *Journal of volcanology and geothermal research* **153**(1-2), 21–36.

Commander, K. W. and Prosperetti, A. (1989), 'Linear pressure waves in bubbly liquids: Comparison between theory and experiments', *The Journal of the Acoustical Society of America* **85**(2), 732–746.

Cox, S. and Matthews, P. (2007), 'Pattern formation in the damped nikolaevskiy equation', *Physical Review E* **76**(5), 056202.

Dontsov, V., Kuznetsov, V. and Nakoryakov, V. (1987), 'Pressure waves in a porous medium saturated with a gassy fluid', *Fluid Dynamics* **22**(4), 564–570.

Dunin, S., Mikhailov, D. and Nikolayevskiy, V. (2006), 'Longitudinal waves in partially saturated porous media: the effect of gas bubbles', *Journal of applied mathematics and mechanics* **70**(2), 251–263.

Dunin, S. and Nikolaevskiy, V. (2005), 'Nonlinear waves in porous media saturated with live oil', *Acoustical Physics* **51**, S61–S66.

Ferry, J. D. (1980), *Viscoelastic properties of polymers*, John Wiley and Sons.

Findley, W. N. and Davis, F. A. (2013), *Creep and relaxation of nonlinear viscoelastic materials*, Courier Corporation.

Fung, Y. C. (2013), *Biomechanics: mechanical properties of living tissues*, Springer Science and Business Media.

Gardner, T. (2000), 'An acoustic study of soils that model seabed sediments containing gas bubbles', *The Journal of the Acoustical Society of America* **107**(1), 163–176.

Ginoux, J. M. (2015), 'Self-excited oscilations: from poincare to andronov', *arXiv preprint arXiv:1501.03282* .

Ginoux, J. M. and Poincaré, A. H. (2017), 'History of nonlinear oscillations theory in france (1880-1940)', *Archimedes (Book 49)* **6**, 381.

Gonze, D. and Kaufman, M. (2015), 'Theory of non-linear dynamical systems'.

Gubaidullin, A., Boldyreva, O. Y. and Dudko, D. (2017), Waves in porous media saturated with bubbly liquid, *in* 'Journal of Physics: Conference Series', Vol. 899, IOP Publishing, p. 032011.

Guschin, V.V., Z. Y. R. S. (1998), 'Nonlinear transformation of high-frequency seismic pulses running in a wet soil', *Izvestiya, Solid Earth Phys* (5), 92–96.

Hadjidemetriou, J. D. and Voyatzis, G. (2011), 'Different types of attractors in the three body problem perturbed by dissipative terms', *International Journal of Bifurcation and Chaos* **21**(08), 2195–2209.

Hara, Y. (2014), 'Function and autonomous behavior of self-oscillating polymer systems', *Polymers* **6**(7), 1958–1971.

Holmes, M. H. (2009), *Introduction to the foundations of applied mathematics*, Vol. 56, Springer Science and Business Media.

Johnson, R., Obaya, R., Novo, S., Núñez, C. and Fabbri, R. (2016), *Nonautonomous Linear Hamiltonian Systems: Oscillation, Spectral Theory and Control*, Vol. 36, Springer.

Kim, Y. I. (2008), Advanced numerical and experimental transient modelling of water and gas pipeline flows incorporating distributed and local effects., PhD thesis.

Kudryashov, N. A. and Sinelshchikov, D. I. (2014), 'Extended models of non-linear waves in liquid with gas bubbles', *International Journal of Non-Linear Mechanics* **63**, 31–38.

Kurzeja, P. S. and Steeb, H. (2012), 'About the transition frequency in biots theory', *The Journal of the Acoustical Society of America* **131**(6), EL454–EL460.

Landa, P. S. (2013), *Nonlinear oscillations and waves in dynamical systems*, Vol. 360, Springer Science and Business Media.

Layek, G. (2015), *An Introduction to Dynamical Systems and Chaos*, Springer.

Lemaitre, J. (2001), *Handbook of Materials Behavior Models, Three-Volume Set: Nonlinear Models and Properties*, Academic Press.

Lévy, T. (1979), 'Propagation of waves in a fluid-saturated porous elastic solid', *International Journal of Engineering Science* **17**(9), 1005–1014.

Liu, H. P., Anderson, D. L. and Kanamori, H. (1976), 'Velocity dispersion due to anelasticity; implications for seismology and mantle composition', *Geophysical Journal International* **47**(1), 41–58.

Lo, W. C., Sposito, G. and Majer, E. (2005), 'Wave propagation through elastic porous media containing two immiscible fluids', *Water Resources Research* **41**(2).

Lozano, R., Brogliato, B., Egeland, O. and Maschke, B. (2013), *Dissipative systems analysis and control: theory and applications*, Springer Science and Business Media.

Lu, J. F., Hanyga, A. and Jeng, D. S. (2007), 'A mixture-theory-based dynamic model for a porous medium saturated by two immiscible fluids', *Journal of Applied Geophysics* **62**(2), 89–106.

Masson, Y., Pride, S. and Nihei, K. (2006), 'Finite difference modeling of biot's poroelastic equations at seismic frequencies', *Journal of Geophysical Research: Solid Earth* **111**(B10).

Matsumoto, Y. and Kameda, M. (1996), 'Propagation of shock waves in dilute bubbly liquids: Governing equations, hugoniot relations, and effect of slippage between two phases', *JSME International Journal Series B Fluids and Thermal Engineering* **39**(2), 264–272.

Matthews, P. and Cox, S. (2000), 'One-dimensional pattern formation with galilean invariance near a stationary bifurcation', *Physical Review E* **62**(2), R1473.

Merxhani, A. (2016), 'An introduction to linear poroelasticity', *arXiv preprint arXiv:1607.04274* .

Mikhailov, A. S. (2012), *Foundations of Synergetics I: Distributed Active Systems*, 2nd edn, Springer Publishing Company, Incorporated.

Mikhailov, A. S. and Loskutov, A. Y. (2013), *Foundations of synergetics II: Chaos and Noise*, Vol. 52, Springer Science and Business Media.

Mikhailov, D. (2010), 'The influence of gas saturation and pore pressure on the characteristics of the frenkel-biot p waves in partially saturated porous media', *Izvestiya Physics of the Solid Earth* **46**(10), 897–909.

Mukherjee, N. and Poria, S. (2012), 'Preliminary concepts of dynamical systems', *International Journal of Applied Mathematical Research* **1**(4), 751–770.

Müller, G., Weber, M., Rümpker, G. and Gajewski, D. (2007), *Theory of elastic waves*, Geoforschungszentrum.

Müller, T. M., Gurevich, B. and Lebedev, M. (2010), 'Seismic wave attenuation and dispersion resulting from wave-induced flow in porous rocksa review', *Geophysics* **75**(5), 75A147–75A164.

Nakoryakov, V., Sobolev, V. and Shreiber, I. (1972), 'Longwave perturbations in a gas-liquid mixture', *Fluid Dynamics* **7**(5), 763–768.

Nikolaevskiy, V. (1985), 'Viscoelasticity with internal oscillators as a possible model of seismoactive medium', *Doklady Akademii Nauk SSSR* **283**(6), 1321–1324.

Nikolaevskiy, V. (1996), *Geomechanics and Fluidodynamics*, Nedra, Moscow and Kluwer, Dordrecht.

Nikolaevskiy, V. (2005), 'Biot–frenkel poromechanics in russia', *Journal of Engineering Mechanics* **131**(9), 888–897.

Nikolaevskiy, V. (2016), 'A real p-wave and its dependence on the presence of gas', *Izvestiya, Physics of the Solid Earth* **52**(1), 1–13.

Nikolaevskiy, V. N. (1989), Dynamics of viscoelastic media with internal oscillators, *in* 'Recent Advances in Engineering Science', Springer, pp. 210–221.

Nikolaevskiy, V. N. (1990), *Mechanics of porous and fractured media*, Vol. 8, World Scientific.

Nikolaevskiy, V. N. (2008), 'Non-linear evolution of p-waves in viscous–elastic granular saturated media', *Transport in Porous Media* **73**(2), 125–140.

Nikolaevskiy, V. and Stepanova, G. (2005), 'Nonlinear seismics and the acoustic action on the oil recovery from an oil pool', *Acoustical Physics* **51**, S131–S139.

Nikolaevskiy, V. and Strunin, D. (2012), The role of natural gases in seismics of hydrocarbon reservoirs, *in* 'Proc. 3rd International Conference Elastic Wave Effect on Fluid in Porous Media EWEF-2012', pp. 25–29.

Novotny, O. (1999), 'Seismic surface waves'.

Özkaya, N., Leger, D., Goldsheyder, D. and Nordin, M. (2017), Mechanical properties of biological tissues, *in* 'Fundamentals of Biomechanics', Springer, pp. 361–387.

Papageorgiou, G. and Chapman, M. (2015), 'Multifluid squirt flow and hysteresis effects on the bulk modulus–water saturation relationship', *Geophysical Journal International* **203**(2), 814–817.

Pechenkin, A. (2002), 'The concept of self-oscillations and the rise of synergetics ideas in the theory of nonlinear oscillations', *Studies in History and Philosophy of Science Part B: Studies in History and Philosophy of Modern Physics* **33**(2), 269–295.

Plona, T. J. (1980), 'Observation of a second bulk compressional wave in a porous medium at ultrasonic frequencies', *Applied Physics Letters* **36**(4), 259–261.

Poon, K. F. (2009), Dynamics of the Nikolaevskiy and related equations, PhD thesis, Dept. of Mathematics-Simon Fraser University.

Pride, S. R., Gangi, A. F. and Morgan, F. D. (1992), 'Deriving the equations of motion for porous isotropic media', *The Journal of the Acoustical Society of America* **92**(6), 3278–3290.

Rabinovich, M. I. and Trubetskov, D. (2012), *Oscillations and waves: in linear and nonlinear systems*, Vol. 50, Springer Science and Business Media.

Regenauer Lieb, K., Veveakis, M., Poulet, T., Wellmann, F., Karrech, A., Liu, J., Hauser, J., Schrank, C., Gaede, O. and Trefry, M. (2013), 'Multiscale coupling and multiphysics approaches in earth sciences: Theory', *Journal of Coupled Systems and Multiscale Dynamics* **1**(1), 49–73.

Roberts, A. (1989), 'Appropriate initial conditions for asymptotic descriptions of the long term evolution of dynamical systems', *The Journal of the Australian Mathematical Society. Series B. Applied Mathematics* **31**(01), 48–75.

Roberts, T. (1998), 'Differential algebraic equation solvers', *MathWorks: https://www.mathworks.com/matlabcentral/fileexchange/28-differential-algebraic-equation-solvers* .

Santos, J. E., Corberó, J. M. and Douglas Jr, J. (1990), 'Static and dynamic behavior of a porous solid saturated by a two-phase fluid', *The Journal of the Acoustical Society of America* **87**(4), 1428–1438.

Sharma, M. and Saini, R. (2012), 'Wave propagation in porous solid containing liquid filled bound pores and two-phase fluid in connected pores', *European Journal of Mechanics-A/Solids* **36**, 53–65.

Shearer, P. M. (2010), 'Introduction to seismology: The wave equation and body waves', *Lecture Notes: http://www. deep-earth. org/2010/Seismo-1-shearer. pdf* .

Silberman, E. (1957), 'Sound velocity and attenuation in bubbly mixtures measured in standing wave tubes', *The journal of the Acoustical Society of America* **29**(8), 925–933.

Simbawa, E., Matthews, P. C. and Cox, S. M. (2010), 'Nikolaevskiy equation with dispersion', *Physical Review E* **81**(3), 036220.

Skrzypek, J. and Ganczarski, A. W. (2015), *Mechanics of Anisotropic Materials*, Springer.

Smeulders, D. (2005), 'Experimental evidence for slow compressional waves', *Journal of Engineering Mechanics* **131**(9), 908–917.

Socolar, J. E. (2007), 'Nonlinear dynamical systems', *Complex Systems Science in Biomedicine* p. 115.

Strogatz, S. H. (2018), *Nonlinear dynamics and chaos: with applications to physics, biology, chemistry, and engineering*, CRC Press.

Strunin, D. (2009), 'Phase equation with nonlinear excitation for nonlocally coupled oscillators', *Physica D: Nonlinear Phenomena* **238**(18), 1909–1916.

Strunin, D. (2014), 'On dissipative nature of elastic waves', *Journal of Coupled Systems and Multiscale Dynamics* **2**(2), 70–73.

Strunin, D. and Ali, A. A. (2016), 'On nonlinear dynamics of neutral modes in elastic waves in granular media', *Journal of Coupled Systems and Multiscale Dynamics* **4**(3), 163–169.

Strunin, D. and Mohammed, M. (2015), 'Range of validity and intermittent dynamics of the phase of oscillators with nonlinear self-excitation', *Communications in Nonlinear Science and Numerical Simulation* .

Sutton, G. P. and Biblarz, O. (2017), *Rocket propulsion elements*, John Wiley and Sons.

Tanaka, D. (2004), 'Chemical turbulence equivalent to nikolavskii turbulence', *Physical Review E* **70**(1), 015202.

Tanaka, D. and Okamura, M. (2010), 'Modal and total power spectra of nikolaevskii turbulence', *Journal of the Physical Society of Japan* **79**(12), 124004.

Thiessen, R. J. and Cheviakov, A. F. (2019), 'Nonlinear dynamics of a viscous bubbly fluid', *Communications in Nonlinear Science and Numerical Simulation* .

Tisato, N., Quintal, B., Chapman, S., Podladchikov, Y. and Burg, J. P. (2015), 'Bubbles attenuate elastic waves at seismic frequencies: First experimental evidence', *Geophysical Research Letters* **42**(10), 3880–3887.

Toksöz, M. N., Cheng, C. H. and Timur, A. (1976), 'Velocities of seismic waves in porous rocks', *Geophysics* **41**(4), 621–645.

Tribelsky, M. I. (2008), 'Patterns in dissipative systems with weakly broken continuous symmetry', *Physical Review E* **77**(3), 035202.

Tribelsky, M. I. and Tsuboi, K. (1996), 'New scenario for transition to turbulence?', *Physical review letters* **76**(10), 1631.

Tribelsky, M. I. and Velarde, M. G. (1996), 'Short-wavelength instability in systems with slow long-wavelength dynamics', *Physical Review E* **54**(5), 4973.

Tuncay, K. and Corapcioglu, M. Y. (1996), 'Body waves in poroelastic media saturated by two immiscible fluids', *Journal of Geophysical Research: Solid Earth* **101**(B11), 25149–25159.

Vilchinska, N. and Nikolaevskiy, V. (1984), 'Acoustical emission and spectrum of seismic signals', *Solid Earth Physics* pp. 91–100.

Vilchinska, N., Nikolaevskiy, V. and Lisin, V. (1985), 'Slow waves and natural oscillations in sandy marine soils', *Izvestiya Acad. Nauk SSSR, Oceanology* (4).

Vyalov, S. S. (2013), *Rheological fundamentals of soil mechanics*, Vol. 36, Elsevier.

Wang, H. F. (2017), *Theory of linear poroelasticity with applications to geomechanics and hydrogeology*, Princeton University Press.

Watanabe, M. and Prosperetti, A. (1994), 'Shock waves in dilute bubbly liquids', *Journal of fluid mechanics* **274**, 349–381.

Watt, S. D. and Roberts, A. J. (1995), 'The accurate dynamic modelling of contaminant dispersion in channels', *SIAM Journal on Applied Mathematics* **55**(4), 1016–1038.

Wayne, C. (2012), 'Dissipative partial differential equations and dynamical systems'.

Wei, C. and Muraleetharan, K. K. (2002), 'A continuum theory of porous media saturated by multiple immiscible fluids: I. linear poroelasticity', *International Journal of Engineering Science* **40**(16), 1807–1833.

Wijngaarden, L. v. (1968), 'On the equations of motion for mixtures of liquid and gas bubbles', *Journal of Fluid Mechanics* **33**(3), 465–474.

Wijngaarden, L. v. (1972), 'One-dimensional flow of liquids containing small gas bubbles', *Annual review of fluid Mechanics* **4**(1), 369–396.

Willems, J. C. (2007), 'Dissipative dynamical systems', *European Journal of Control* **2**(13), 134–151.

Yang, L., Yang, D. and Nie, J. (2014), 'Wave dispersion and attenuation in viscoelastic isotropic media containing multiphase flow and its application', *Science China Physics, Mechanics and Astronomy* **57**(6), 1068–1077.

Zhi-jun, F., Jia-ming, Z. and Hong-suo, Y. (2014), 'A constitutive model for mudstone shear creep', *Electronic Journal of Geotechnical Engineering* **19**, Z6.

Appendix A

Maxima program

The following Maxima program is used to calculate the coefficients (6.14).

```
A2:a1*A1+b1*A1c+a2*A1*A1c+m2*A1^2+n2*A1c^2+a3*A1^2*A1c+b3*A1c^2*A1
+g3*A1^3+h3*A1c^3 +w4*A1^4+x4*A1^3*A1c+y4*A1^2*A1c^2 +z4*A1*A1c^3+
l4*A1c^4;
%---------------------------------------------------------------%
A3:p1*A1+q1*A1c+p2*A1*A1c+f2*A1^2+k2*A1c^2+p3*A1^2*A1c+q3*A1c^2*A1
+v3*A1^3+y3*A1c^3;
%---------------------------------------------------------------%
A2c:a1*A1c+b1*A1+a2*A1c*A1+m2*A1c^2+n2*A1^2+a3*A1c^2*A1+b3*A1^2*A1c
+g3*A1c^3+h3*A1^3+w4*A1c^4+x4*A1c^3*A1+y4*A1c^2*A1^2 +z4*A1c*A1^3
+l*A1^4;
%---------------------------------------------------------------%
A3c:p1*A1c+q1*A1+p2*A1c*A1+f2*A1c^2+k2*A1^2+p3*A1c^2*A1+q3*A1^2*A1c
+v3*A1c^3+y3*A1^3;
%---------------------------------------------------------------%
EQA2:diff(A2,A1)*dotA1+diff(A2,A1c)*dotA1c+36*A2+A1^2-6*A3*A1c;
EQA3:diff(A3,A1)*dotA1+diff(A3,A1c)*dotA1c+576*A3+4*A1*A2;
%---------------------------------------------------------------%
```

```
FA2:expandwrt(subst([dotA1=4*A2*A1c+12*A3*A2c,dotA1c=4*A2c*A1+12*
A3c*A2],EQA2),A1,A1c);
/*FA3:expandwrt(subst([dotA1=4*A2*A1c+12*A3*A2c,dotA1c=4*A2c*A1+
12*A3c*A2],EQA3),A1,A1c);*/
%---------------------------------------------------------------%
subst([A1^8=0,A1c^8=0,A1^7=0,A1c^7=0,A1^6=0,A1c^6=0,A1^5=0,A1c^5=0]
,FA2);
/*subst([A1^9=0,A1c^9=0,A1^8=0,A1c^8=0,A1^7=0,A1c^7=0,A1^6=0,A1c^6=0
,A1^5=0,A1c^5=0],FA3);*/
%---------------------------------------------------------------%
collectterms(%,A1,A1c,A1*A1c,A1^2,A1c^2,A1^2*A1c,A1*A1c^2,A1^3,A1c^3
,A1^3*A1c,A1^2*A1c^2,A1*A1c^3,A1^4,A1c^4);
```

Appendix B

An extract from the paper of Nikolaevskiy (2008)

1 Introduction

The dominant frequency effect consists in transfer of any type of mechanical impact at a soil/rock massive to a wave with this frequency (Nikolaevskiy 1996). It is also known that these waves are disturbing its structure the most effectively. It was found experimentally for marine sands (Vilchinska and Nikolaevskiy 1984) but typical for all weak soils (Nikolaev 1965; Guschin 1998) or fragmented rocks, that is, for granular media. The term *dominant* frequency exists in the book by Biot (1965) and it is used here in the same sense as it appears sometimes in the engineering literature (ISRM 1992).

The aim of publications (Nikolaevskiy 1989; Beresnev and Nikolàevskiy 1993) and this article is to explain the dominant frequency effect by free oscillations of porous matrix fragments (grains, for instance) under the complex elastic–viscous response of grain contacts, wetted with foreign fluid or fluid films of special state due to close presence of solid matter.

In the literature there are known many attempts of generalization of porodynamics by the changes of the state laws for deformation or fluid flows (Nikolaevskiy 1996; Donskoy 1997; Hokstadt 2004). Here the viscous–elastic properties of the matrix in the Frenkel–Biot model (Frenkel 2005; Biot 1956; Nikolaevskiy 2005) are generalized in a manner, essential for dynamic processes. The latter is used in a form of non-linear balances with constitutive laws, based on the thermodynamics, conventional for continuum theories, as it was done long ago (Nikolaevskiy et al. 1970).

In articles (Nikolaevskiy 1989; Beresnev and Nikolàevskiy 1993) the key role is given to introduction of higher time derivatives into the laws, connecting stress and strains. The corresponding coefficients are determined in the rheologic scheme by masses of internal oscillators (of free granules or blocks) and additional viscosities (existed at granules contact due wetting effects) of the matrix (skeleton) itself. As a result, the wave-evolution equation appeared to be the further generalization of the Korteweg–de Vries–Burgers equation with positive coefficients at its right side and this reflects the decaying of oscillations in the earth materials. The negative values of coefficients correspond to a raw of solitons (Kawahara 1983), typical for shallow water dynamics.

However, in a simple numerical example (Beresnev and Nikolàevskiy 1993) it was found that stable solution could exist for some short time, but afterwards the calculations became impossible. Later, the skilled analytical studies, added with calculations by supercomputers, had shown (Tribelsky and Tsuboi 1996; Tribelsky and Velarde 1996; Tribelsky 1997; Xi et al. 2000) the nature of appearing chaos and the need of bulk dissipating sink to get stable asymptotic waves (Tribelsky 2007).

Let consider if the Darcy term responsible for involvement of saturating fluid phase can generate the bulk dissipation necessary for stabilization of the evolution process.

2 One-Dimension Dynamics Equations

For simplicity, we consider only one-dimensional case. Then the momentum balance for the solid matrix has the form:

$$\frac{\partial}{\partial t}(1-\phi)\rho^{(s)}v + \frac{\partial}{\partial x}(1-\phi)\rho^{(s)}vv = \frac{\partial}{\partial x}\sigma^{f} - (1-\phi)\frac{\partial p}{\partial x} - R \tag{2.1}$$

here, v is its velocity, ϕ is porosity, R is interfacial viscous force, created due to the relative fluid flow, μ_f is fluid viscosity and k is intrinsic permeability:

$$R = \delta\phi\,(v-u), \quad \delta = \mu_f\phi/k \tag{2.2}$$

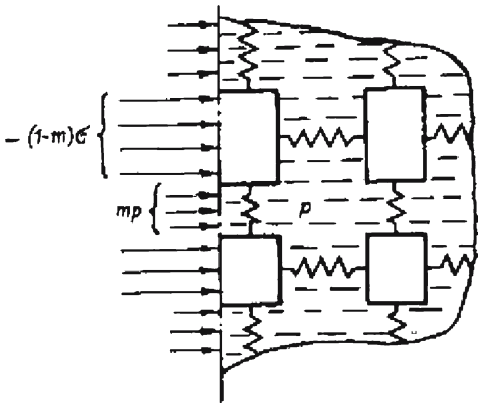

Fig. 1 The scheme of stresses distribution in a porous saturated medium: the effective stresses acts in springs

The non-divergent form of (2.1) is evident in non-linear cases. The effective stresses are introduced as (Fig. 1):

$$\sigma^f = (1-\phi)(\sigma + p) = \Gamma + p \tag{2.3}$$

where σ is the true stress in the solid matrix, $\rho^{(s)}$ is solid density, p is the pore pressure and Γ are the total stresses, acting at a cross-section of the medium:

$$\Gamma = (1-\phi)\sigma - \phi p \tag{2.4}$$

The effective stress (2.3) is one of possible linear combinations in the constitutive law for solid matrix but it is selected by its role in the failure conditions (for example, in the Coulomb criterion for fluid saturated soils as it was found in 1925 by Karl Terzaghi, see Nikolaevskiy (1996); Nikolaevskiy et al. (1970)). Besides (2.3) includes the only measurable variables and all other variants are needed in knowledge of elastic modules that will be found after interpretation of tests with samples. The corresponding thermodynamics was developed in Nikolaevskiy et al. (1970) and reproduced in Nikolaevskiy (1996). The balances forms, used in Nikolaevskiy (1996), permits to get a non-linear variant of the Frenkel–Biot model and to eliminate its some shortcomings.

The impulse balance for a fluid part of the medium looks as

$$\frac{\partial}{\partial t}\phi\rho^{(f)}u + \frac{\partial}{\partial x}\phi\rho^{(f)}u\,u = -\phi\frac{\partial p}{\partial x} + R \tag{2.5}$$

Mass balances for a porous medium have the following form:

$$\frac{\partial}{\partial t}(1-\phi)\rho^{(s)} + \frac{\partial}{\partial x}(1-\phi)\rho^{(s)}v = 0; \quad \frac{\partial}{\partial t}\phi\,\rho^{(f)} + \frac{\partial}{\partial x}\phi\,\rho^{(f)}u = 0 \tag{2.6}$$

Here u is the fluid velocity, indices (s) and (f) are symbols of solid and fluid parameters, respectively, $\rho^{(f)}$ is the fluid density. The true stress, σ, determines the density changes of solid intact material:

$$\begin{aligned}\rho^{(s)} &= \rho_0^{(s)}(1-\beta^{(s)}\sigma) = \rho_0^{(s)}\left[1+\beta^{(s)}p - \beta^{(s)}\sigma^f/(1-\phi)\right] \\ &\approx \rho_0^{(s)}\left[1+\beta^{(s)}p - \beta^{(s)}\sigma^f\right]\end{aligned} \tag{2.7}$$

The equation of the fluid phase state has the same form but for fluid (pore) pressure p:

$$\rho^{(f)} = \rho_0^f (1 + \beta^{(f)} p) \tag{2.8}$$

It is known that the description of solid dynamics in terms of displacement velocities is preferable than displacements themselves to avoid an integral stress–strain links, typical for elastic–viscous bodies. However, let remind that in this case there is a need to use the Oldroyd derivatives to get the same determination of strains through displacement as in non-linear elasticity (Nikolaevskiy 1996).

In one-dimension case the Oldroyd derivative is the usual Lagrange one and this gives the following relation exists between deformation e and solid velocity v:

$$\frac{De}{Dt} \equiv \frac{\partial e}{\partial t} + v\frac{\partial e}{\partial x} = \frac{\partial v}{\partial x} \tag{2.9}$$

Let account for these derivatives in the effective stress and the strain tensors in pore-elastic law, where the polynomial viscous terms are added:

$$\sigma^f + \sum_{q=1}^{n} a_q \frac{D^q \sigma^f}{Dt^q} = E[e + \beta^{(s)} Kp] + \sum_{q=1}^{m} b_q \frac{D^q e}{Dt^q} \tag{2.10}$$

where $E = \lambda_1 + 2\lambda_2$ is elastic ID modulus, $K = \lambda_1 + (2/3)\lambda_2$ is the bulk elastic module of the porous matrix, λ_1, λ_2 are the Lame coefficients, a_q, b_q is the elastic–viscous coefficients, assumed constants. By introduction of pore pressure p, we are generalizing the constitutive equation, suggested in Nikolaevskiy (1989).

It is possible to illustrate (2.10) by rheological scheme in Fig. 2 which generalizes the Maxwell–Voigt element by attaching free oscillators (grains of a porous medium, given in Fig. 1) to elastic contact springs (Nikolaevskiy 1996; Nikolaevskiy 1989). These oscillators possess own masses M_i that are included into constants a_q and b_q as well as the piston viscosities (see Nikolaevskiy (1989)).

It can be seen that Fig. 2 corresponds to the case in which $n = 3$ and $m = 5$. Two internal concentrated masses M have a dimension $[M] = [\rho][L^2]$. Because the matrix impulse itself includes the density, ρ, the oscillator mass means practically the introduction of internal length scale l such that

$$l^2 = M/\rho \tag{2.11}$$

That is, law (2.10) reflects dynamics of the medium fragments (sand grain conglomerates, for example) in a continuum theory. Figure 2 describes the response of the scheme of Fig. 1

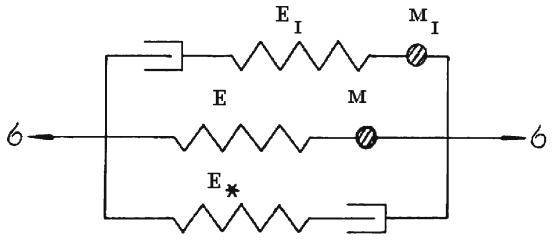

Fig. 2 Elastic springs (E_I, E and E_*) and viscous pistons of the Maxwell–Voigt rheology are added with internal oscillators M_I and M

to dynamical loads with account for the grain's oscillation and viscous delay due to a special rheology of contacts where another fluid is present.

3 Evolution of P_2 Wave in Wet Soils

In the impulse balance of wet matrix (2.1) it is possible to neglect fluid inertia, that is:

$$\frac{\partial}{\partial t}(1-\phi)\rho^{(s)}v + \frac{\partial}{\partial x}(1-\phi)\rho^{(s)}vv = \frac{\partial \sigma^f}{\partial x} - \frac{\partial p}{\partial x} \tag{3.1}$$

Really, density of air, saturating soil, is extremely small (gas under low pressure). Because air phase is soft and matrix grains are practically rigid, we have porosity changes connected with grain repacking and the mass balance for gas phase may be represented as:

$$\frac{\partial}{\partial t}\phi p + \frac{\partial}{\partial x}\phi p u = 0, \quad \frac{\rho^{(f)}}{\rho_0^{(f)}} = \frac{p}{p_0} \tag{3.2}$$

here, index zero corresponds to the reference sate and isothermal condition is assumed. In impulse balance of fluid phase (2.5) now we can neglect the inertial terms and it takes a form of the Darcy law:

$$R \equiv \delta\,\phi(v-u) \;=\; \phi\frac{\partial p}{\partial x_i} \tag{3.3}$$

that excludes pore pressure from the matrix dynamics equation:

$$\frac{\partial}{\partial t}[(1-\phi)\rho^{(s)}v] + \frac{\partial}{\partial x}[(1-\phi)\rho^{(s)}vv] = \frac{\partial \sigma^f}{\partial x} - \delta(v-u) \tag{3.4}$$

Due to incompressibility of grains ($\beta^{(s)} = 0$), the stress–strain rate law of the matrix (2.10) has the form as for a single continuum case (Nikolaevskiy 1989):

$$\sigma^f + \sum_{q=1}^{n} a_q \frac{D^q \sigma^f}{Dt^q} = Ee + \sum_{q=1}^{m} b_q \frac{D^q e}{Dt^q} \tag{3.5}$$

As it usual for treatment of weak non-linear waves, let use the running coordinate system with simultaneous scale changes:

$$\begin{gathered} \xi = \eta^\alpha (x - ct), \quad \tau = \left(\frac{1}{2}\right)\eta^\beta t \\ \frac{\partial}{\partial x} \to \eta^\alpha \frac{\partial}{\partial \xi}; \quad \frac{\partial}{\partial t} \to \eta^\alpha \left(\frac{1}{2}\eta^{\beta-\alpha}\frac{\partial}{\partial \tau} - c\frac{\partial}{\partial \xi}\right) \end{gathered} \tag{3.6}$$

where $\beta = \alpha + 1$, $\alpha = 1$ and $\eta << 1$ is a small parameter. We assume that air viscosity is extremely small, that is $\delta = \eta \mathrm{O}(v)$ at least. Then

$$\begin{gathered} \left(\frac{1}{2}\eta^{\beta-\alpha}\frac{\partial}{\partial \tau}(1-\phi)\rho^{(s)}v\right) = \frac{\partial \sigma^f}{\partial \xi} - \frac{\partial p}{\partial \xi} - (v-c)\frac{\partial}{\partial \xi}(1-\phi)\rho^{(s)}v \\ \delta\phi(v-u) \;= \eta^\alpha \phi \frac{\partial p}{\partial \xi}, \quad \left(\delta = \frac{\mu\,\phi}{k}, \quad v - u \approx \mathrm{O}(v), \quad u \approx 0\right) \end{gathered} \tag{3.7}$$

$$\frac{1}{2}\eta^{\beta-\alpha}\frac{\partial(1-\phi)}{\partial \tau} = -\frac{\partial}{\partial \xi}(1-\phi)(v-c)$$

$$\sigma^f - Ee = T \equiv -\sum_{q=1}^{n} a_q \Pi_{p=1}^{q} \eta^q \left[\eta \frac{1}{2}\frac{\partial}{\partial \tau} + (v-c)\frac{\partial}{\partial \xi}\right]^q \sigma^f + \sum_{q=1}^{m} b_q \Pi_{p=1}^{q} \eta^q \left[\eta \frac{1}{2}\frac{\partial}{\partial \tau} + (v-c)\frac{\partial}{\partial \xi}\right]^q e \tag{3.8}$$

Also apply the following series for dynamical variables of a wave:

$$\begin{aligned} p &= p_0 + \eta p_1 + \eta^2 p_2 + \cdots; \quad v = \eta\, v_1 + \eta^2 v_2 + \cdots; \\ e &= e_0 + \eta\, e_1 + \eta^2 e_2 + \cdots \phi = \phi_0 + \eta\, \phi_1 + \eta^2 \phi_2 + \cdots; \\ \sigma^f &= \sigma_0^f + \eta\, \sigma_1^f + \eta^2 \sigma_1^f + \cdots \end{aligned} \tag{3.9}$$

In order to consider the first approximation, we select the momentum equation, the strain definition through velocity field, the strain-stress law and material balance, consequently:

$$\begin{aligned} &\frac{\partial {\sigma_1}^f}{\partial \xi} + (1-\phi_0)\rho_0^{(s)} c \frac{\partial v_1}{\partial \xi} = \eta\Sigma, \quad \frac{\partial v_1}{\partial \xi} + c\frac{\partial e_1}{\partial \xi} = \eta F, \\ &\sigma_1^f - Ee_1 = \eta T, \quad \frac{\partial}{\partial \xi}[v_1(1-\phi_0) + c\phi_1] = \eta\left(\frac{1}{2}\frac{\partial \phi_1}{\partial \tau} - c\frac{\partial v_1 \phi_1}{\partial \xi}\right) \end{aligned} \tag{3.10}$$

here, stress and strain of the reference state satisfy (3.9) and

$$\Sigma = (1-\phi_0)\rho_0^{(s)}\left(\frac{1}{2}\frac{\partial v_1}{\partial \tau}\right) + \rho_0^{(s)}\frac{\partial}{\partial \xi}[(1-\phi_0)v_1 - \phi_1 c]v_1 + \frac{\delta}{\eta}v_1,$$

$$F = \frac{1}{2}\frac{\partial e_1}{\partial \tau} + v_1\frac{\partial e_1}{\partial \xi},$$

neglecting the right sides of this set of equations gives the integrals as well as the first porosity increment as well as the first porosity increment from (3.10):

$$\begin{aligned} &{\sigma_1}^f + (1-\phi_0)\rho^{(s)} c v_1 = 0; \quad \sigma_1^f = -Ev_1/c \\ &e_1 = -v_1/c; \quad \phi_1 = -(1-\phi_0)(v_1/c) \end{aligned} \tag{3.11}$$

Integrals (3.11) determine the wave velocity through the 1D elastic modulus of the matrix and its total density $\rho = (1-\phi_0)\rho^{(s)}$:

$$c = +\sqrt{\frac{E}{(1-\phi_0)\rho^{(s)}}} = +\sqrt{\frac{E}{\rho}}; \tag{3.12}$$

In the second approximation, the same system of equations is valid but relatively to three variables (v_2, σ_2^f and e_2) but with not negligible right-side parts:

$$(1-\phi_0)\rho^{(s)} c\frac{\partial v_2}{\partial \xi} + \frac{\partial {\sigma_2}^f}{\partial \xi} = \Sigma, \quad \frac{\partial v_2}{\partial \xi} + c\frac{\partial e_2}{\partial \xi} = F, \quad \sigma_2^f - Ee_2 = T \tag{3.13}$$

$$T = -\sum_{q=1}^{n} a_q \Pi_{p=1}^{q} \eta^q (-c)^{q-1} \left(\frac{\partial v_1}{\partial \xi}\right)^q E + \sum_{q=1}^{m} b_q \Pi_{p=1}^{q} \eta^q (-c)^{q-1} \left(\frac{\partial v_1}{\partial \xi}\right)^q \quad (3.14)$$

The determinant of (3.13) is equal to zero if the wave velocity has value (3.12). Therefore we need the compatibility condition of Eq. 3.13

$$\begin{vmatrix} 1 & \Sigma \\ c & EF + cT \end{vmatrix} = 0 \quad \text{or} \quad EF - c\Sigma + c\frac{\partial T}{\partial \xi} = 0, \quad (3.15)$$

which one may consider as the evolution equation for the wave under consideration.

Use right sides of (3.9), expressing all variables through $v \equiv v_1$, according to (3.11). Then we get the evolution equation that includes rather small bulk dissipation of η - order (if the air viscosity μ_f in soils has the order η^γ, $\gamma \sim 2$):

$$\frac{\partial v}{\partial \tau} + Nv\frac{\partial v}{\partial \xi} + \varsigma v = \sum_{q=1}^{n} A_{q+1} \frac{\partial^{q+1}}{\partial \xi^{q+1}} v, \quad \varsigma = \frac{\delta/\eta}{(1-\phi_0)\rho^{(s)}} \equiv \frac{\mu_f \phi_0}{k\rho\eta} = \mathrm{O}(\eta) \quad (3.16)$$

where $v \equiv v_1$, $n = 6$, coefficients

$$A_{q+1} = c(-c)^q (Y_{m-q} b_q - Y_{n-q} a_{n-q} E), \quad Y_p = 1, \ p \geq 0; \quad Y_p = 0, \ p < 0 \quad (3.17)$$

Here $A_{2q} \geq 0$, $A_{2q-1} \leq 0$ as well as non-linearity coefficient N (equal in this case to 1) are constants. This choice of their signs corresponds to positive viscosities of the medium (the negative signs $A_{2q} \leq 0$ would give the solitons case, see Kawahara (1983)).

Let the underline that the considered wave is P_2 by the Frenkel–Biot terminology, observed in soils of arbitrary but small fluid wetness. Really, it is controlled by developed deformation of the matrix (modulus E) with the Darcy law. Wave P_1 is absent in this case.

However, in the case of full saturation the wave P_2 is fast decaying because mass velocities v and u have the opposite signs and the Darcy resistance is extremely high. Then another Frenkel–Biot wave (P_1) becomes practically the only observable. This explains "sudden" jump in wave velocity curves if fluid saturation is selected as its argument (Nikolaevskiy et al. 1970; Nakagawa et al. 1997). Mikhailov (2006) has studied the pore pressure effect on waves in gas-saturated media when such a change takes place.

Two waves are seen in the case of gas bubbles presence in water/oil-saturated media (Bedford and Stern 1983; Gardner 2000) but in this case the bubbles resonance makes the situation more complicated. The physics of this phenomenon is explained in Dunin et al. (1978).

4 P_1 Wave in Fluid Saturated Media: The First Approximation

Let us consider the wave P_1 observable in porous materials under its full saturation. In this case we consider the full dynamics system. The key point now is that in wave P_1 the mass velocities v and u have the same sign and we can assume that

$$v_1 = u_1 + \eta^\gamma v_1, \quad v - u = \mathrm{O}(\eta v) \quad (4.1)$$

Then the interfacial (Darcy) force has the order as shown:

$$R = \eta^\gamma \delta\phi\,(v-u) = \eta^\gamma \delta\,\phi v; \quad \delta = \phi\mu/k = \mathrm{O}(1) \quad (4.2)$$

Due to (4.2), the first approximation of Eq. 2.1, if one applies representations (3.6), (3.7), means

$$\eta^{\beta-\alpha}\frac{1}{2}\frac{\partial(1-\phi)\rho^{(s)}v}{\partial\tau}+\frac{\partial}{\partial\xi}(1-\phi)\rho^{(s)}v(v-c)=\frac{\partial\sigma^{f}}{\partial\xi}-(1-\phi)\frac{\partial p}{\partial\xi}+\eta^{\gamma-\alpha}\delta\,\phi v,$$

$$\eta^{\beta-\alpha}\frac{1}{2}\frac{\partial\phi\rho^{(f)}u}{\partial\tau}+\frac{\partial}{\partial\xi}\phi\rho^{(f)}u(u-c)=-\phi\frac{\partial p}{\partial\xi}-\eta^{\gamma-\alpha}\delta\,\phi v, \tag{4.3}$$

$$\eta^{\beta-\alpha}\frac{1}{2}\frac{\partial(1-\phi)\rho^{(s)}}{\partial\tau}+\frac{\partial}{\partial\xi}(1-\phi)\rho^{(s)}(v-c)=0;$$

$$\eta^{\beta-\alpha}\frac{1}{2}\frac{\partial\phi\rho^{(f)}}{\partial\tau}+\frac{\partial}{\partial\xi}\phi\rho^{(f)}(u-c)=0$$

If assume $\beta=\alpha+1$, $\alpha=1$ and the following equations are valid:

$$(1-\phi_0)\rho_0^{(s)}c\frac{\partial v_1}{\partial\xi}+\frac{\partial\sigma_1^{f}}{\partial\xi}-(1-\phi_0)\frac{\partial p_1}{\partial\xi}=\eta\Sigma$$

$$\Sigma\equiv(1-\phi_0)\rho_0^{(s)}\left(\frac{1}{2}\frac{\partial v_1}{\partial\tau}+\frac{\partial v_1v_1}{\partial\xi}\right)+c[\phi_1\rho_0^{(s)}-(1-\phi_0)\rho_1^{(s)}]\frac{\partial v_1}{\partial\xi} \tag{4.4}$$
$$-\phi_1\frac{\partial p_1}{\partial\xi}-\eta^{\gamma-1}\delta\phi_0\,v_1$$

Expression (3.10) for strain is still valid but the constitutive law is changed:

$$\sigma_1^{f}-Ee_1-K\beta^{(s)}p_1=\eta T \tag{4.5}$$

$$T\equiv-\sum_{q=1}^{n}a_q(-c)^q\Pi_{p=1}^{q}\eta^{q-1}\frac{\partial^q}{\partial\xi^q}\sigma_1^{f}+\frac{1}{\eta}\sum_{q=1}^{m}b_q(-c)^q\Pi_{p=1}^{q}\eta^{q-1}\frac{\partial^q}{\partial\xi^q}e_1 \tag{4.6}$$

The left sides of Eqs. 4.4, 4.4, 3.8 and (4.5) give us the following integrals:

$$\begin{aligned}&(1-\phi_0)\rho_0^{(s)}v_1c=-\sigma_1^{f}+(1-\phi_0)p_1,\quad \phi_0\rho_0^{(f)}u_1c=\phi_0p_1\\&v_1+ce_1=0,\quad \sigma_1^{f}=Ee_1+K\beta^{(s)}p_1\end{aligned} \tag{4.7}$$

Condition (4.1) in the first approximation means $v_1=u_1$. Therefore the impulse balance gives the following result

$$\rho_0v_1c=-\sigma_1^{f}+p_1,\qquad \rho_0=(1-\phi_0)\rho_0^{(s)}+\phi_0\rho_0^{(f)} \tag{4.8}$$

The Hooke law (with introduced pressure of saturating fluid) follows (4.5):

$$\sigma_1^{f}=-Ev_1/c+K\beta^{(s)}p_1 \tag{4.9}$$

The combination of (4.8) and (4.9) will be used further:

$$(\rho_0c^2-E)v_1-(1-K\beta^{(s)})cp_1=0 \tag{4.10}$$

Now, let us consider mass balance to be:

$$\begin{aligned}&\frac{\partial}{\partial\xi}\left\{(1-\phi_0)\rho_0^{(s)}v_1-\left[\rho_1^{(s)}(1-\phi_0)-\rho_0^{(s)}\phi_1\right]\,c\right\}=\eta\Lambda^{(s)}\\&\Lambda^{(s)}\equiv\frac{1}{2}\frac{\partial[\rho_1^{(s)}(1-\phi_0)-\rho_0^{(s)}\phi_1]}{\partial\tau}-\frac{\partial}{\partial\xi}\left[\rho_0^{(s)}\phi_1v_1-\rho_1^{(s)}\phi_1c-(1-\phi_0)\rho_1^{(s)}v_1\right];\end{aligned}\tag{4.11}$$

$$\begin{aligned}&\frac{\partial}{\partial\xi}\left\{\rho_0^{(f)}\phi_0u_1-\left[\rho_0^{(f)}\phi_1+\rho_1^{(f)}\phi_0\right]\,c\right\}=\eta\Lambda^{(f)}\\&\Lambda^{(f)}\equiv\frac{1}{2}\frac{\partial(\rho_0^{(f)}\phi_1+\rho_1^{(f)}\phi_0)}{\partial\tau}-\frac{\partial}{\partial\xi}\left(\rho_0^{(f)}\phi_1u_1-c\rho_1^{(f)}\phi_1-\rho_1^{(f)}\phi_0u_1\right)\end{aligned}\tag{4.12}$$

This set of equations gives us the following integrals if we neglect values of η-order.

$$\begin{aligned}(1-\phi_0)\rho_0^{(s)}v_1&=(-\rho_0^{(s)}\phi_1+\rho_1^{(s)}(1-\phi_0))c;\\\phi_0\rho_0^{(f)}u_1&=(\rho_0^{(f)}\phi_1+\rho_1^{(f)}\phi_0)c;\end{aligned}\tag{4.13}$$

According (2.7), (2.8), the first approximations of the densities are

$$\rho_1^{(f)}=\rho_0^{(f)}\beta^{(f)}p_1;\quad \rho_1^{(s)}=\rho_0^{(s)}[\beta^{(s)}p_1-\beta^{(s)}\sigma_1^f/(1-\phi)]\tag{4.14}$$

Now one can express the first approximations of phase velocities through wave velocity $c(>> v_1, u_1)$:

$$(1-\phi_0)v_1=(-\phi_1+(1-\phi_0)\beta^{(s)}p_1-\beta^{(s)}\sigma_1^f)c;\quad \phi_0u_1=(\phi_1+\phi_0\beta^{(f)}p_1)c$$

After summation one can get

$$(1-\phi_0)v_1+\phi_0u_1=(\phi_0\beta^{(f)}p_1+(1-\phi_0)\beta^{(s)}p_1-\beta^{(s)}\sigma_1^f)c\equiv(\beta p_1-\beta^{(s)}\sigma_1^f)c\tag{4.15}$$

Due to $v_1=u_1$, (4.15) means

$$v_1=(\beta p_1-\beta^{(s)}\sigma_1^f)c;\tag{4.16}$$

Exclusion of the effective stress (4.10) gives:

$$(1-\beta^{(s)}E)v_1-(\beta-\beta^{(s)}\beta^{(s)}K)p_1c=0\tag{4.17}$$

The condition of coincidence of Eqs. 4.10 and 4.17 relatively v_1 and cp_1 determines the wave velocity:

$$\begin{vmatrix}1-\beta^{(s)}E & -(\beta-\beta^{(s)}\beta^{(s)}K)\\ \rho_0c^2-E & -(1-\beta^{(s)}K)\end{vmatrix}=0\tag{4.18}$$

that is,

$$c^2=\frac{E+(1-\beta^{(s)}K)B}{\rho_0},\qquad B=\frac{1-\beta^{(s)}E}{\beta-\beta^{(s)}\beta^{(s)}K}\tag{4.19}$$

If the solid material is ideally cemented (Nikolaevskiy et al. 1970), that is $\beta^{(s)}K=1$, (4.19) gives the usual 1D wave velocity.

In the first approximation we can express all variables through the velocity v_1:

$$e_1 = -\frac{v_1}{c}; \quad \rho_1^{(f)} = \rho_0^{(f)}\beta^{(f)}B\frac{v_1}{c}, \quad \rho_1^{(s)} = \rho_0^{(s)}\beta^{(s)}[B(1-\beta^{(s)}K)+E]\frac{v_1}{c};$$
$$\phi_1 = (1-\phi_0)[(1-\beta^{(s)}K)\beta^{(s)}B + (\beta^{(s)}E-1)]\frac{v_1}{c}; \quad p_1 = B\frac{v_1}{c}; \tag{4.20}$$
$$\sigma_1^f = -(E-\beta^{(s)}KB)\frac{v_1}{c}$$

In the case of "soft" rocks (fully saturated soils), that is, if $\beta E << 1, \quad \beta^{(s)}K << 1$,

$$B\beta = 1, \quad p_1 = v_1/(\beta c), \quad \sigma_1^f = -p_1(\beta E - \beta^{(s)}K),$$
$$\phi_1 = -(1-\phi_0)(v_1/c)[1-(\beta^{(s)}/\beta)],$$
$$e_1 = -(v_1/c); \quad \rho_1^{(f)} = \rho_0^{(f)}(\beta^{(f)}/\beta)(v_1/c), \quad \rho_1^{(s)} = \rho_0^{(s)}(\beta^{(s)}/\beta)(v_1/c) \tag{4.21}$$
$$c = +1/\sqrt{\beta\rho_0}$$

This coincides with the results, got earlier (Nikolaevskiy 1996; Nikolaevskiy et al. 1970) for this type of porous rocks.

5 The Second Approximation of Wave P_1

Assumption (4.1) selects practically (Nikolaevskiy 1996) the first P-wave in the full equation system. The second approximation will give us the evolution equation. Firstly, one has to pay attention to the impulse equation, where right side is determined by Eq. 4.3:

$$(1-\phi_0)\rho_0^{(s)}c\frac{\partial v_2}{\partial\xi} + \frac{\partial\sigma_2^f}{\partial\xi} - (1-\phi_0)\frac{\partial p_2}{\partial\xi} = \Sigma \tag{5.1}$$

The constitutive law of the matrix has the form of:

$$\sigma_2^f - Ee_2 - p_2\beta^{(s)}K = T \tag{5.2}$$

The expression of strain through displacement velocity is the following one:

$$\frac{\partial}{\partial\xi}(ce_2 + v_2) = F \tag{5.3}$$

The second approximation of mass balances (2.6)—with account for analysis of (4.11), (4.12)—is as follows:

$$\frac{\partial}{\partial\xi}[v_2 - (\beta p_2 - \beta^{(s)}\sigma_2^f)c] = \Lambda \equiv (\Lambda_s/\rho_0^{(s)}) + (\Lambda_f/\rho_0^{(f)}) \tag{5.4}$$

The combination of (5.2) and (5.3) results in

$$\frac{\partial}{\partial\xi}(c\sigma_2^f + Ev_2 - p_2c\beta^{(s)}K) = EF + c\frac{\partial T}{\partial\xi} \tag{5.5}$$

Now exclude the second approximation of the effective stress. Then Eqs. 5.4 and 5.5 give:

$$\frac{\partial}{\partial\xi}[(1-\beta^{(s)}E)v_2 - (\beta - \beta^{(s)}\beta^{(s)}K)cp_2] = \Lambda - \beta^{(s)}EF - \beta^{(s)}c\frac{\partial T}{\partial\xi} \tag{5.6}$$

Eqs. 5.1 with 5.5 result in the following one:

$$\frac{\partial}{\partial\xi}[(\rho_0 c^2 - E)v_2 - (1-\beta^{(s)}K)cp_2] = EF - c\Sigma + c\frac{\partial T}{\partial\xi} \tag{5.7}$$

The determinant of Eqs. 5.6, 2.5 coincides with (4.18) that had given the wave velocity c. According to the linear algebra rules, the compatibility condition is the equation, got from (4.18) by change of one of columns with right side of (5.6), (5.7). Then we have:

$$\begin{vmatrix} \rho_0 c^2 - E & \frac{\partial}{\partial\xi}\left(EF - c\Sigma + c\frac{\partial T}{\partial\xi}\right) \\ 1-\beta^{(s)}E & \frac{\partial}{\partial\xi}\left(\Lambda - \beta^{(s)}EF - \beta^{(s)}c\frac{\partial T}{\partial\xi}\right) \end{vmatrix} = 0 \tag{5.8}$$

This is the evolution equation relatively to $v \cong v_1$:

$$\begin{aligned}(\rho_0\, c^2 - E)\Lambda - [1 - 2\beta^{(s)}E + \beta^{(s)}\rho_0 c^2]EF + c(1-\beta^{(s)}E)\Sigma \\ = [\beta^{(s)}(\rho_0\, c^2 - E) + (1-\beta^{(s)}E)]c\frac{\partial T}{\partial\xi}\end{aligned} \tag{5.9}$$

This equation has the form of (3.16) with the coefficients N and A_q can be calculated with help of the expressions given above. The sink term with the coefficient $\zeta \sim O(\eta)$ is responsible for permanent generation of the P-wave of the second type, which is parasitic in this case.

For soft rocks (soils), saturated with fluid, we have $\beta E << 1$, $\beta^{(s)}K << 1$, and expressions (4.20) are valid. Then (5.9) is simplified:

$$c\Lambda - [\beta + \beta^{(s)}]EcF + c^2\beta\Sigma = (\beta + \beta^{(s)})c^2\frac{\partial T}{\partial\xi} \tag{5.10}$$

$$c\Lambda = \frac{1}{2}\frac{\partial v}{\partial\tau} + \left[1 + (1-\phi_0)\frac{\beta^{(f)} - \beta^{(s)}}{\beta}\left(1 - \frac{\beta^{(s)}}{\beta}\right)\right]\frac{\partial vv}{\partial\xi} \tag{5.11}$$

$$cF = -\left(\frac{1}{2}\frac{\partial v}{\partial\tau} + \frac{1}{2}\frac{\partial vv}{\partial\xi}\right) \tag{5.12}$$

$$c^2\Sigma = c^2(1-\phi_0)\rho_0^{(s)}\left\{\frac{1}{2}\frac{\partial v}{\partial\tau} + \left[\left(1 - \frac{\beta_s}{\beta}\right)\frac{\rho_0}{\rho_0^{(s)}}\right]\frac{\partial vv}{\partial\xi}\right\} \tag{5.13}$$

Collecting all necessary expressions will give again Eq. 3.16 with the following coefficients. Correspondingly, one can see that deviations of value $N = 1$ are connected with the physical differences of solid and fluid phases.

$$\frac{\partial v}{\partial\tau} + Nv\frac{\partial v}{\partial\xi} + \varsigma v = \frac{\beta + \beta^{(s)}}{\Delta}c^2\frac{\partial T}{\partial\xi}, \quad \varsigma = \frac{\delta\eta}{\rho_0\Delta} \equiv \frac{\mu_f\phi_0}{k\rho_0\Delta} = \mathrm{O}(\eta) \tag{5.14}$$

$$N = 2\frac{1 + (1-\phi_0^2)}{\phi_0 + \phi_0(1-\phi_0)(\rho_0^{(s)}/\rho_0)}\Delta, \quad \Delta = \frac{1}{2}\left[1 + (1-\phi_0)\frac{\rho_0^{(s)}}{\rho_0}\right] \tag{5.15}$$

Appendix C

Example

Equation (4.57) can be illustrated by the following simple example

$$v_1 + cR_1 = 0\,,$$

$$2v_1 + 4R_1 = 0\,.$$

A non-zero solution of the system exists only if $c = 2$ (the eigenvalue of the problem). Here v_1 and R_1 are analogous to the first approximation from our main text. The second approximation, v_2 and R_2, satisfies the system

$$v_2 + cR_2 = f[v_1]\,,$$

$$2v_2 + 4R_2 = g[v_1]\,,$$

which is solvable only if the right-hand sides satisfy the condition $g[v_1] = 2f[v_1]$. This solvability condition is the analogy to the Nikolaevskiy-type equation that we aim to derive.